2007

Copper(II) oxide mediated formation and stabilization of combustion generated persistent free radicals

Hieu Truong
Louisiana State University and Agricultural and Mechanical College

COPPER(II) OXIDE MEDIATED FORMATION AND STABILIZATION OF COMBUSTION GENERATED PERSISTENT FREE RADICALS

A Dissertation

Submitted to the Graduate Faculty of the
Louisiana State University and
Agricultural and Mechanical College
In partial fulfillment of the
Requirements for the degree of
Doctor of Philosophy

In

The Department of Chemistry

By

Hieu Truong
B.S., Louisiana State University, Baton Rouge, 2001
August 2007

TABLE OF CONTENTS

LIST OF TABLES

LIST OF FIGURES

ABSTRACT

Biologically damaging semiquinone-type radicals have been reported in cigarette smoke, their likely origin being hydroquinone (HQ) and catechol (CT) molecular precursors contained by the tobacco. Since other biomass contains HQ and CT-type species, it is likely that combustion of other biomass will also form semiquinone-type radicals. All hydrocarbon fuels will form phenol and substituted phenol that can form substituted phenoxyl radicals. Because each of these radicals has the potential to be environmentally persistent and biologically active, their formation and stabilization from various molecular precursors was studied with the focus on surface-bound radicals formed in association with combustion-generated fly-ash particles.

Comprehensive product yield determinations from the high-temperature, gas-phase degradation of HQ and CT revealed the formation of dibenzofuran, dibenzo-p-dioxin, benzoquinone, phenol, benzene, phenylethyne, styrene, indene, naphthalene and biphenylene. The formation of semiquinone, phenoxyl, and cyclopentadienyl radical is strongly implied because of the observation of benzoquinone, phenol, and naphthalene, respectively during the thermal decomposition of HQ and CT process.

Radicals were generated and stabilized on the surface of 5% copper (II) oxide/silica dioxide (CuO/SiO_2) particles, which was used as a surrogate for combustion-generated fly-ashes. These radicals were generated from the following precursors through chemisorption and electrons transfer between the matrix and the adsorbed molecules: monochlorobenzene (MCBz), 1,2-dichlorobenzene (1,2-DCBz), phenol (P), 2-monochlorophenol (2-MCP), HQ and CT. Electron paramagnetic resonance (EPR) was used to investigate the characteristic of radicals. Gas chromatography-mass spectroscopy (GC-MS) was used to identify molecular

species formed during solvent extraction using polar solvents; methyl alcohol, isopropyl alcohol, and dichloromethane; and non-polar solvents; toluene, and *tert*-butylbenzene.

All of precursors generated surface-associated radicals with maximum yields between 200°C - 230°C and were very persistent in the air. Polar solvents extracted more free radicals than non-polar solvents. GC/MS analysis identified many molecular dimer species in solution indicating radical-radical reaction in the extract solution.

These studies indicate that CuO/SiO_2 surface mediates the formation and stabilization of substituted phenol-type surface-associated radicals that can be environmentally persistent. Solvent extraction converts these radicals to molecular species that may result in their misidentification in the literature as molecules rather than radicals.

CHAPTER 1: INTRODUCTION

A persistent free radical (PFR) is defined as a radical that is sufficiently stable towards decomposition and resistant to further reaction that it can exist for long period of time in the atmosphere. These radicals that potentially include semiquinone-type and phenoxyl-type radicals are highly resonance stabilized that can be formed in combustion systems or thermal processes such as burning of cigarette, biomass fuels, fossil fuels, coal, and hazardous materials [1-3].

Recently, many studies have been reported that semiquinone and phenoxyl radicals are persistent when they are associated with combustion generated fly-ash such they can exist very long time and transport over considerable atmospheric distances [4-8]. Semiquinone radicals are highly active in oxidative stress that can lead to cancer, mutations, and alter DNA [9-11]. Phenoxyl radicals can also combine to form polychlorinated dibenzo-p-dioxin/ dibenzofuran (PCDD/F) which is the most toxic known environmental pollutant [12]. Due to the structural similarity of semiquinone and phenoxyl radicals; hydroquinone, catechol, chlorinated benzenes, phenol, and chlorinated phenols are chosen to be precursors for studying the formation and stabilization of corresponding persistent free radicals.

1.1 Occurrence, Use and Health Impacts of Phenol, Hydroquinone and Catechol

Phenol occurs naturally in animal waste and by decomposition of organic wastes [13] or even in hardwood [14, 15]. Phenol was detected in the water of lakes, rivers and in fish tissue [16]. In contrast, hydroquinone (HQ) and catechol (CT) are found in a variety of forms as natural products from plants and animals. HQ and CT have been identified in roasted coffee beans [17] and in the leaves of blueberry, cranberry, cowberry and bearberry plants [18];

however, tea is prepared from these leaves that have been reported to contain HQ at some concentration up to 1% of total ingredients [19]. The hazardous substances data bank (HSDB) in 1993 reported CT is found in onions, apples, and even in the leaves or branches of oak and willow trees. HQ was observed in the tissue cultures of *Antennaria-microphylla* and *Euphorbia-esula* [20, 21]. HQ is also found in the explosion chamber of beetle [22, 23] that is ready to shoot toward the enemy in the form of hot quinone cloud.

Phenol is used in a variety of indoor products including mouth washes, shave creams, and throat lozenges [24] or in the manufacture of plastics, fibers, adhesives, resins, and rubber (HSDB, 1991). HQ and CT are used in many fields including graphic arts, photographic developers, antioxidants, polymerization inhibitors, and pharmaceuticals. They are used in cosmetics and medical skin preparations as de-pigmenting agent to lighten small areas of hyper-pigmented skin [18] or in ingredient of permanent hair dyes and color preparations [25, 26]. HQ and CT are used in medical and industrial X-ray films [27] as well as developer in black-and-white photography or related graphic arts such as lithography and rotogravure [18, 27-29]. They are widely used in the manufacture of rubber antioxidants, monomer inhibitors, and food antioxidants to prevent deterioration in many oxidizable products [18, 30]. Application of a CT antioxidant protocatechuic acid on 12-O-tetradecanoylphorbol-13-acetate induces inflammatory responses in mouse skin [31]. An abietic acid-derived CT scavenges hypochlorous acid, a powerful pro-inflammatory oxidant produced by activated neutrophils, to protect liposomes against iron-ascorbate-induced oxidation [32]. Phenol, HQ and CT are very useful in our life; on the other hand, they are also very harmful if we misuse them.

Cigarette smoking is the leading cause of preventable death in the United States, claiming more than 400,000 lives per year (clinnimmune-immunotoxicology report, 2003). A typical smoker receives more than 100 µg of HQ or CT per cigarette [33] and ~280 µg of phenol per cigarette [34]. Environmental Protection Agency (EPA) database in U.S. (revised in January 2000) reported vapor pressure of phenol and CT are 0.357 mmHg and 0.03 mmHg, respectively at 20°C while HQ exhibits as much lower vapor pressure of 1.9×10^{-5} mmHg at 25°C. However, they can be oxidized in the presence of moisture to form quinone, which is more volatile. Inhalation of phenol, HQ or CT has been shown to induce coughing, burning sensations, labored breathing in humans [35-38] as well as reduced bone marrow and corneal damage in mice [38-42].

The use of phenol in the surgical procedure of skin peeling may produce cardiac arrhythmias [43]. Concentration of HQ or CT as low as 10µM inhibits ribo-nucleotide reductase that causes an immediate cessation of DNA synthesis in proliferating lymphocytes [44, 45]. Even worse, 50µM of HQ or CT will instantaneously blocks more than 90% DNA synthesis [46]. The major concern is HQ and CT may exist as semiquinone radical form causing cancer, mutations, and many health symptoms in our life.

Semiquinone radical has been reported in cigarette smoke [4, 10] and demonstrated to be highly redox active toward producing reactive oxygen species (ROS) in biological systems [10, 47, 48]. ROS induces oxidative stress in living organisms which is currently considered to be a significant causes of the health impacts of airborne fine particulate matter [4, 11, 47, 49, 50]. Cigarette smoke enhances tumor cell invasions and metastasis, which increase the spread of cancer in the body [51]. The study of the effect of cigarette smoking on oxidative stress in lung tissues from 14 smokers and non-smokers has shown that oxidative DNA

damage is induced in lung DNA by cigarette smoke related to semiquinone radicals and reactive oxygen species (ROS) [52-55]. Semiquinone radical also has reported in wood smoke and other combustion sources. A study of wood burning indicates the generation of radicals and ROS that break cellular DNA strands in cultured RAW 264.7 mouse macrophage cells [56]. Although the initial DNA cell is damaged, our immune system has the ability to repair it. However, a study of 22 patients with systematic lupus erythematosus and 16 healthy people has demonstrated that radicals in the blood cell is the main cause of the decrease in DNA-repair capability and suggested that ROS damages the enzymes responsible for DNA repair [57].

Phenol may exist in form of phenoxyl radicals and may also have a major impact on human health effects as well as semiquinone radicals. However, it is not clear if this type of radicals is highly reactive with oxygen or other molecular species to produce superoxide or hydroxyl radicals. Furthermore, phenoxyl radicals tend to undergo radical-radical recombination process to form PCDD/Fs or poly-aromatic hydrocarbon (PAH) at high temperature in post-flame region of the combustion process [12]. Semiquinone and phnoxyl radicals are being formed in gas-phase or on the surface of combustion-generated particles that contribute to ambient air pollution.

Ambient air pollution is a complex mixture of volatiles and particulates from various sources including vehicle exhaust pipes, flaring of hydrocarbons at refineries sites, coal burning at power plants, burning trash or crops after harvest that still happen in many developed countries [50]. The size and composition distribution of fine particulate matter from motor vehicles, wood burning, and cigarette smoke [58-62] contribute a significant impact in our health.

Particles with the sizes greater than 10 μm can pass through nose and mouth to penetrate on the larynx. Those particles with the sizes between 10 μm and 2.5 μm, can follow air stream through the larynx and enter the trachea and the bronchial regions of the lung. However, those particles with sizes less than 2.5 μm deposit deep into the alveolar regions of the lung and even diffuse directly into the blood stream. Research suggested that fine particulate matters produces an acute cardiovascular malfunction indirectly through the induction and perpetuation of inflammatory responses in the lung [50]. Other review suggests that particles with the sizes 0.1 μm can penetrate deep into the lower respiratory tract and diffuse into the blood stream then circulate to the heart whereas they may cause many symptoms related to heart diseases including the influences of the cardiac myocytes and cardiovascular functioning [63-65].

Exposure to fine particulate matter causes an acute inflammatory response [66], asthma and chronic obstructive pulmonary disease [67]. The number of deaths due to respiratory viral infections is increased on high concentration of ambient air pollution days [68]. Some studies have shown cardiac myocyte degeneration [69] and changes in heart rate [70] when exposed to environmental pollutant for even a short period of time.

Significant contribution to ambient air pollution is anthropogenic combustion sources including cigarette smoke. The government and EPA have set the limit of environmental exposure to hazardous compounds for producers to protect our environment concerning human health.

1.2 Combustion Sources and Environmental Exposure

Combustion sources are a process of burning hydrocarbon fuel including burning coal in many power plants, burning wood in firestones or bonfire for heating and cooking,

burning gasoline in internal combustion engine found in motor vehicles, lawnmowers, air planes, open burning biomass in agricultures. Phenol, HQ, and CT are thought to originate from thermal degradation of lignin and other polymeric plant materials that usually contain aryl ether and aryl alcohol linkages [71-74]. They can be a significant decomposition product in burning of other biomass [73-79] and some coals [80-82]. Wood and biomass fuels are still the major source of energy for cooking and space heating in the world. Field burning of the post-harvest residuals in urban also contributes to their source.

Their derivative including quinones of PAHs have been reported in both atmospheric aerosols and combustion-generated particulate matter (PM). They have been reported in concentrations of 5.0-730 $\mu g/m^3$ in atmospheric total suspended particulate (TSP) [83]. The emissions of HQ and CT from wood-burning fireplaces were reported to be 0.3-10 mg/g and 1.7-9.8 mg/g of organic carbon, respectively [78, 84]. The emissions of CT from open burning of agricultural biomass were reported to be 0.060-1.2 mg/g of organic carbon and 0.11-4.0 mg/g for other quinones [75]. Methoxyhydroquinones and methoxyphenols (e.g. syringols) are frequently reported in biomass combustion emissions as partial decomposition products of lignin [71]. They have been reported to be 0.50-3.0 % of total biomass burned [85]. Methoxyphenol concentrations were reported in airborne PM at concentrations of 0.10-22 ng/m^3 [86]. Burning wood and biomass release a huge amount of methoxyphenol in the range 900-4200 mg/kg of fuel in vapor and particle-phase [87-89].

Phenol, HQ, and CT are also found as one of a major organic components of combustion of tobacco[44, 90-96]. Despite cancer and other symptoms caused by cigarette smoke, people do not want to quit smoke. The United State and other countries have limited

cigarette smoke by not allowing people smoke at work or restaurants; however, more young people become regular smoker everyday.

Along with refinery site and power plant, motor vehicles contribute significantly to their sources. Although both motor vehicle designs and gasoline formulations have changed to reduce the emissions of air pollution, they are still a major concern. The emissions of quinone for catalyst-equipped gasoline-powered motor vehicle are reported 0.849 μg/km versus 25.4 μg/km for noncatalyst-equipped gasoline-powered motor vehicle [97]. Also, The emissions of quinones were reported to be 15-140 μg/g in gasoline exhaust particles [98] and 7.90-40.4 μg/g in diesel exhaust particles [83]. Light-duty gasoline vehicles technology classes reported the emission of benzoquinone in low emission vehicles (LEV), three-way catalyst equipped vehicles (TWC), and smoking vehicles to be 2.0 μg/L, 85 μg/L, 3200 μg/L of fuel consumed respectively in gas-phase and 1.8 μg/L, 46 μg/L, 1500 μg/L of fuel consumed respectively in particle-phase [99]. Significant reduction of benzoquinone emission level of heavy-duty diesel vehicles in the year of 1999 versus 1995 from 28000 μg/L to 510 μg/L of fuel consumed in gas-phase and from 1600 μg/L to 230 μg/L of fuel consumed in particle-phase [99].

These data indicate a wide variety of related compounds are formed that contribute to environmental ambient air pollution. **Table 1** presents a review of the literature (1998-2006) concerning the emission of phenol, HQ, CT, and their derivative from combustion sources. In combustion, chain reaction of radicals is a major reaction. Free radicals in general, and particularly semiquinone-type and phenoxyl-type radicals, play a very important role and may have a significant impact on our environmental health. However, how do they form? The next section will explain their formation.

Table 1.1: Summary of the Key Finding of the Emission of Phenol, HQ, CT, and Their Derivative from combustion sources

(Year), Authors, and Journal	Title	Key Finding of Phenol, HQ, CT, and Their Derivative
(2006) Valavanidis, A; Fiotakis, K; Vlahogianni T.; Papadimitriou, V.; Pantikaki, V.; *Environmental Chemistry*	Determination of Selective Quinones and Quinoid Radicals in Airborne Particulate Matter and Vehicular Exhaust Particles	The average concentrations of individual target quinones ranged of 15-140 ng/mg in diesel and gasoline exhaust particles, ranged of 1.5-60 ng/mg or 150-1100 pg/m^3 in airborne particulate matter
(2006) Jakober, Chris A.; Charles, J.; Kleeman, M.; Green, P; *Analytical Chemistry*	LC-MS Analysis of Carbonyl Compounds and Their Occurrence in Diesel Emission	Heavy-duty diesel vehicle emissions were collected in Riverside, CA containing 1,4-benzoquinone at a rate of 150 ± 7 µg/km (gas-phase), 1,4-naphthoquinone at a rate of 70 ± 3 µg/km (gas-phase) and 2.1 ± 0.1 µg/km (particle-phase).
(2005) Simpson, C.; Paulsen, M.; Dills, R.; Liu, S.; Kalman, D.; *Environmental Science & Technology*	Determination of Methoxyphenols in Ambient Atmospheric Particulate Matter: Tracers for Wood Combustion	Particle-bound methoxyphenol concentrations in the range of 0.1-22 ng/m^3 were observed and the methoxyphenols were almost exclusively in the fine particle size fraction
(2005) Hays, M.; Fine, P.; Geron, C.; Kleeman, M.; Gullett, B; *Atmospheric Environment*	Open Burning of Agricultural Biomass: Physical and Chemical Properties of Particle-Phase Emissions	The emission (mg/g of organic carbon) from open burning of agricultural biomass rice straw and wheat straw for CT (1.179; 0.060), methyl benzenediol (0.710; 0.104), methoxybenzenediol (0.371; 0.095), and anthracene-9,10-dione (ND; 0.033).
(2004) Cho, A.; Stefano, E.; You, Y.; Rodriguez, C.; Schmitz, D.; Kumagai, Y.; Miguel, A.; Eiguren-Fernandez, A.; Kobayashi, T.; Avol, E.; Froines, J.; *Aerosol Science and Technology*	Determination of Four Quinones in Diesel Exhaust Particles, SRM 1649a, an Atmospheric PM2.5	Mean concentration of individual target quinones ranged from 7.9-40.4 µg /g in the diesel exhaust particles, and from 5-730 pg/m^3 in the PM2.5 samples.

(Table con'd)

(Year), Authors, and Journal	Title	Key Finding of Phenol, HQ, CT, and Their Derivative
(2002) Fine, P.; Cass, G.; Simoneit, B.; *Environmental Science & Technology*	Chemical Characterization of Fine Particle Emissions from the Fireplace Combustion of Woods Grown in the Southern United States	The concentration emitted from southern U.S. wood: yellow poplar, white ash, sweet-gum, mochemut hickory, loblolly pine, and slash pine for HQ (7.609, 1.621, 1.435, 10.119, 0.763, and 0.295 mg/g of organic carbon) and CT (4.127, 1.741, 1.383, 9.865, 2.600, and 1.711 mg/g of organic carbon), respectively.
(2002) Schauer, J.; Kleeman, M.; Cass, G.; Simoneit, B.; *Environmental Science & Technology*	Measurement of Emissions from Air Pollution Sources. 5. C_1-C_{32} Organic Compounds from Gasoline-Powered Motor Vehicles	Emission of anthracene-9,10-dione were 0.849 µg/km for catalyst-equipped gasoline-powered motor vehicle and 25.4 µg/km for noncatalyst- equipped gasoline-powered motor vehicle
(2002) Zheng, M.; Cass, G.; Schauer, J.; Edgerton, E.; *Environmental Science & Technology*	Source Apportionment of PM2.5 in the Southeastern United States Using Solvent-extractable Organic Compounds as Tracers	The concentration was calculated from Centreville, North Birmingham, Jefferson, and Pensacola for anthracene-9,10-dione (0.12, 0.51, 0.32, and 0.15) ng/m^3 and benz[a]anthracene-7-12-dione (0.02, 0.26, 0.05, and 0.01) ng/m^3, respectively.
(2002) Hays, M.; Geron, C.; Linna, K.; Smith, D.; *Environmental Science & Technology*	Speciation of Gas-Phase and Fine Particle Emissions from Burning of Foliar Fuels	Gas-phase emissions from open burning of six fine fuels common to U.S. ecosystems were invested that containing methoxyphenol ranged 0.5-3% of total PM2.5 mass.
(2001) Fine, P.; Cass, G.; Simoneit; B.; *Environmental Science & Technology*	Chemical Characterization of Fine Particle Emissions from Fireplace Combustion of Woods Grown in the Northeastern United State	The concentration emitted from northeastern U.S. wood: red maple, northern red oak, paper birch, eastern white pine, eastern hemlock, and balsam fir for HQ (0.625, 5.570, 0.919, 0.356, 1.146, and 4.793 mg/g of organic carbon) and CT (0.799, 5.434, 1.110, 1.512, 0.952, and 7.114 mg/g of organic carbon), respectively.

(Table con'd)

(Year), Authors, and Journal	Title	Key Finding of Phenol, HQ, CT, and Their Derivative
(2001) Nolte, C.; Schauer, J.; Cass, G.; Simoneit, B.; *Environmental Science & Technology*	Highly Polar Organic Compounds Present in Wood Smoke and in the Ambient Atmosphere	The emission (µg /g of wood burned) of lignin breakdown substituted phenol products in wood smoke of the San Joaquin Valley, California for oak (0.3-68), eucalyptus (0.1-106), and pine (0.1-125), respectively.
(2000) Fraser, M.; Kleeman, M.; Schauer, J.; Cass, G.; *Environmental Science & Technology*	Modeling the Atmospheric Concentrations of Individual Gas-Phase and Particle-Phase Organic Compound	A formal evaluation of model performance has shown that primary emission sources of anthracene-9,10-dione were from catalyst and noncatalyst-equipped gasoline-powered vehicles or natural gas combustion with the concentration of 0.3 ± 0.2 ng/m^3
(1999) Fine, P.; Cass, G.; *Environmental Science & Technology*	Characterization of Fine Particle Emissions from Burning Church Candles	The concentration emitted from unburned wax and candle smoke for anthracenedione (paraffin: 0.09 and 0.04 mg/g of wax; beeswax: 0.07 and 0.05 mg/g of wax) and benz[a]anthracene-7-12-dione (paraffin: 0.002 and 0.007 mg/g of wax; beeswax: 0.002 and 0.02 mg/g of wax)
(1998) Trenholm, A.; *Waste Management*	Identification of PICs in hazardous waste combustion emission	Benzoquinone, 1,4-naphthaquinone, and phenol were identified by EPA method for semivolatile compound (MM5-SV with GC/MS). The concentration of benzoquinone and 1,4-naphthaquinone from 1-5 µg/cm^3 and phenol from 5-25 µg/cm^3.
(1998) Fraser, M.; Cass, G.; Simoneit, B.; *Environmental Science & Technology*	Gas-Phase and Particle-Phase Organic Compounds Emitted from Motor Vehicle Traffic in a Los Angeles Roadway Tunnel	The concentration emitted from motor vehicle traffic in a Los Angeles roadway tunnel for anthracene-9,10-dione (14.7 µg/L vapor-phase and 9.8 µg/L particle-phase) and benz[a]anthracene-7-12-dione (3.3 µg/L particle-phase).

1.3 Formation of Semiquinone and Phenoxyl Radicals

HQ and CT are isomers, and the only difference in structure between them is the position of hydroxyl groups on the benzene ring, which is *para* position for HQ versus *ortho* position for CT. **Figure 1.1** presents the formula structure of HQ and CT molecular as well as p-semiquinone and o-semiquinone radical.

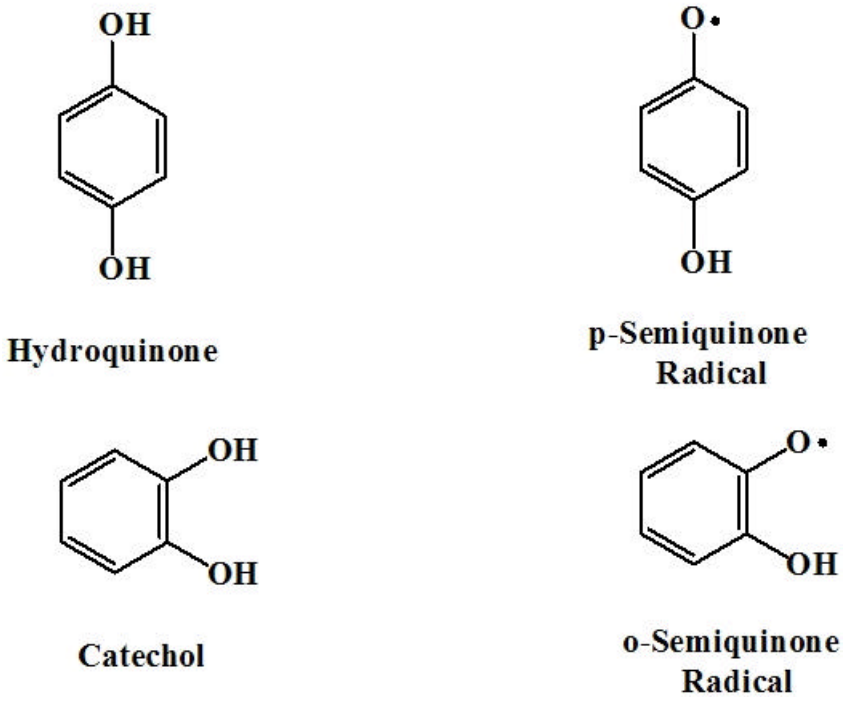

Figure 1.1: Hydroquinone, Catechol, and Semiquinone Radicals

In the gas-phase, endothermic dissociation of semiquinone-hydrogen bond from HQ or CT forms semiquinone radical or abstraction of semiquinone-hydrogen from HQ or CT in the presence of high concentration of initiated radicals also forms semiquinone radical [100, 101]. **Scheme 1.1** displays possible routers of formation of semiquinone radical form HQ and CT molecules in gas-phase.

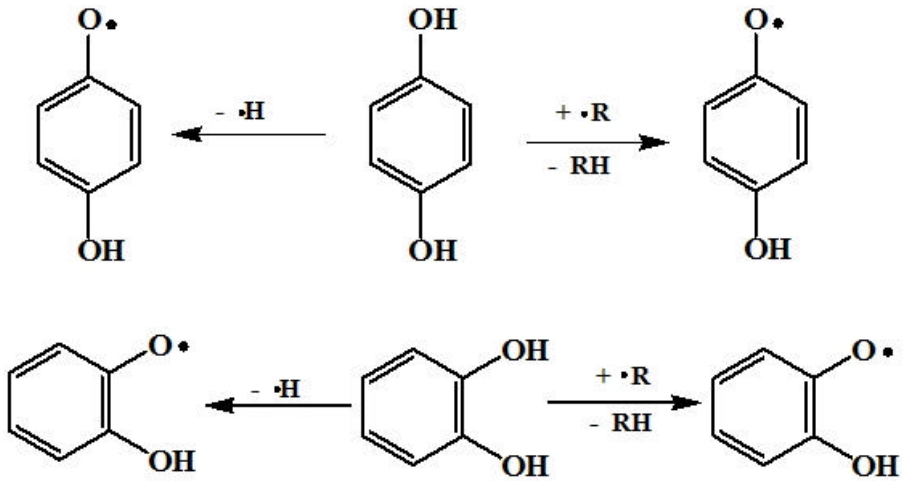

Scheme 1.1: General Formation of Semiquinone Radical in Gas-Phase

Semiquinone radicals may also form on the surface of combustion generated fly-ash through the elimination of water and electron transfer to the metal surface in chemisorption process [5, 102, 103]. **Scheme 1.2** depicts possible routes of formation of semiquinone radical from HQ and CT on the metal surface.

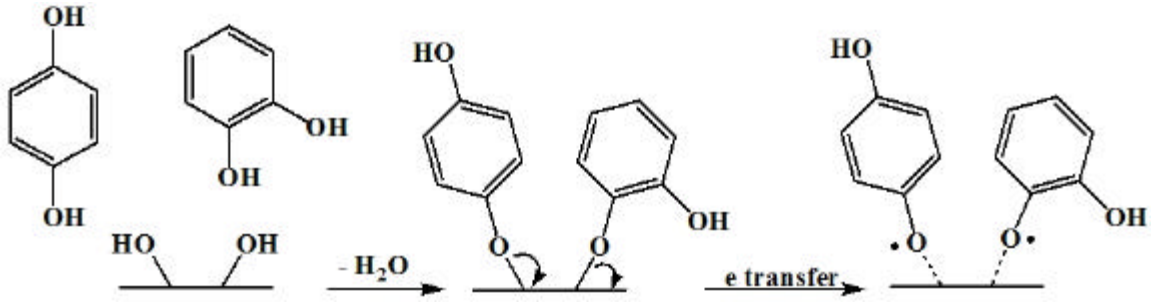

Scheme 1.2: Semiquinone Radical Formation on the Metal Surface from HQ or CT

2-Monochlorophenol (2-MCP) and 1,2-dichlorobenzene (1,2-DCBz) may form 2-chlorophenoxyl radical and may also form semiquinone radicals while phenol (P) and Monochlorobenzene (MCBz) may form phenoxyl radical when chemisorb on the particle.

Figure 1.2 presents the formula structure of MCBz, 1,2-DCBz, 2-MCP, Phenol, phenoxyl radical, and 2-chlorophenoxyl radical.

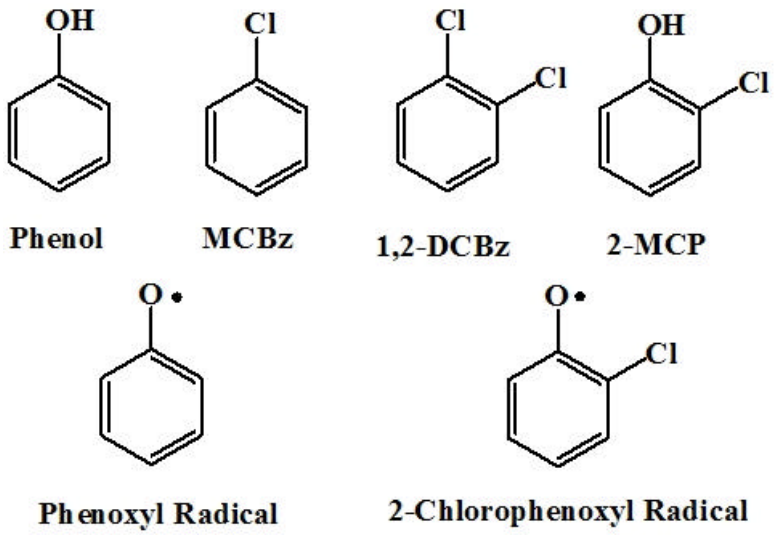

Figure 1.2: Precursors of Phenoxyl Radical and Chlronated Phenoxyl Radical

Similar to semiquinone radical formation, phenoxyl radical can be generated in gas-phase through unimolecular endothermic decomposition [104] or abstraction of phenoxyl-hydrogen from phenol in the presence of high concentration of initiated radical [105-107] due to the phenoxyl-hydrogen bond being weak (81-86kcal/mol) [101]. **Scheme 1.3** displays possible routers of formation of phenoxyl radical form phenol molecules in gas-phase.

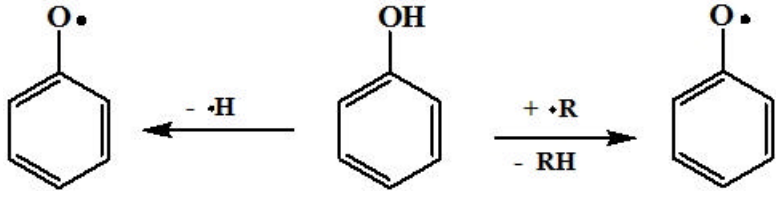

Scheme 1.3: General Formation of Phenoxyl Radical in Gas-Phase

Phenol may also eliminate water to bind to the surface of combustion generated fly-ash and form phenoxyl radicals through electron transfer in chemisorption process. Chlorinated benzenes such as MCBz and 1,2-DCBz may bind to the surface of particulate mater and form phenoxyl radical or chlorinated phenoxyl radical through hydrogen chloride elimination and electron transfer [6, 102] as shown in **scheme 1.4**.

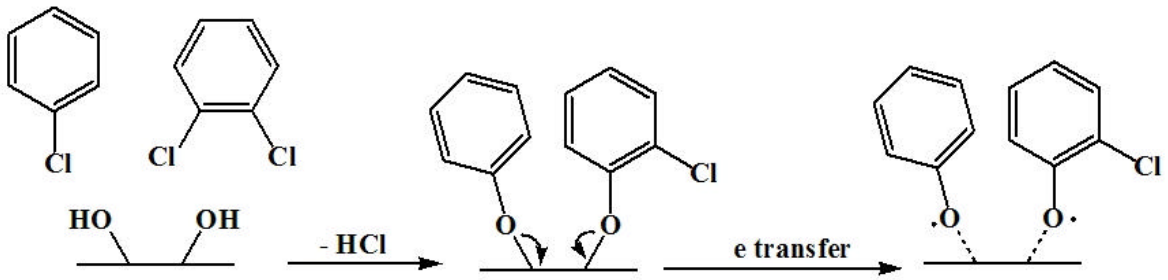

Scheme 1.4: Formation of Phenoxyl Radical and Chlorinated Phenoxyl Radical on the Metal Surface from Chlorinated Benzene

Radicals exhibit very short lifetime in the gas-phase or in solution [108-110]; however, they can be stabilized and exist for a very long period of time when they associate with surface of some particulate matter that contain transition metals [5-8, 11]. Fine particles of fly-ash are normally generated from combustion sources that contain transition metals and persistent radicals [1-3, 60, 111]. The interaction between phenoxyl-type radicals may result in the formation of (PCDD/F) [12] that has more detail in the next section.

1.4 Formation of PCDD/Fs

PCDD/Fs are common trace products from many combustion and other thermal processes; they are also found in fish, sediment, and soil [112]. PCDD/Fs are the target of research through many decades because of their extremely toxicity. The most toxic among PCDD/F is the 2,3,7,8-tetrachlorodibenzo-p-dioxin (TCDD) that causes birth defects,

cancer, skin disorder, liver damage, and others suppression of the immune system even with very small dose concentration [113].

In combustion processes, radical-radical interaction of phenoxyl and/or chloro-phenoxyl radicals is the main mechanism pathway of the formation of PCDD/Fs [114-117]. **Scheme 1.5** presents the general formation of PCDD/F.

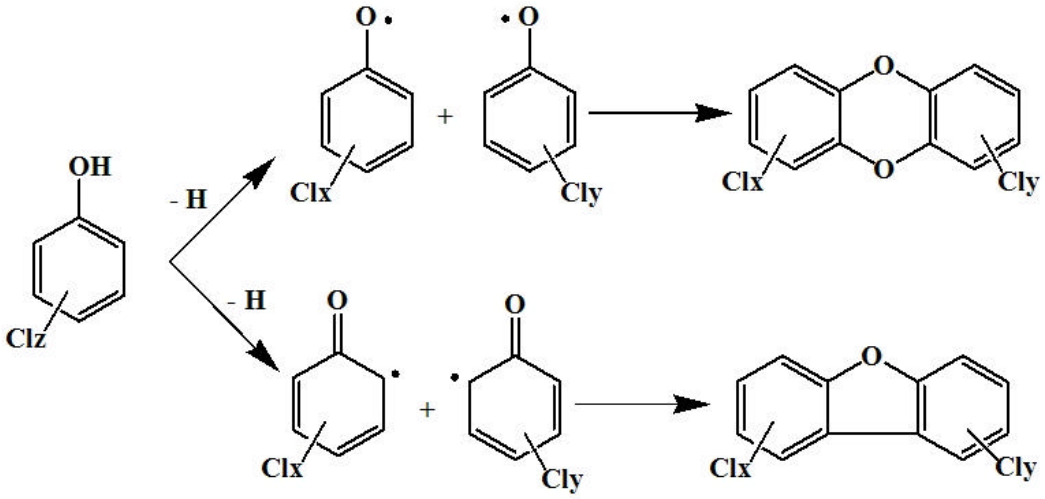

Scheme 1.5: Formation of PCDD/F from radical-radical interaction pathway

Other researchers have suggested that phenoxyl or chlorinated phenoxyl radicals react with molecular aromatic chlorinated phenol to form PCDD/F [115, 118-120]. **Scheme 1.6** displays the general formation of PCDD/F form the radical-molecule interaction pathway.

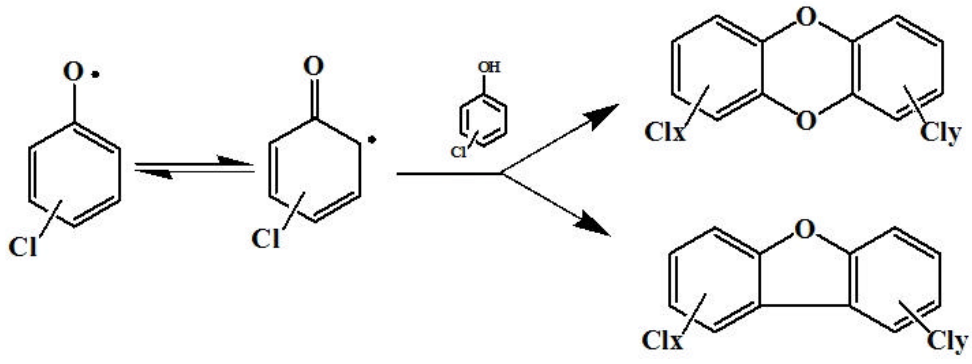

Scheme 1.6: Formation of PCDD/F from radical-molecule interaction pathway

Gas-phase formation of PCDD/F only accounts for 30% of dioxins emission [121] while surface-mediated processes with transition metal plays important role in dioxins formation that accounts for 70% of dioxins emission [5, 122]. In fact, most of reactions in combustion process deal with radicals, and these radicals with very short lifetime tend to react with high concentration molecules (oxygen and water vapor). However, some radicals may be stabilized and extend their lifetime when they associate with fly-ashes containing transition metal which also were generated by combustion. Many studies have shown transition metals are present in combustion generated fly-ashes and airborne particulate mater [1-3, 123]. Recently, researchers have proven that metal-mediated PCDD/F formation on the surface of fly-ashes [5, 124-127] results in significantly increased PCDD/F formation. **Scheme 1.7** displays the general mechanism of dioxin formation on the surface of fly-ashes.

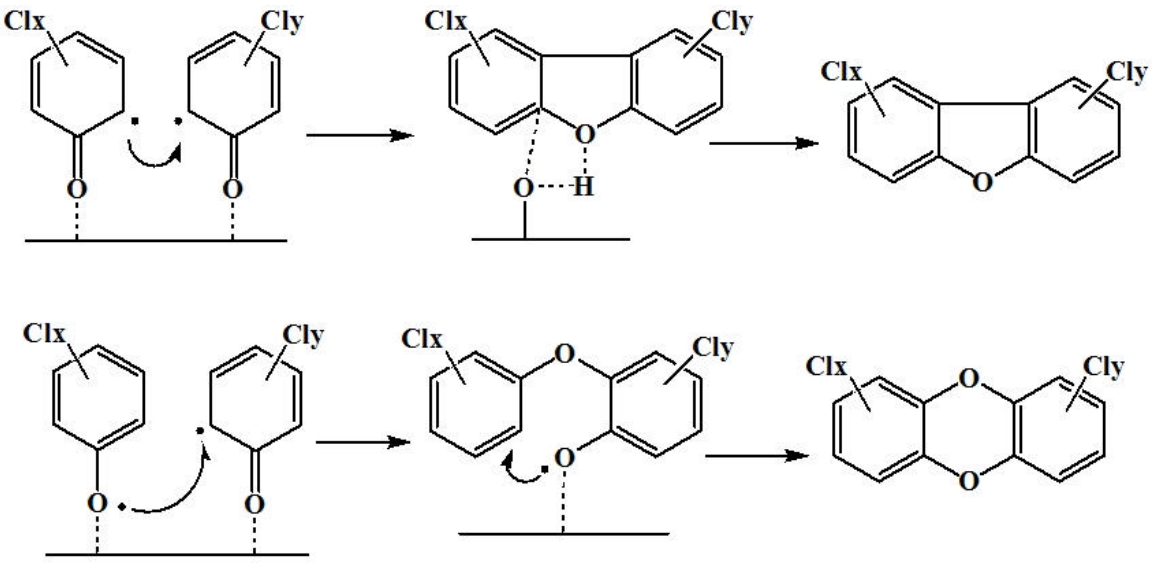

Scheme 1.6: Formation of PCDD/F on Metal Surface of Fly-ashes

In the gas-phase thermal degradation of chlorinated phenol, dioxins products form above 600°C under pyrolytic condition and above 400°C under oxidative condition [120, 128,

[129]. Thus, oxygen enhances PCDD/F formation at low temperature due to formation of phenoxyl radicals [117, 130] and many studies have strongly suggested that phenoxy radicals are the key intermediates of the formation of PCDD/F [116, 117, 119]. Normally, the initial step of PCDD/F formation is the dissociation of hydroxyl hydrogen bond of phenol or chlorinated phenol to form phenoxyl radicals following chlorine displacement or radical-radical combination.

In general, chlorinated benzene or chlorinated phenol adsorbed on the surface of fly-ash through water or hydrogen chloride elimination at surface oxide and hydroxyl sites leads to the formation of surface chlorophenolate. Electron transfer occurs between the chlorophenolate electron donors to the metal cation site through chemisorption that results in bound chlorophenoxyl radicals on the surface. Interaction between phenoxyl or chlorophenoxyl radicals on the surface of fly-ash assists the formation of PCDD/F.

Hazardous wastes contain chlorinated hydrocarbons (CHCs), form chlorinated phenols and chlorinated phenoxyl radicals that are isoelectronic with semiquinone radicals. Because each of these radicals has the potential to be environmentally persistent and biologically active, their formation and stabilization from various molecular precursors was studied with the focus on surface-bound radicals formed in association with combustion-generated fly-ash particles.

1.5 Approach to the Current Study of Semiquinone and Phenoxyl Radicals

Evaluation of PCDD/Fs from combustion sources has been a major environmental issue for many years. Phenol, chlorinated benzene and chlorinated phenols are the precursors for the formation of PCDD/Fs through phenoxyl radicals intermediates [116, 117, 119]. HQ and CT have been identified significantly as the product in combustion sources [73-82] and

a major organic components in mainstream cigarette smoke [44, 90-94]. They structurally similar to phenol with an extra hydroxyl group and are suspected to form semi-quinone and phenoxyl type radicals which in turn further form dioxin-type products. Thus, there is ample justification for the study of semiquinone-type and phenoxyl-type radicals in gas-phase and on the metal surface.

The study of the thermal degradation of HQ and CT helps to identify which persistent radical is formed during the thermal process. It also helps to understand the mechanism of dioxin formation as well as other poly aromatic hydrocarbon (PAH) products. This study reports the comprehensive products yield determination from the high temperature, gas-phase thermal degradation of HQ and CT under pyrolytic and oxidative condition.

If phenoxyl radicals are intermediate in PCDD/F formation on surface, they are probably bound-radicals on the surface of fly-ash. In order to investigate this hypothesis, six precursors including HQ, CT, P, 2-MCP, MCBz, and 1,2-DCBz were chemisorbed on the 5% copper oxide supported silica dioxide (CuO/SiO_2) surface by using vacuum and thermoelectric furnace system. Typical 5% CuO/SiO_2 surface was used as a surrogate of combustion generated fly-ash. Copper was chosen as the transition metal because it is easy to reduce to copper (I) and oxidize back to copper (II). Supported silicon dioxide with surface area of $500 m^2/g$ is similar to typical fly-ash combustion generated particles in any combustion system. After chemisorption of molecular precursors onto the CuO/SiO_2 surface, the samples were subjected to Electrons Paramagnetic Resonance (EPR) analysis to determine the nature and concentration of surface bound radicals. Samples were also

prepared for the toxicological testing on human epithelial cells by Dr. Stephania Cormier in the LSU Department of Biological Science.

Once bound-radicals bind on the surface, they may persist without being destroyed [6, 11]; however, they may be removable from the surface by some type of solvent extraction for. Various polar and non-polar solvents such as methyl alcohol (MEA), isopropyl alcohol (IPA), dichloromethane (DCM), toluene (TOL), and *tert*-butylbenzene (TBB) were used to investigate the extractability of surface-bound radicals. After extraction, the extracts and residues were separated and analyzed by EPR to determine any bound-radicals were still on the surface of the residue or that had been extracted into solvents. Lifetimes of radicals in the solution are very short, and they tend to react with molecular oxygen or hydrogen in the solution to convert into more stable molecules or they interact with each other to build up a bigger molecule. In order to identify the products of radical-radical interaction, the extracts were introduced immediately into a Gas Chromatograph Mass Spectrometer (GCMS) for chemical analysis.

1.6 References

1. Huffman, G. P.; Huggins, F. E.; Shah, N.; Huggins, R.; Linak, W. P.; Miller, C. A.; Pugmire, R. J.; Meuzelaar, H. L. C.; Seehra, M. S.; Manivannan, A., Characterization of fine particulate matter produced by combustion of residual fuel oil. *Journal of the Air & Waste Management Association* **2000,** 50, (7), 1106-1114.

2. Yan, L.; Gupta, R. P.; Wall, T. F., The implication of mineral coalescence behaviour on ash formation and ash deposition during pulverised coal combustion. *Fuel* **2001,** 80, (9), 1333-1340.

3. Chen, Y. Z.; Shah, N.; Huggins, F. E.; Huffman, G. P., Transmission electron microscopy investigation of ultrafine coal fly ash particles. *Environmental Science & Technology* **2005,** 39, (4), 1144-1151.

4. Dellinger, B.; Pryor, W. A.; Cueto, R.; Squadrito, G.; Deutsch, W. A., The role of combustion-generated radicals in the toxicity of PM2.5. *Proceedings of the Combustion Institute* **2000,** 28, 2675-2681.

5. Lomnicki, S.; Dellinger, B., A detailed mechanism of the surface-mediated formation of PCDD/F from the oxidation of 2-chlorophenol on a CuO/silica surface. *Journal of Physical Chemistry A* **2003,** 107, (22), 4387-4395.

6. Dellinger, B., Formation and Stabilization of Persistent Free Radicals. *Combustion Institute* **Accepted, 2006**.

7. Rodrigues, M. A.; Bemquerer, M. P.; Tada, D. B.; Bastos, E. L.; Baptista, M. S.; Politi, M. J., Synthesis and characterization of silica gel particles functionalized with bioactive materials. *Adsorption* **2005,** 11, (5/6), 595-602.

8. Hurrell, L.; Johnston, L. J.; Mathivanan, N.; Vong, D., Photochemistry of Lignin Model Compounds on Solid Supports. *Canadian Journal of Chemistry-Revue Canadienne De Chimie* **1993,** 71, (9), 1340-1348.

9. Pryor, W. A.; Hales, B. J.; Premovic, P. I.; Church, D. F., The Radicals in Cigarette Tar - Their Nature and Suggested Physiological Implications. *Science* **1983,** 220, (4595), 425-427.

10. Pryor, W. A.; Stone, K.; Zang, L. Y.; Bermudez, E., Fractionation of aqueous cigarette tar extracts: Fractions that contain the tar radical cause DNA damage. *Chemical Research in Toxicology* **1998,** 11, (5), 441-448.

11. Dellinger, B.; Pryor, W. A.; Cueto, R.; Squadrito, G. L.; Hegde, V.; Deutsch, W. A., Role of free radicals in the toxicity of airborne fine particulate matter. *Chemical Research in Toxicology* **2001,** 14, (10), 1371-1377.

12. Berho, F.; Lesclaux, R., The phenoxy radical: UV spectrum and kinetics of gas-phase reactions with itself and with oxygen. *Chemical Physics Letters* **1997,** 279, (5,6), 289-296.

13. Amlathe, S.; Upadhyay, S.; Gupta, V. K., Spectrophotometric Determination of Trace Amounts of Phenol in Waste-Water and Biological-Fluids. *Analyst* **1987,** 112, (10), 1463-1465.

14. Shariff, A. J.; Lowe, R. W.; Berthiaume, D.; Bryce, J. R. G.; Mclean, R. A. N., Unexpected Source of Phenol in the Sulfur-Free Semichemical Pulping of Hardwood. *Tappi Journal* **1989,** 72, (3), 177-183.

15. Luten, J. B.; Ritskes, J. M.; Weseman, J. M., Determination of Phenol, Guaiacol and 4-Methylguaiacol in Wood Smoke and Smoked Fish-Products by Gas-Liquid-Chromatography. *Zeitschrift Fur Lebensmittel-Untersuchung Und-Forschung* **1979,** 168, (4), 289-292.

16. Michalowicz, J.; Duda, R. O. W., Analysis of chlorophenols, chlorocatechols, chlorinated methoxyphenols and monoterpenes in communal sewage of Lodz and in the Ner River in 1999-2000. *Water Air and Soil Pollution* **2005,** 164, (1-4), 205-222.

17. Hogl, O., Some nonvolatile extracts of coffee. *Mitteilungen aus dem Gebiete der Lebensmitteluntersuchung und Hygiene* **1958,** 49, 433-41.

18. Varagnat, J., Hydroquinone, resorcinol, and catechol. *Kirk-Othmer Encycl. Chem. Technol., 3rd Ed.* **1981,** 13, 39-69.

19. Deichmann, W. B.; Keplinger, M. L., Industrial toxicology. Phenols and phenolic compounds. *Patty's Ind. Hyg. Toxicol. (3rd Revis. Ed.)* **1981,** 2A, 2567-627.

20. Hogan, M. E.; Manners, G. D., Allelopathy of Small Everlasting (Antennaria-Microphylla) Phytotoxicity to Leafy Spurge (Euphorbia-Esula) in Tissue-Culture. *Journal of Chemical Ecology* **1990,** 16, (3), 931-939.

21. Hogan, M. E.; Manners, G. D., Differential Allelochemical Detoxification Mechanism in Tissue-Cultures of Antennaria-Microphylla and Euphorbia-Esula. *Journal of Chemical Ecology* **1991,** 17, (1), 167-174.

22. Eisner, T.; Jones, T. H.; Hicks, K.; Silberglied, R. E.; Meinwald, J., Defense-Mechanisms of Arthropods .53. Quinones and Phenols in Defensive Secretions of Neotropical Opilionids. *Journal of Chemical Ecology* **1977,** 3, (3), 321-329.

23. Meinwald, J.; Jones, T. H.; Eisner, T.; Hicks, K., Defense-Mechanisms of Arthropods .56. New Methylcyclopentanoid Terpenes from Larval Defensive Secretion of a Chrysomelid Beetle (Plagiodera-Versicolora). *Proceedings of the National Academy of Sciences of the United States of America* **1977,** 74, (6), 2189-2193.

24. Hodgson, A. T.; Wooley, J. D. *Assessment of indoor concentrations, indoor sources and source emissions of selected volatile organic compounds*; Thomas J. Watson Res. Cent.,IBM,Yorktown Heights,NY,USA.: 1991; p 35 pp.

25. Jung, C. T.; Wickett, R. R.; Desai, P. B.; Bronaugh, R. L., In vitro and in vivo percutaneous absorption of catechol. *Food and Chemical Toxicology* **2003,** 41, (6), 885-895.

26. Meybeck, A. Pharmaceuticals or cosmetics containing hydroquinone - kojic acid mixtures encapsulated in liposomes or in lamellar lipid phases. 88-FR295, 8809659, 19880610., 1988.

27. Loblaw, J. C. High contrast photographic elements exhibiting reduced stress sensitivity. 86-109090, 209010, 19860703., 1987.

28. Yamane, K.; Noda, T. Support for photography. 95-111745, 08304961, 19950510., 1996.,29. Yurow, H. W. Photographic developer for direct production of equal density images on a high contrast film. 99-356536,6083671, 19990719., 2000.

30. Mattill, H. A.; Crawford, B., Autoxidation of corn oil as related to its unsaponifiable constituents. *Industrial and Engineering Chemistry* **1930,** 22, 341-344.

31. Nakamura, Y.; Torikai, K.; Ohigashi, H., A catechol antioxidant protocatechuic acid potentiates inflammatory leukocyte-derived oxidative stress in mouse skin via a tyrosinase bioactivation pathway. *Free Radical Biology and Medicine* **2001,** 30, (9), 967-978.

32. Justino, G. C.; Correia, C. F.; Mira, L.; Dos Santos, R. M. B.; Simoes, J. A. M.; Silva, A. M.; Santos, C.; Gigante, B., Antioxidant activity of a catechol derived from abietic acid. *Journal of Agricultural and Food Chemistry* **2006,** 54, (2), 342-348.

33. Hecht, S. S.; Carmella, S.; Mori, H.; Hoffmann, D., A Study of Tobacco Carcinogenesis .20. Role of Catechol as a Major Cocarcinogen in the Weakly Acidic Fraction of Smoke Condensate. *Journal of the National Cancer Institute* **1981,** 66, (1), 163-169.

34. Daisey, J. M.; Mahanama, K. R. R.; Hodgson, A. T., Toxic volatile organic compounds in simulated environmental tobacco smoke: Emission factors for exposure assessment. *Journal of Exposure Analysis and Environmental Epidemiology* **1998,** 8, (3), 313-334.

35. Bruce, R. M.; Santodonato, J.; Neal, M. W., Summary Review of the Health-Effects Associated with Phenol. *Toxicology and Industrial Health* **1987,** 3, (4), 535-568.

36. Flickinger, C. W., Benzenediols - Catechol, Resorcinol and Hydroquinone - Review of Industrial Toxicology and Current Industrial Exposure Limits. *American Industrial Hygiene Association Journal* **1976,** 37, (10), 596-606.

37. Leanderson, P.; Tagesson, C., Cigarette Smoke-Induced DNA-Damage - Role of Hydroquinone and Catechol in the Formation of the Oxidative DNA-Adduct, 8-Hydroxydeoxyguanosine. *Chemico-Biological Interactions* **1990,** 75, (1), 71-81.

38. Bilimoria, M. H., Detection of Mutagenic Activity of Chemicals and Tobacco-Smoke in a Bacterial System. *Mutation Research* **1975,** 31, (5), 328-328.

39. Leanderson, P.; Tagesson, C., Cigarette Smoke-Induced DNA Damage in Cultured Human Lung-Cells - Role of Hydroxyl Radicals and Endonuclease Activation. *Chemico-Biological Interactions* **1992,** 81, (1-2), 197-208.

40. Wierda, D.; Irons, R. D., Hydroquinone and Catechol Reduce the Frequency of Progenitor Lymphocytes-B in Mouse Spleen and Bone-Marrow. *Immunopharmacology* **1982,** 4, (1), 41-54.

41. King, A. G.; Landreth, K. S.; Wierda, D., Hydroquinone Inhibits Bone-Marrow Pre-B Cell Maturation Invitro. *Molecular Pharmacology* **1987,** 32, (6), 807-812.

42. Gaido, K. W.; Wierda, D., Suppression of Bone-Marrow Stromal Cell-Function by Benzene and Hydroquinone Is Ameliorated by Indomethacin. *Toxicology and Applied Pharmacology* **1987,** 89, (3), 378-390.

43. Warner, M. A.; Harper, J. V., Cardiac Dysrhythmias Associated with Chemical Peeling with Phenol. *Anesthesiology* **1985,** 62, (3), 366-367.

44. McCue, J. M.; Link, K. L.; Eaton, S. S.; Freed, B. M., Exposure to cigarette tar inhibits ribonucleotide reductase and blocks lymphocyte proliferation. *Journal of Immunology* **2000,** 165, (12), 6771-6775.

45. McCue, J. M.; Lazis, S.; Cohen, J. J.; Modiano, J. F.; Freed, B. M., Hydroquinone and catechol interfere with T cell cycle entry and progression through the G(1) phase. *Molecular Immunology* **2003,** 39, (16), 995-1001.

46. Li, Q.; Aubrey, M. T.; Christian, T.; Freed, B. M., Differential inhibition of DNA synthesis in human T cells by the cigarette tar components hydroquinone and catechol. *Fundamental and Applied Toxicology* **1997,** 38, (2), 158-165.

47. Squadrito, G. L.; Cueto, R.; Dellinger, B.; Pryor, W. A., Quinoid redox cycling as a mechanism for sustained free radical generation by inhaled airborne particulate matter. *Free Radical Biology and Medicine* **2001,** 31, (9), 1132-1138.

48. Hirakawa, K.; Oikawa, S.; Hiraku, Y.; Hirosawa, I.; Kawanishi, S., Catechol and hydroquinone have different redox properties responsible for their differential DNA-damaging ability. *Chemical Research in Toxicology* **2002,** 15, (1), 76-82.

49. Maskos, Z.; Khachatryan, L.; Dellinger, B., Precursors of radicals in tobacco smoke and the role of particulate matter in forming and stabilizing radicals. *Energy & Fuels* **2005,** 19, (6), 2466-2473.

50. Cormier, S. A.; Lomnicki, S.; Backes, W.; Dellinger, B., Origin and health impacts of emissions of toxic by-products and fine particles from combustion and thermal treatment of hazardous wastes and materials. *Environmental Health Perspectives* **2006,** 114, (6), 810-817.

51. Gopalakrishna, R.; Chen, Z. H.; Gundimeda, U., Tobacco-Smoke Tumor Promoters, Catechol and Hydroquinone, Induce Oxidative Regulation of Protein-Kinase-C and Influence Invasion and Metastasis of Lung-Carcinoma Cells. *Proceedings of the National Academy of Sciences of the United States of America* **1994,** 91, (25), 12233-12237.

52. Marsh, J. P.; Mossman, B. T., Role of Asbestos and Active Oxygen Species in Activation and Expression of Ornithine Decarboxylase in Hamster Tracheal Epithelial-Cells. *Cancer Research* **1991,** 51, (1), 167-173.

53. Kensler, T. W.; Trush, M. A., Role of Oxygen Radicals in Tumor Promotion. *Environmental Mutagenesis* **1984,** 6, (4), 593-616.

54. Cerutti, P. A., Prooxidant States and Tumor Promotion. *Science* **1985,** 227, (4685), 375-381.

55. Asami, S.; Manabe, H.; Miyake, J.; Tsurudome, Y.; Hirano, T.; Yamaguchi, R.; Itoh, H.; Kasai, H., Cigarette smoking induces an increase in oxidative DNA damage, 8-hydroxydeoxyguanosine, in a central site of the human lung. *Carcinogenesis* **1997,** 18, (9), 1763-1766.

56. Leonard, S. S.; Wang, S. W.; Shi, X. L.; Jordan, B. S.; Castranova, V.; Dubick, M. A., Wood smoke particles generate free radicals and cause lipid peroxidation, DNA damage, NF kappa B activation and TNF-alpha release in macrophages. *Toxicology* **2000,** 150, (1-3), 147-157.

57. Lisitsyna, T. A.; Vasil'eva, I. M.; Durnev, A. D.; Zasukhina, G. D.; Seredenin, S. V., Free radicals and the DNA Damage repair in the repair-deficient human cells. *Doklady Akademii Nauk* **1999,** 365, (2), 263-266.

58. Kleeman, M. J.; Schauer, J. J.; Cass, G. R., Size and composition distribution of fine particulate matter emitted from motor vehicles. *Environmental Science & Technology* **2000,** 34, (7), 1132-1142.

59. Kleeman, M. J.; Schauer, J. J.; Cass, G. R., Size and composition distribution of fine particulate matter emitted from wood burning, meat charbroiling, and cigarettes. *Environmental Science & Technology* **1999,** 33, (20), 3516-3523.

60. Okeson, C. D.; Riley, M. R.; Fernandez, A.; Wendt, J. O. L., Impact of the composition of combustion generated fine particles on epithelial cell toxicity: influences of metals on metabolism. *Chemosphere* **2003,** 51, (10), 1121-1128.

61. Chen, Y. Z.; Shah, N.; Huggins, F. E.; Huffman, G. P., Investigation of the microcharacteristics of PM2.5 in residual oil fly ash by analytical transmission electron microscopy. *Environmental Science & Technology* **2004,** 38, (24), 6553-6560.

62. Linak, W. P.; Miller, C. A., Comparison of particle size distributions and elemental partitioning from the combustion of pulverized coal and residual fuel oil. *Journal of the Air & Waste Management Association* **2000,** 50, (8), 1532-1544.

63. Nemmar, A.; Vanbilloen, H.; Hoylaerts, M. F.; Hoet, P. H. M.; Verbruggen, A.; Nemery, B., Passage of intratracheally instilled ultrafine particles from the lung into the

systemic circulation in hamster. *American Journal of Respiratory and Critical Care Medicine* **2001,** 164, (9), 1665-1668.

64. Calderon-Garciduenas, L.; Mora-Tiscareno, A.; Fordham, L. A.; Chung, C. J.; Garcia, R.; Osnaya, N.; Hernandez, J.; Acuna, H.; Gambling, T. M.; Villarreal-Calderon, A.; Carson, J.; Koren, H. S.; Devlin, B., Canines as sentinel species for assessing chronic exposures to air pollutants: Part 1. Respiratory pathology. *Toxicological Sciences* **2001,** 61, (2), 342-355.

65. Calderon-Garciduenas, L.; Gambling, T. M.; Acuna, H.; Garcia, R.; Osnaya, N.; Monroy, S.; Villarreal-Calderon, A.; Carson, J.; Koren, H. S.; Devlin, R. B., Canines as sentinel species for assessing chronic exposures to air pollutants: Part 2. cardiac pathology. *Toxicological Sciences* **2001,** 61, (2), 356-367.

66. Carter, J. D.; Ghio, A. J.; Samet, J. M.; Devlin, R. B., Cytokine production by human airway epithelial cells after exposure to an air pollution particle is metal-dependent. *Toxicology and Applied Pharmacology* **1997,** 146, (2), 180-188.

67. Boezen, M.; Schouten, J.; Rijcken, B.; Vonk, J.; Gerritsen, J.; van der Zee, S.; Hoek, G.; Brunekreef, B.; Postma, D., Peak expiratory flow variability, bronchial responsiveness, and susceptibility to ambient air pollution in adults. *American Journal of Respiratory and Critical Care Medicine* **1998,** 158, (6), 1848-1854.

68. Schwartz, J., What Are People Dying of on High Air-Pollution Days. *Environmental Research* **1994,** 64, (1), 26-35.

69. Kodavanti, U. P.; Moyer, C. F.; Ledbetter, A. D.; Schladweiler, M. C.; Costa, D. L.; Hauser, R.; Christiani, D. C.; Nyska, A., Inhaled environmental combustion particles cause myocardial injury in the Wistar Kyoto rat. *Toxicological Sciences* **2003,** 71, (2), 237-245.

70. Gordon, T.; Nadziejko, C.; Schlesinger, R.; Chen, L. C., Pulmonary and cardiovascular effects of acute exposure to concentrated ambient particulate matter in rats. *Toxicology Letters* **1998,** 96-7, 285-288.

71. Nolte, C. G.; Schauer, J. J.; Cass, G. R.; Simoneit, B. R. T., Highly polar organic compounds present in wood smoke and in the ambient atmosphere. *Environmental Science & Technology* **2001,** 35, (10), 1912-1919.

72. Troughton, G. E.; Manville, J. F.; Chow, S. Z., Lignin utilization. II. Resin properties of 4-alkyl-substituted catechol compounds. *Forest Products Journal* **1972,** 22, (9), 108-10.

73. Font, R.; Esperanza, M.; Garcia, A. N., Toxic by-products from the combustion of Kraft lignin. *Chemosphere* **2003,** 52, (6), 1047-1058.

74. Simoneit, B. R. T., Biomass burning - A review of organic tracers for smoke from incomplete combustion. *Applied Geochemistry* **2002,** 17, (3), 129-162.

75. Hays, M. D.; Fine, P. M.; Geron, C. D.; Kleeman, M. J.; Gullett, B. K., Open burning of agricultural biomass: Physical and chemical properties of particle-phase emissions. *Atmospheric Environment* **2005,** 39, (36), 6747-6764.

76. Visser, R.; Harbers, A. A. M.; Hovestad, A.; Stevens, T. W., Identification of organic compounds in waste water of wood gasifiers with capillary gas chromatography. *Proc. Int. Symp. Capillary Chromatogr., 6th* **1985**, 281-7.

77. Fine, P. M.; Cass, G. R.; Simoneit, B. R. T., Chemical characterization of fine particle emissions from the fireplace combustion of wood types grown in the Midwestern and Western United States. *Environmental Engineering Science* **2004,** 21, (3), 387-409.

78. Fine, P. M.; Cass, G. R.; Simoneit, B. R. T., Chemical characterization of fine particle emissions from fireplace combustion of woods grown in the northeastern United States. *Environmental Science & Technology* **2001,** 35, (13), 2665-2675.

79. Sheesley, R. J.; Schauer, J. J.; Chowdhury, Z.; Cass, G. R.; Simoneit, B. R. T., Characterization of organic aerosols emitted from the combustion of biomass indigenous to South Asia. *Journal of Geophysical Research-Atmospheres* **2003,** 108, (D9), -.

80. Wroblewski, A. E.; Lensink, C.; Markuszewski, R.; Verkade, J. G., P-31 Nmr Spectroscopic Analysis of Coal Pyrolysis Condensates and Extracts for Heteroatom Functionalities Possessing Labile Hydrogen. *Energy & Fuels* **1988,** 2, (6), 765-774.

81. Gagarin, S. G.; Gladun, T. G., Evaluation of the formation enthalpy of the organic matter of brown coals. *Khimiya Tverdogo Topliva (Moscow, Russian Federation)* **2002**, (5), 11-21.

82. Rayalu, S. S.; Kumaran, P.; Rao, K. S. M., Chemical transformation of phenolics in coal carbonization wastewater. *Indian Journal of Environmental Protection* **1992,** 12, (3), 210-18.

83. Cho, A. K.; Di Stefano, E.; You, Y.; Rodriguez, C. E.; Schmitz, D. A.; Kumagai, Y.; Miguel, A. H.; Eiguren-Fernandez, A.; Kobayashi, T.; Avol, E.; Froines, J. R., Determination of four quinones in diesel exhaust particles, SRM 1649a, an atmospheric PM2.5. *Aerosol Science and Technology* **2004,** 38, 68-81.

84. Fine, P. M.; Cass, G. R.; Simoneit, B. R. T., Chemical characterization of fine particle emissions from the fireplace combustion of woods grown in the southern United States. *Environmental Science & Technology* **2002,** 36, (7), 1442-1451.

85. Hays, M. D.; Geron, C. D.; Linna, K. J.; Smith, N. D.; Schauer, J. J., Speciation of gas-phase and fine particle emissions from burning of foliar fuels. *Environmental Science & Technology* **2002,** 36, (11), 2281-2295.

86. Simpson, C. D.; Paulsen, M.; Dills, R. L.; Liu, L. J. S.; Kalman, D. A., Determination of methoxyphenols in ambient atmospheric particulate matter: Tracers for wood combustion. *Environmental Science & Technology* **2005,** 39, (2), 631-637.

87. Schauer, J. J.; Kleeman, M. J.; Cass, G. R.; Simoneit, B. R. T., Measurement of emissions from air pollution sources. 3. C-1-C-29 organic compounds from fireplace combustion of wood. *Environmental Science & Technology* **2001,** 35, (9), 1716-1728.

88. Hawthorne, S. B.; Krieger, M. S.; Miller, D. J.; Mathiason, M. B., Collection and Quantitation of Methoxylated Phenol Tracers for Atmospheric-Pollution from Residential Wood Stoves. *Environmental Science & Technology* **1989,** 23, (4), 470-475.

89. Rogge, W. F.; Hildemann, L. M.; Mazurek, M. A.; Cass, G. R.; Simoneit, B. R. T., Sources of fine organic aerosol. 9. Pine, oak and synthetic log combustion in residential fireplaces. *Environmental Science & Technology* **1998,** 32, (1), 13-22.

90. Lee, M. R.; Jeng, J. E.; Hsiang, W. S.; Hwang, B. H., Determination of pyrolysis products of smoked methamphetamine mixed with tobacco by tandem mass spectrometry. *Journal of Analytical Toxicology* **1999,** 23, (1), 41-45.

91. Schlotzhauer, W. S.; Walters, D. B.; Snook, M. E.; Higman, H. C., Characterization of Catechols, Resorcinols, and Hydroquinones in an Acidic Fraction of Cigarette-Smoke Condensate. *Journal of Agricultural and Food Chemistry* **1978,** 26, (6), 1277-1288.

92. Carmella, S. G.; Hecht, S. S.; Tso, T. C.; Hoffmann, D., Chemical Studies on Tobacco-Smoke .77. Roles of Tobacco Cellulose, Sugars, and Chlorogenic Acid as Precursors to Catechol in Cigarette-Smoke. *Journal of Agricultural and Food Chemistry* **1984,** 32, (2), 267-273.

93. Kallianos, A. G.; Means, R. E.; Mold, J. D., Effect of nitrates in tobacco on the catechol yield in cigaret smoke. *Tobacco Science* **1968,** 12, 125-9.

94. Schlotzhauer, W. S.; Martin, R. M.; Snook, M. E.; Williamson, R. E., Pyrolytic Studies on the Contribution of Tobacco Leaf Constituents to the Formation of Smoke Catechols. *Journal of Agricultural and Food Chemistry* **1982,** 30, (2), 372-374.

95. Talbot, P.; DiCarlantonio, G.; Knoll, M.; Gomez, C., Identification of cigarette smoke components that alter functioning of hamster (Mesocricetus auratus) oviducts in vitro. *Biology of Reproduction* **1998,** 58, (4), 1047-1053.

96. Riveles, K.; Roza, R.; Talbot, P., Phenols, quinolines, indoles, benzene, and 2-cyclopenten-1-ones are oviductal toxicants in cigarette smoke. *Toxicological Sciences* **2005,** 86, (1), 141-151.

97. Schauer, J. J.; Kleeman, M. J.; Cass, G. R.; Simoneit, B. R. T., Measurement of emissions from air pollution sources. 5. C-1-C-32 organic compounds from gasoline-powered motor vehicles. *Environmental Science & Technology* **2002,** 36, (6), 1169-1180.

98. Valavanidis, A.; Fiotakis, K.; Vlahogianni, T.; Papadimitriou, V.; Pantikaki, V., Determination of selective quinones and quinoid radicals in airborne particulate matter and vehicular exhaust particles (vol 3, pg 118, 2006). *Environmental Chemistry* **2006,** 3, (3), 233-U12.

99. Jakober, C. A.; Riddle, S. G.; Robert, M. A.; Destaillats, H.; Charles, M. J.; Green, P. G.; Kleeman, M. J., Quinone Emissions from Gasoline and Diesel Motor Vehicles. *Environmental Science & Technology*, ACS ASAP.

100. Ledesma, E. B.; Marsh, N. D.; Sandrowitz, A. K.; Wornat, M. J., An experimental study on the thermal decomposition of catechol. *Proceedings of the Combustion Institute* **2003,** 29, 2299-2306.

101. Khachatryan, L.; Adounkpe, J.; Maskos, Z.; Dellinger, B., Formation of cyclopentadienyl radical from the gas-phase pyrolysis of hydroquinone, catechol, and phenol. *Environmental Science & Technology* **2006,** 40, (16), 5071-5076.

102. Farquar, G. R.; Alderman, S. L.; Poliakoff, E. D.; Dellinger, B., X-ray spectroscopic studies of the high temperature reduction of Cu(II)0 by 2-chlorophenol on a simulated fly ash surface. *Environmental Science & Technology* **2003,** 37, (5), 931-935.

103. Dellinger, B.; Lomnicki, S.; Khachatryan, L.; Maskos, Z.; Hall, R. W.; Adounkpe, J.; McFerrin, C.; Truong, H., Formation and stabilization of persistent free radicals. *Proceedings of the Combustion Institute* **2007,** 31, (Pt. 1), 521-528.

104. Lin, C. Y.; Lin, M. C., Unimolecular Decomposition of the Phenoxy Radical in Shock-Waves. *International Journal of Chemical Kinetics* **1985,** 17, (10), 1025-1028.

105. Lovell, A. B.; Brezinsky, K.; Glassman, I., The Gas-Phase Pyrolysis of Phenol. *International Journal of Chemical Kinetics* **1989,** 21, (7), 547-560.

106. Brezinsky, K.; Pecullan, M.; Glassman, I., Pyrolysis and oxidation of phenol. *Journal of Physical Chemistry A* **1998,** 102, (44), 8614-8619.

107. Cooke, S.; Labes, M. M., Destruction of the Environmentally Hazardous Monochlorinated Phenols Via Pyrolysis in an Inert Atmosphere. *Carbon* **1994,** 32, (6), 1055-1058.

108. Black, G.; Jusinski, L. E., Radiative Lifetimes of the V'3 = 0, 1, and 2 Levels of Ch3s(A2a1). *Journal of Chemical Physics* **1986,** 85, (9), 5379-5380.

109. Falvey, D. E.; Schuster, G. B., Picosecond Time Scale Dynamics of Perester Photodecomposition - Evidence for an Acyloxy Radical Intermediate in the Photolysis of

Tert-Butyl 9-Methylfluorene-9-Percarboxylate. *Journal of the American Chemical Society* **1986,** 108, (23), 7419-7420.

110. Okamura, T.; Tanaka, I., Radiative Lifetimes of Benzyl, Deuterated Benzyl, and Methyl-Substituted Benzyl Radicals. *Journal of Physical Chemistry* **1975,** 79, (25), 2728-2731.

111. Mohapatra, R.; Rao, J. R., Some aspects of characterisation, utilisation and environmental effects of fly ash. *Journal of Chemical Technology and Biotechnology* **2001,** 76, (1), 9-26.

112. Safe, S., Polychlorinated-Biphenyls (Pcbs), Dibenzo-Para-Dioxins (Pcdds), Dibenzofurans (Pcdfs), and Related-Compounds - Environmental and Mechanistic Considerations Which Support the Development of Toxic Equivalency Factors (Tefs). *Critical Reviews in Toxicology* **1990,** 21, (1), 51-88.

113. Silbergeld, E. K.; Mattison, D. R., Experimental and Clinical-Studies on the Reproductive Toxicology of 2,3,7,8-Tetrachlorodibenzo-P-Dioxin. *American Journal of Industrial Medicine* **1987,** 11, (2), 131-144.

114. Sidhu, S. S.; Maqsud, L.; Dellinger, B.; Mascolo, G., The Homogeneous, Gas-Phase Formation of Chlorinated and Brominated Dibenzo-P-Dioxin from 2,4,6-Trichlorophenols and 2,4,6-Tribromophenols. *Combustion and Flame* **1995,** 100, (1-2), 11-20.

115. Wiater-Protas, I.; Louw, R., Gas-phase chemistry of chlorinated phenols - Formation of dibenzofurans and dibenzodioxins in slow combustion. *European Journal of Organic Chemistry* **2001**, (20), 3945-3952.

116. Born, J. G. P.; Louw, R.; Mulder, P., Formation of Dibenzodioxins and Dibenzofurans in Homogenous Gas-Phase Reactions of Phenols. *Chemosphere* **1989,** 19, (1-6), 401-406.

117. Weber, R.; Hagenmaier, H., Mechanism of the formation of polychlorinated dibenzo-p-dioxins and dibenzofurans from chlorophenols in gas phase reactions. *Chemosphere* **1999,** 38, (3), 529-549.

118. Khachatryan, L.; Asatryan, R.; Dellinger, B., Development of expanded and core kinetic models for the gas phase formation of dioxins from chlorinated phenols. *Chemosphere* **2003,** 52, (4), 695-708.

119. Louw, R.; Ahonkhai, S. I., Radical/radical vs radical/molecule reactions in the formation of PCDD/Fs from (chloro)phenols in incinerators. *Chemosphere* **2002,** 46, (9-10), 1273-1278.

120. Mulholland, J. A.; Akki, U.; Yang, Y.; Ryu, J. Y., Temperature dependence of DCDD/F isomer distributions from chlorophenol precursors. *Chemosphere* **2001,** 42, (5-7), 719-727.

121. Altwicker, E. R., Some Laboratory Experimental-Designs for Obtaining Dynamic Property Data on Dioxins. *Science of the Total Environment* **1991,** 104, (1-2), 47-72.

122. Stieglitz, L., Selected topics on the de novo synthesis of PCDD/PCDF on fly ash. *Environmental Engineering Science* **1998,** 15, (1), 5-18.

123. Hsiao, M. C.; Wang, H. P.; Huang, Y. J.; Yang, Y. W., EXAFS study of copper in waste incineration fly ashes. *Journal of Synchrotron Radiation* **2001,** 8, 931-933.

124. Hagenmaier, H.; Brunner, H.; Haag, R.; Kraft, M., Copper-Catalyzed Dechlorination Hydrogenation of Polychlorinated Dibenzo-Para-Dioxins, Polychlorinated Dibenzofurans, and Other Chlorinated Aromatic-Compounds. *Environmental Science & Technology* **1987,** 21, (11), 1085-1088.

125. Hagenmaier, H.; Kraft, M.; Brunner, H.; Haag, R., Catalytic Effects of Fly-Ash from Waste Incineration Facilities on the Formation and Decomposition of Polychlorinated Dibenzo-Para-Dioxins and Polychlorinated Dibenzofurans. *Environmental Science & Technology* **1987,** 21, (11), 1080-1084.

126. Born, J. G. P.; Louw, R.; Mulder, P., Fly-Ash Mediated (Oxy)Chlorination of Phenol and Its Role in Pcdd/F Formation. *Chemosphere* **1993,** 26, (12), 2087-2095.

127. Ryu, J. Y.; Mulholland, J. A., Metal-mediated chlorinated dibenzo-p-dioxin (CDD) and dibenzofuran (CDF) formation from phenols. *Chemosphere* **2005,** 58, (7), 977-988.

128. Evans, C. S.; Dellinger, B., Mechanisms of dioxin formation from the high-temperature oxidation of 2-chlorophenol. *Environmental Science & Technology* **2005,** 39, (1), 122-127.

129. Evans, C. S.; Dellinger, B., Mechanisms of dioxin formation from the high-temperature pyrolysis of 2-chlorophenol. *Environmental Science & Technology* **2003,** 37, (7), 1325-1330.

130. Addink, R.; Olie, K., Role of Oxygen in Formation of Polychlorinated Dibenzo-P-Dioxins/Dibenzofurans from Carbon on Fly-Ash. *Environmental Science & Technology* **1995,** 29, (6), 1586-1590.

CHAPTER 2: EXPERIMENTAL

2.1 System for Thermal Diagnostic Studies

2.1.1 Description

The System for Thermal Diagnostic Studies (STDS) is a high-temperature, flow reactor analytical system that provides flexibility and versatility for conducting a broad range of thermal related studies [1-3]. This system is ideal for the study of thermal decomposition analysis of various organic materials from hazardous waste incineration. There are four main component units: the control instrumentation console, a thermal reactor compartment, a cryogenic trapping, analysis equipments for effluent analyzes that make up the whole STDS as shown in **figure 2.1**.

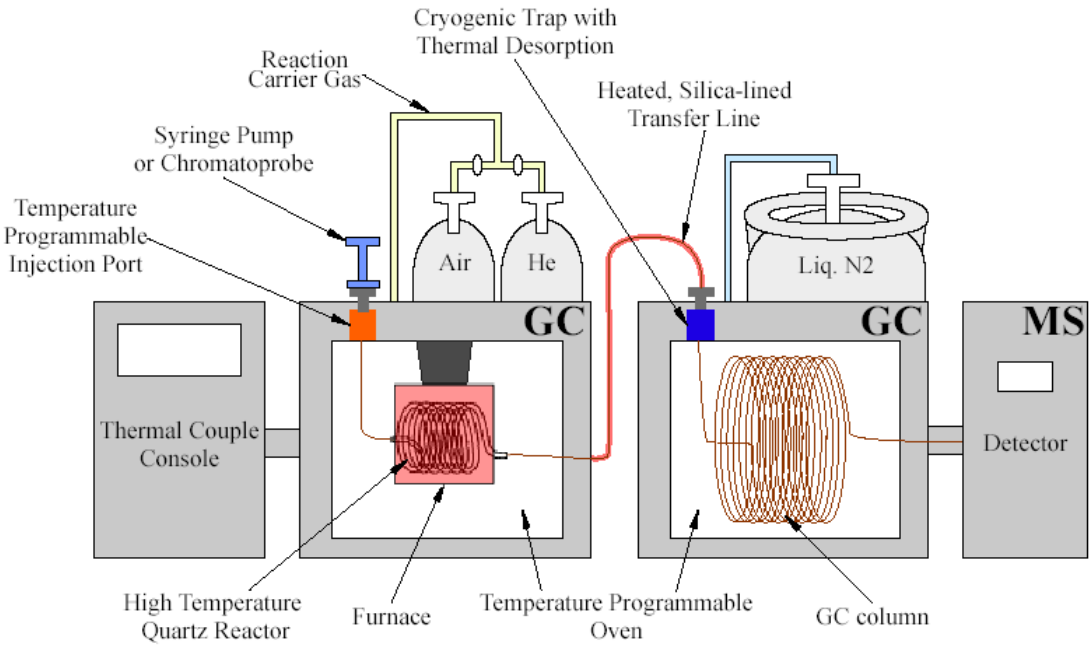

Figure 2.1: System for Thermal Diagnostic Studies

The STDS consists of a high temperature fused silica flow reactor placed inside a high temperature furnace that is controlled by a separate temperature controller with maximum operating temperature of 1200°C (c.f. **Figure 2.2**). This furnace is housed inside the thermal reactor compartment that is a gas chromatograph (GC) oven (Varian, CP 3800). Basically, this GC is just an oven and it is designed to act as a temperature control that maintain the temperature of all connection and the lines coming from the injection port to the reactor and the line going from the reactor to the heated transfer line. The temperature inside this thermal reactor compartment was controlled at constant temperature of 200°C to facilitate transport of gas-phase reactants and products.

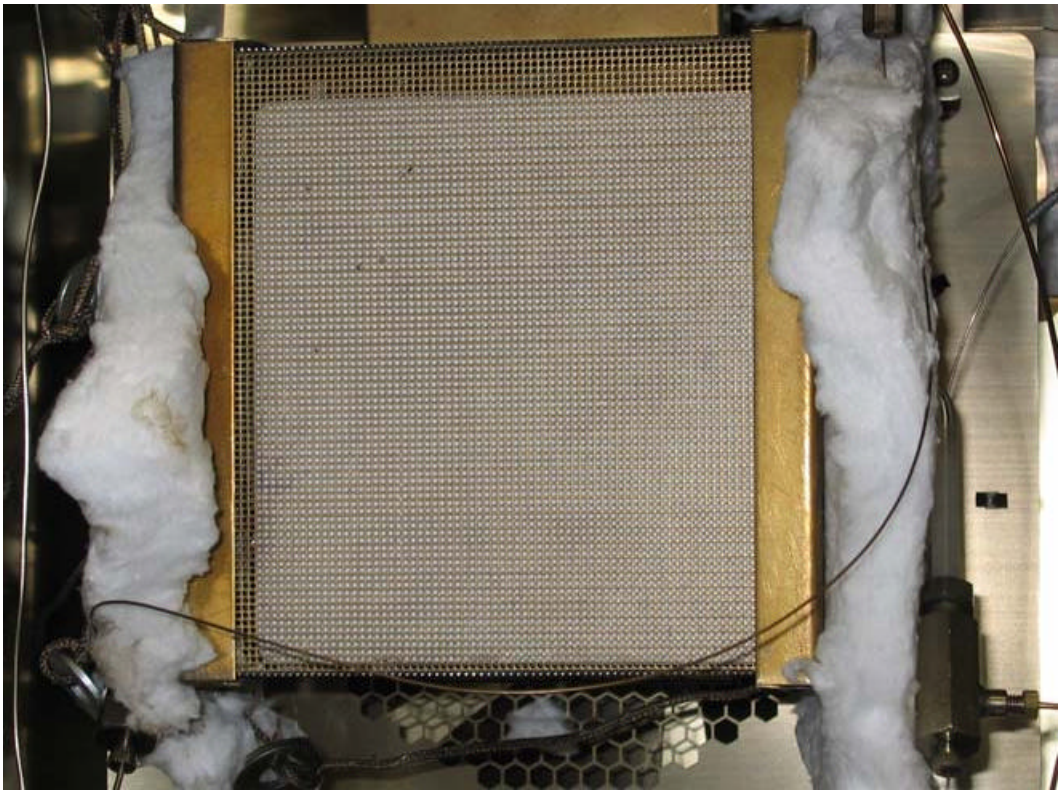

Figure 2.2: High Temperature Furnace

The flow reactor is made of quartz that is stable at very high temperature up to 1200^{o}C and typically is designed for the purpose of studying the thermal decomposition of organic material (c.f. **Figure 2.3**). It has a length of 35 cm and 1 cm inside diameter and is helically shaped in order to maximize the distance for gas-phase sample traveling in a short length of the furnace. The volume of this flow reactor is 2.7 x 10^{-5} m^3.

Figure 2.3: Quartz Flow-Reactor

All of the connections to the quartz flow-reactor are composed of fused silica to maintain an inert atmosphere. Helium is the gas carrier for pyrolytic condition while the mixture of helium-oxygen is the gas carrier for oxidative condition. The gas carrier was controlled by a digital mass flow controller (McMillan, model 80D) to maintain a constant residence time inside the reactor. A Chromatoprobe® (Varian) was also used to introduce

solid samples into the system. A Chromatoprobe® is a solid phase vaporizer that is inserted into injection port of the thermal reactor compartment reactor. It has a precisely programmable temperature controller to maintain constant concentration of vapors from solid samples. Pure solid samples were placed into the quartz micro-vial at the bottom of the chromatoprobe shaft. The temperature of injection in the chormatoprobe was programmed in order to maintain a constant gas-phase concentration of sample inside the flow-reactor.

A digital syringe pump (Kd Scientific, model 100) was used to maintain a constant rate flow of liquid sample into injection port of the thermal reactor compartment that help to maintain a constant initial concentration of sample inside the flow-reactor. The injection port contained a quartz tube to maintain an inert atmosphere inside the STDS. This injection port has the temperature controller to vaporize all of liquid sample before entering the flow-reactor.

The flow-reactor effluent is transported through a heated, temperature-controlled transfer line (deactivated silica lined stainless steel tube) where it is trapped cryogenically at the head of the capillary column of Gas Chromatograph Mass Spectrometer (GC-MS) system (Varian, Saturn 2000). The temperature controller in the transfer line maintains a reasonable temperature to ensure transport of gas-phase products without thermal degradation. Additionally, there is a splitter in the transfer line to delivery only small amount of sample to the GC-MS system without damage to the detector. Also, the splitter helps to maintain the constant pressure around 1.0 atm inside the flow-reactor. This splitter is controlled by a needle valve and pressure gauge. The effluent of the splitter flowed through a charcoal trap and out to a fume hood.

Liquid nitrogen is used to cryogenically trap gas-phase products at the head of the 30m long, 0.25mm id., 0.25µm film thickness capillary column (Restek, Rtx®-5MS) inside GC (Varian, CP 3800). Initially, all the products were trapped in the head of capillary column at the temperature of -60°C, followed by temperature programmed ramping of the column from –60°C to 300°C at 15°C/min. Separated products with molecular weights from 40 to 650amu were analyzed with a Mass Spectrometer (MS) operating in the full-scan mode. The mass-spectral library (NIST 98 version 1.6d) was used to identify the products.

2.1.2 Experimental Set-Up

A 2.0 seconds gas residence time [4] was designed to use for all experiments. Equation 1[4] was used to calculate the rate of the main flow need to maintain the residence time of 2.0 seconds inside the flow-reactor; where $\bar{t}_r$ (seconds) is the mean residence time distribution for gas-phase molecules passing through a flow-reactor; T_o (Kelvin, K) is ambient temperature; T_e (Kelvin, K) is average exposure temperature within the flow-reactor; V_E (m^3) is effective volume of the flow-reactor; F_o (m^3/s) is volumetric flow rate; P_o (atm) is ambient pressure; P_d (atm) is positive differential pressure relative to P_o within the flow-reactor. **Table 2.1** shows the main flow rate base on the **equation 1**. Pure helium gas was used as a gas carrier for pyrolytic conditions and the mixture 80% of helium and 20% of oxygen was used as a gas carrier for oxidative conditions for all thermal degradation of HQ and CT.

$$\bar{t}_r = \left(\frac{T_o}{T_e}\right)\left(\frac{V_E}{F_o}\right)\left(1+\frac{P_d}{P_o}\right) \qquad \text{(Equation 1)}$$

Table 2.1 Total Flow Rate Vary with Temperature inside the Furnace

Temperature (°C)	Temperature (°K)	Flow Rate (mL/min)
200	473	586.9
250	523	530.8
300	573	484.4
350	623	445.6
400	673	412.5
450	723	383.9
500	773	359.1
550	823	337.3
600	873	318.0
650	923	300.7
700	973	285.3
725	998	278.1
750	1023	271.3
775	1048	264.9
800	1073	258.7
825	1098	252.8
850	1123	247.2
875	1148	241.8
900	1173	236.6
925	1198	231.7
950	1223	227.0
975	1248	222.4
1000	1273	218.1

HQ and CT are polar solids; therefore, isopropyl alcohol was chosen as the solvent. The molarity of the solution was 1.0 M and the volume of sample HQ or CT that injected into the STDS was chosen to be 1.0 µL. The density of isopropyl alcohol is 0.781 g/mL that means in 1.0 µL of 1.0 M solution, there are 0.781 mg of isopropyl alcohol and 0.110 mg of HQ or CT. As the result, the sample contains 12% HQ or CT by mass in the solution. The concentration of the solution in gas-phase inside the reactor was selected to be 500 ppm; thus the concentration of HQ or CT is 60 ppm and isopropyl alcohol is 440 ppm.

In order to maintain a constant concentration of sample inside the reactor, a syringe pump was used to control the flow rate of the sample injection into the STDS. The

injection rate for the sample was determined based on the main flow rate of the gas carrier through the flow-reactor. The concentration of the solution is 500 ppm (gas-phase), thus the ratio of the injection flow rate (F_{inj}) in gas-phase to the helium flow rate (F_o) should be 500 ppm for all temperature inside the furnace. From the volume of sample injection, the time and the injection flow-rate can be obtained from **table 2.2**. The injection port was operated at the temperature of 180°C to vaporize all of liquid sample before entering the flow-reactor.

Table 2.2 Time and Injection Rate Vary with Temperature inside the Furnace

Temperature (°C)	Temperature (°K)	Injection Time (min)	Injection Rate (µL/hr)
200	473	1.0	60.5
250	523	1.1	54.7
300	573	1.2	49.9
350	623	1.3	45.9
400	673	1.4	42.5
450	723	1.5	39.6
500	773	1.6	37.0
550	823	1.7	34.7
600	873	1.8	32.8
650	923	1.9	31.0
700	973	2.0	29.4
725	998	2.1	28.7
750	1023	2.1	28.0
775	1048	2.2	27.3
800	1073	2.3	26.7
825	1098	2.3	26.0
850	1123	2.4	25.5
875	1148	2.4	24.9
900	1173	2.5	24.4
925	1198	2.5	23.9
950	1223	2.6	23.4
975	1248	2.6	22.9
1000	1273	2.7	22.5

The vaporizer chormatoprobe was used to introduce pure HQ or CT into STDS. The main flow rate of helium carrier gas was operated varying with temperature inside the

furnace in table 1 to maintain a residence time of 2 seconds inside the flow-reactor. The injection port was operated at the temperature of 90°C for HQ and 80°C for CT to maintain a constant concentration of 35ppm inside the flow-reactor. This concentration was obtained from the ratio of sample vapor pressure to total pressure inside the flow-reactor.

The STDS system was baked out at high temperature over night prior to use and the blank test was run before and after each trial to ensure a high quality of products. The syringe was submerged in isopropyl solvent and the new thermal septa were changed everyday to eliminate the contamination. Leak tests were performed at all connections using a leak detector to ensure that the sample was quantitatively transported.

2.1.3 Detailed Procedure

a. Dissolve HQ or CT in isopropyl alcohol at the concentration of 1.0 mole per litter

b. Set the infection port temperature at 180°C to vaporize all of liquid sample before entering the flow-reactor.

c. Set the thermal reactor compartment oven and the transfer line at 200°C facilitate transport of gas-phase reactants and products.

d. Set the furnace temperature to desired temperature for each trial of experiment.

e. Set the helium flow rate to desired flow rate as table 1 for each trial of experiment from the mass flow controller.

f. Measure the effluent flow rate from the transfer line and the splitter. Set the flow rate from the transfer line around 70 mL/min by controlling the needle nose valve to delivery only small amount of sample to the GC-MS system without damage the detector.

g. Record the flow rate from the splitter and the transfer line.

h. Program the GC/MS run from -60°C (hold for 5 minutes) to 300°C (hold for 1 minute) at the rate of 15°C/min. The total time will be 30 minutes.

i. Open the liquid nitrogen valve to help the GC oven initial temperature reach -60^{o}C in order to trap the products.

j. Program the MS for the full scan mode from 10 amu to 650 amu for 30 minutes. Turn on the detector after 9 minutes to eliminate a huge solvent peak.

k. Set the injection rate to the desire rate as table 2 for each trial of experiment from the syringe pump. If using vaporizer chormatoprobe, go to step o-q.

l. When all of the temperatures are stabilized and the system is ready, insert the transfer line into the injection port of the GC/MS system.

m. Draw 1.0 µL of sample HQ or CT into syringe and place syringe in the syringe pump.

n. Insert syringe needle into the injection port of the thermal reactor compartment and start the syringe pump as well as the GC/MS system.

o. Measure 5.0 mg of HQ or CT and place into the quartz micro-vial at the bottom of the chromatoprobe shaft.

p. Insert chromatoprobe into the injection port of the thermal reactor compartment and set the temperature of the injection port at 90^{o}C for HQ and 80^{o}C for CT.

q. When all of the temperatures are stabilized and the system is ready, insert the transfer line into the injection port of the GC/MS system and start the trial immediately.

r. Remove the syringe pump and transfer line from the injection ports after 5.0 minutes of cryogenic trapping.

s. Set the new desired temperature for the furnace to be ready for the next trial.
t. When the trial is complete, analyze the peaks and repeat the steps for the next trial.

2.1.4 GC-MS Analysis and Calculation of Product Yields

The mass-spectral library (NIST 98 version 1.6d) was used for helping to identify the products from the mass spectrum and gas chromatogram that were generated by the MS. Quantization of reactants and products was performed based on the calibration curves using

analytical standards (Sigma-Aldrich). Calibration was based on the area counts of the peaks on the chromatogram. Multiple trials were performed for each temperature to eliminate the error. The yields of the products were calculated using a following formula:

$$Y = \frac{P}{P_O} \times 100 \qquad \text{(Equation 2)}$$

Where: Y (%) is percent yield, P (moles) is the total mole of the particular product formed, and P_o (moles) is the initial mole of HQ or CT sample injected into the system.

2.2 Vacuum and Thermoelectric Furnace System

2.2.1 System Description

The vacuum and thermoelectric furnace system was custom designed for studying the surface-induced formation and stabilization of combustion generated persistent free radical. This custom designed system can be used as multiple tools such as adsorption, extraction, and electron paramagnetic resonance (EPR) measurement. There are four main components in this system: high power vacuum pumps, a high temperature thermoelectric ceramic heater, a vacuum exposure chamber, and an EPR-extraction cell as shown in **Figure 2.4**.

The pumping system consists of a vacuum pump (Edwards, model E2MO.7) and a high power turbo-molecular pump (Edwards, model EXT70). The vacuum pump is on all the time during the experiment while the turbo pump is turned on only after adsorption to remove excess and physisorbed molecules. This turbo pump is a high power vacuum pump and it can evacuate to lower pressure down to 10^{-6} torr. The outlet from the vacuum pump is connected to a carbon capsule filter (Pall, model 12011) and vented to a fume.

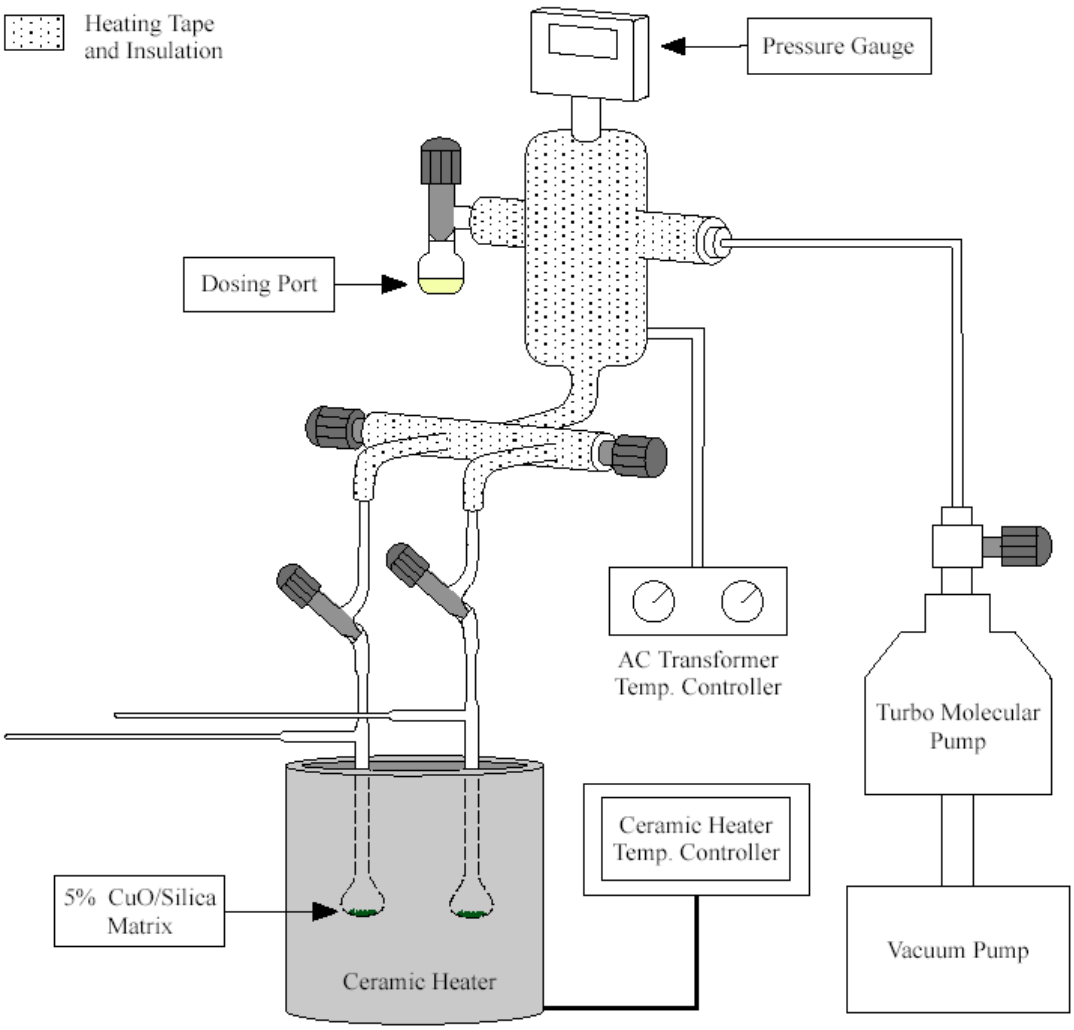

Figure 2.4: Vacuum and Thermoelectric Furnace System Apparatus

The vacuum exposure glass chamber is separated from the pumps by a vacuum valve. Rope heaters (Omegalux®, model FGR) and aluminum foil are wrapped around this glass chamber to prevent adsorption on the wall of chamber. These rope heaters are connected to the variable AC transformer (Electrothermal, model MC240X1) that controls the temperature surround the chamber. The digital pressure gauge (Varian, eyesys convectorr) monitors the pressure inside the system. The dosing port with a high vacuum valve is connected to the vacuum exposure chamber and is easily removed for cleaning.

Two custom-designed EPR-extraction cells (c.f. **Figure 2.5**) are hooked up to the vacuum exposure chamber through a quarter inch stainless steel adapter. Again, these EPR-extraction cells are very simple to dissemble from the vacuum exposure chamber. This specially designed cell is a 12 inches quartz tube composed of a 9 inches suprasil EPR side arm and a 1.5 inches diameter quartz bulb. The side arm has a diameter of 3mm and is made of suprasil necessary for EPR measurements. The quartz bulb contains the surface matrix that is used for adsorption and extraction experiments. This special design is ideal for non-diffusion limited interaction of the gas-phase molecules with the surface matrix as well as transferring the matrix to EPR tubes under vacuum condition.

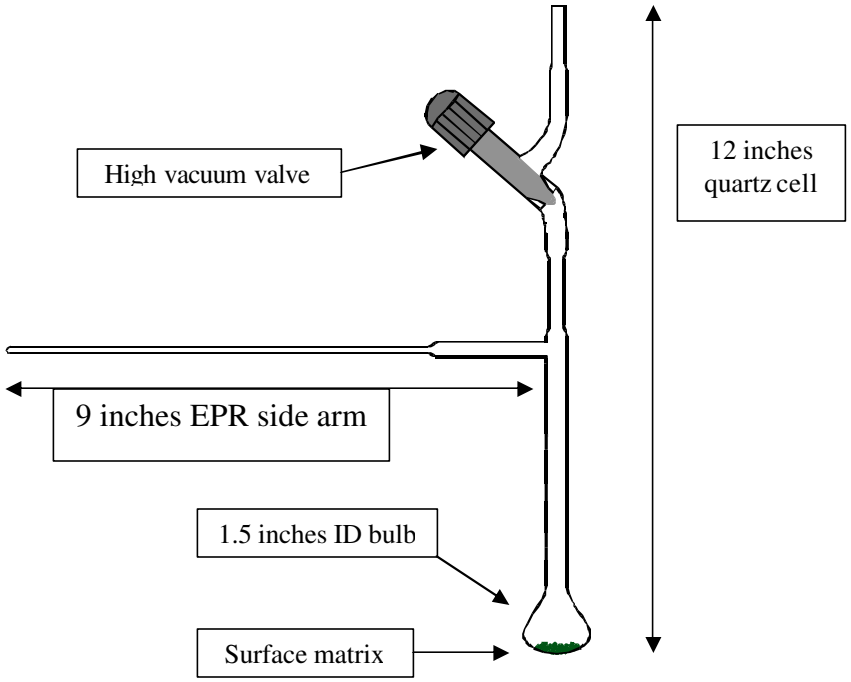

Figure 2.5: Custom-Designed EPR-Extraction Cells

The two bulbs, part of the custom-designed EPR-extraction cells, are housed inside a high-temperature cylindrical ceramic heater (Omegalux®, model CRFC) with the maximum operating temperature of 950°C. The temperature inside the heater is controlled by the relay

temperature controller (Omegalux®, model SSRL240DC25). In order to keep the temperature constant inside the heater, both ends of the cylinder are covered with thermal insulation.

2.2.2 Bound Radical Matrix Preparation

In this study, 5% of copper oxide (CuO) on supported silica oxide (SiO_2) [5-7] was used as a matrix for adsorption. CuO is supported on SiO_2 (Sigma Aldrich) by the method of incipient wetness, with a copper loading of 5%, on a mass basis.

- ✓ The first step in this preparation is determination of the amount of water needed to achieve incipient wetness for a given amount of silica gel powder. This silica powder is a very small size (200 mesh), and the surface area is 500m^2/g. Incipient wetness is the term used when the water added to the silica is either contained within the pore structure and/or bound to adsorption sites on the surface, i.e. no bulk water is present.

- ✓ Once the correct volume of water has been determined, the necessary amount of copper (II) nitrate hemipenta-hydrate ($Cu(NO_3)_2 \cdot 2.5\ H_2O$ from Sigma Aldrich) needed to yield 5% Cu in the CuO/SiO_2 substrate was calculated. For example, there are 5g of Cu(II)O and 95g of SiO_2 for every 100g of CuO/SiO_2 to make up the yield of 5% Cu in the CuO/SiO_2 substrate. In order to obtain 5g of Cu(II)O, 15g of $Cu(NO_3)_2 \cdot 2.5\ H_2O$ was added.

- ✓ Dissolve the calculated amount of $Cu(NO3)_2 \cdot 2.5\ H_2O$ in the correct volume of water that is needed for incipient wetness.

- ✓ Pour this aqueous solution of $Cu(NO_3)_2$ into the correct amount of silica gel powder and stir to mix well.

- ✓ Allow the resulting gel to stand for 2 hours with occasional stirring at room temperature.

- ✓ Dry for 6 hours at 120 °C in the oven.

- ✓ Calcinate the blue-green powder at 450 °C in the furnace for 12 hours to convert all $Cu(NO3)_2$ to CuO.

- ✓ Thoroughly grind the resulting green-black powder with a mortar and pestle.

- ✓ Sieve the powder to small size and store in the valve to use.

2.2.3 Detailed Surface-Bound Radical Adsorption Procedure

In this experiment, six precursors of phenoxyl radicals and semiquinone type radicals were chosen to study on temperature dependence of EPR g-value and concentrate of radicals in the range of 50°C to 300°C. Using a vacuum system and thermoelectric furnace, HQ, CT, monochlorobenzene (MCBz), 1,2-dichlorobenzene (1,2-DCBz), phenol (P) and 2-monochlorophenol (2-MCP) were chemisorbed at various temperatures onto 5% copper oxide supported on silica oxide (5% CuO/SiO_2) that was used as a surrogate for combustion generated particulate matter.

- Measure 100mg of 5% CuO/SiO_2 sample and place inside a customize design EPR-extraction cell.
- Hook up two EPR-extraction cells to the vacuum exposure chamber and level the bulbs in the middle of cylinder ceramic heater.
- Load the radical precursor in a dosing port and connect to the vacuum exposure chamber with the valve close.
- Turn on the vacuum pump while the turbo-molecular pump remains off.
- Slowly open the vacuum valve to evacuate samples until the catalyst is stable and slowly heat the matrix sample to the desired temperature of 120°C under vacuum to evaporate all of water out of system for 10min, and then close the vacuum valve.
- Open and remove the valve of EPR-extraction cells completely to expose the matrix sample to the air and dry it at the temperature of 400°C for 1 hour to remove all organic impurities on the matrix sample surface.
- Close the valve of EPR-extraction cells to the air, but keep the matrix sample air-to-vacuum feed through the vacuum exposure chamber.
- Set the temperature of ceramic heater to desired adsorption temperature and slowly open the vacuum valve.
- Open the water line and turn on the turbo-molecular pump when the pressure inside the system around 0.1 torr.
- Turn on the variable AC transformer to warm the vacuum exposure chamber.

- Evacuate the system down to 10^{-4} torr and close the EPR-extraction cell valves to get ready for adsorption.

- Slowly open the dosing port valve to remove all of the air inside, and then close the vacuum valve.

- Open the EPR-extraction cell valves to adsorb radical precursors onto a surface matrix sample for 5min while warm the rest or glass parts that not cover with rope heaters using a heat gun in order to prevent condensation.

- Close the dosing valve and open the vacuum valve to evacuate all of the excess and physisorbed molecules out of the system at 10^{-4} torr for 2 hours. This should leave only chemisorbed molecules bound on the matrix surface.

- Switch off the transformer and lower the temperature of the ceramic heater to room temperature to cool down the sample.

- Close the EPR-extraction cell and vacuum valves. Disassemble the EPR-extraction cells from the exposure chamber.

- Tilt EPR-extraction cell to transfer the matrix sample into the suprasil EPR side arm tube and perform EPR analysis.

2.2.4 Persistence of Surface Bound Radicals

When surface bound-radicals associate with metal surface, they can exist for significant time periods without being destroyed. In this experiment, the same six precursors MCBz, 1,2-DCBz, P, 2-MCP, HQ, and CT were adsorbed on 5% CuO/SiO_2 surface following the above steps. After performing EPR analysis for the intensity and g-value of surface bound-radicals, the matrix sample was transferred to a clean weighing boat in order to expose them to the air at room temperature for 30min. The matrix sample was transferred back to the EPR-extraction cell and evacuated down to the pressure of 10^{-2} torr before take EPR measurement again. The exposure was repeated in 30 min interval, until the EPR signal of bound-radicals completely disappeared.

2.3 Extraction of Chemisorbed Bound-Radicals

Once the precursors adsorb on the surface, they can be removed from that surface by extraction with some solvents. Several polar and non-polar solvents such as methyl alcohol (MEA), isopropyl alcohol (IPA), dichloromethane (DCM), toluene (TOL), and tert-butylbenzene (TBB) were chosen to extract surface-bound radicals from the above six precursors.

- Perform chemisorption of a precursor on 5% CuO/SiO_2 using the above procedures.
- Analyze EPR properties on surface bound- radicals.
- Tilt the EPR-extraction cell to transfer all of sample back into the bulb.
- Introduce 1.5mL for one of above solvents into EPR-extraction cell.
- Close EPR-extraction cell valve and place inside the sonicator (Fisher Scientific, model FS20).
- Sonicate the sample for 1 hour to extract surface bound-radicals into solvent.
- Pour the extract into a 1.5mL micro-valve and centrifuge to separate any of trace residues in the extract.
- Decant the extract into two clean 1.5mL micro-valves for GC/MS and EPR analysis.
- Connect the EPR-extraction cell back to vacuum exposure chamber for evacuation then take EPR measurement on residue sample.
- For GC/MS analysis, draw 1.0µL of the extract and load it in the GC (Agilent Technologies, model 6890N) equipped with the 30 m long, 0.25 mm id., 0.25 µm film thickness capillary column (HP-5MS) to separate products then analyze in the full scan mode 20amu to 600aum in MS (Agilent Technologies, model 9873).

2.4 EPR Analysis

EPR is the spectroscopic technique that uses to detect species having one or more unpaired electrons. When an external magnetic field is applied, the paramagnetic electrons

can either orient in a direction parallel or anti-parallel to the direction of the magnetic field. This phenomenon creates two different energy levels for the unpaired electrons and making it possible for absorption of electron-magnetic radiation to occur when electrons are driven between the two energy levels. The condition where the magnetic field and the microwave frequency are "just right" to produce an absorption is known as the resonance condition (c.f. **figure 2.6**). The g-value is one characteristic of EPR analysis, and is a dimensionless constant or the proportionality constant between the frequency and the field at resonance condition (**equation 3**).

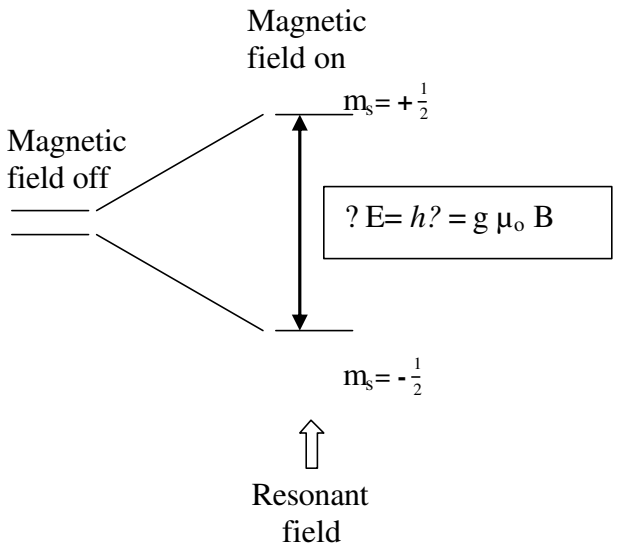

Figure 2.6: Resonance Condition

$$h? = g\ \mu_o\ B \qquad \text{(equation 3)}$$

Where: *h* is a Planck's constant value ($h = 6.63 \times 10^{-34}$ J s); *?* (hz) is the frequency of the radio waves; μ_o is Bohr magneton constant value ($\mu_o = 9.27 \times 10^{-24}$ J T^{-1}); B (T, tesla) is magnetic field.

2.4.1 EPR Parameters

All of samples were analyzed on a Bruker model EMX 10/2.7 EPR spectrometer (Bruker Instruments, Billerica, MA) with dual cavities. The parameters for all solid samples spectra were microwave frequency of 9.67 GHz, microwave power of 2.02mW, center field of 3250 G, sweep width of 2000 G, resolution of 2048 points, receiver gain 1.0 x 10^4, modulation frequency of 100 kHz, modulation amplitude of 4.0 G, time constant of 163.84 ms, and sweep time of 167.77 seconds.

However, due to the low concentration of radicals in the extract, the EPR parameter for the liquid samples were quite difference from EPR parameters for the solid samples. The microwave frequency was 9.71 GHz, while the microwave power was 20.19mW which is 10 times greater than solid samples parameters in order to detect a weak signal from liquid sample. Other parameters were center field of 3462 G, sweep width of 100 G, resolution of 2048 points, receiver gain 4.0 x 10^5, modulation frequency of 100 kHz, modulation amplitude of 4.0 G, time constant of 10.24 ms, and sweep time of 20.97 seconds.

2.4.2 Analysis and Calculation

Values of the g-factor were calculated using Bruker's WINEPR software for all liquid samples and Origin 7.0 software for all solid samples. The concentrations of free radicals in the samples (**Equation 4**) were calculated using the double integration method of the first derivative signal and comparison with a standard sample of 2,2-di(4-tert-octylphenyl)-1-picrylhydrazyl (DPPH)[8, 9].

$$C = \frac{Spins \times A \times RG_{DPPH}}{A_{DPPH} \times RG \times m} \qquad \text{(Equation 4)}$$

Where: C (spins/g) is concentration of radicals in the sample, A is the area count of sample; RG is received gain of sample; m (grams) is the mass of sample; A_{DPPH} is the area count of 1,1-diphenyl-2-picrylhydrazyl (DPPH) and RG_{DPPH} is received gain of DPPH.

In order to investigate the persistence to radicals, the **Equation 5, and Equation 6** were used to calculate the lifetime of radicals. Where C is the concentration of sample; k (min^{-1}) is the first order kinetic rate constant; and t (min) is the lifetime of radicals.

$$-\int \frac{d[C]}{[C]} = k\int dt \qquad \text{(Equation 5)}$$

$$-\ln\frac{[A_t]}{[A_o]} = kt$$

$$\ln\frac{[A_t]}{[A_o]} = -kt$$

$$\frac{[A_t]}{[A_o]} = e^{-kt}$$

$$\tau = \frac{1}{k} \qquad \text{(Equation 6)}$$

The automated mass spectral deconvolution and identification system (AMSDIS 97 version 1.1) and mass-spectral library (NIST/EPA/NIH 98 version 1.6) were used to identify the extracted products from the mass spectrum and gas chromatogram that were generated by the MS.

2.5 References

1. Rubey, W. A.; Grant, R. A., Design Aspects of a Modular Instrumentation System for Thermal Diagnostic Studies. *Review of Scientific Instruments* **1988,** 59, (2), 265-269.

2. Striebich, R. C.; Rubey, W. A., A System for Thermal Diagnostic Studies. *American Laboratory* **1990,** 22, (1), 64-&.

3. Striebich, R. C.; Rubey, W. A.; Tirey, D. A., The thermal decomposition of various organic materials using the system for thermal diagnostic studies (STDS). *International SAMPE Environmental Conference* **1991,** 1, (Environment in the 1990's: A Global Concern), 155-62.

4. Rubey, W. A.; Carnes, R. A., Design of a Tubular Reactor Instrumentation Assembly for Conducting Thermal-Decomposition Studies. *Review of Scientific Instruments* **1985,** 56, (9), 1795-1798.

5. Lomnicki, S.; Dellinger, B., A detailed mechanism of the surface-mediated formation of PCDD/F from the oxidation of 2-chlorophenol on a CuO/silica surface. *Journal of Physical Chemistry A* **2003,** 107, (22), 4387-4395.

6. Lomnicki, S.; Dellinger, B., Formation of PCDD/F from the pyrolysis of 2-chlorophenol on the surface of dispersed copper oxide particles. *Proceedings of the Combustion Institute* **2003,** 29, 2463-2468.

7. Evans, C. S.; Dellinger, B., Surface-mediated formation of polybrominated dibenzo-p-dioxins and dibenzofurans from the high-temperature pyrolysis of 2-bromophenol on a CuO/silica surface. *Environmental Science & Technology* **2005,** 39, (13), 4857-4863.

8. Maskos, Z.; Khachatryan, L.; Dellinger, B., Precursors of radicals in tobacco smoke and the role of particulate matter in forming and stabilizing radicals. *Energy & Fuels* **2005,** 19, (6), 2466-2473.

9. Maskos, Z.; Khachatryan, L.; Cueto, R.; Pryor, W. A.; Dellinger, B., Radicals from the pyrolysis of tobacco. *Energy & Fuels* **2005,** 19, (3), 791-799.

CHAPTER 3: RESULTS

STDS, EPR and GC-MS instrumentation were used to obtain all of the data in this work. The STDS is a flow reactor analytical system that was used to study the thermal degradation of HQ and CT. EPR is a spectroscopic technique that was used to detect bound radicals from chemisorption of the six precursors including HQ, CT, MCBz, 1,2-DCBz, P, 2-MCP as well as measure g-value and the intensity of radicals. GC-MS was used to separate and identify the extraction products.

3.1 Thermal Degradation of HQ and CT Using STDS

Comprehensive product yields were determined from the thermal degradation of HQ and CT at a reaction time of 2.0 seconds. Both pyrolytic and oxidative conditions, which described in previous chapter, were performed in thermal degradation of the precursors using STDS.

3.1.1 Hydroquinone

3.1.1.1 Gas-Phase Pyrolysis of Hydroquione

Gas-phase pyrolysis of hydroquinone was performed in the temperature range of 250^{o}C to 1000^{o}C for the reaction time of 2.0 seconds. However, HQ was pyrolyzed in two reaction modes:

- HQ in the presence of isopropyl alcohol (hydrogen-rich source) in a helium gas carrier.
- Pure HQ (hydrogen-lean source) in a helium gas carrier.

3.1.1.1.1 Hydrogen-Rich Conditions

The thermal degradation behavior and the yields of product formation from the pyrolysis of HQ in the presence of isopropyl alcohol (hydrogen-rich condition) are presented

in **Figure 3.1** and **Table 3.1**. In this case, the thermal degradation of HQ was initiated at 250°C and gradually increases with temperature. The thermal degradation of HQ under the hydrogen-rich condition increased rapidly at 700°C and HQ was completely degraded around 750°C.

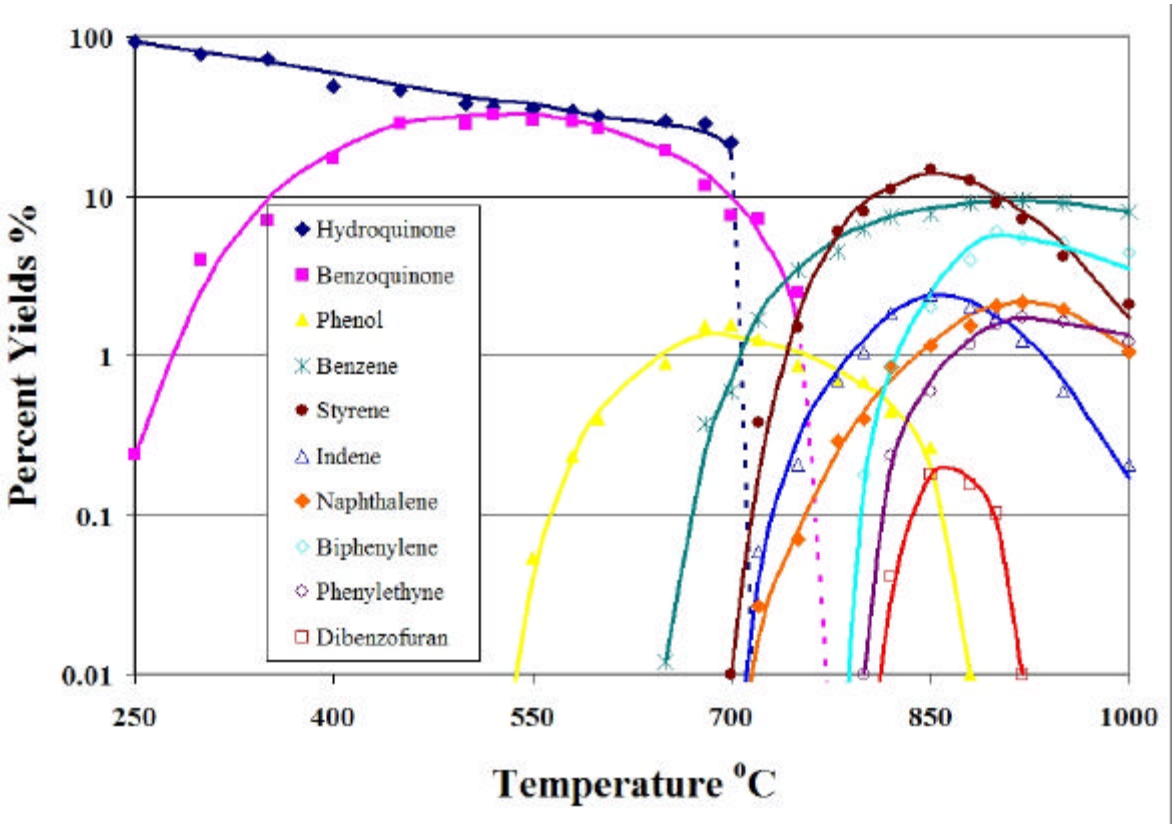

Figure 3.1: Percent Yield of Products from the Gas-phase Pyrolysis of HQ under Hydrogen-Rich Conditions

p-Benzoquinone formation occurred immediately upon degradation of HQ at 250°C with a maximum yield of 33% at 550°C persisting until 750°C. p-Benzoquinone and phenol were the only observable products at low temperature below 650°C while many products were detected above 650°C . Phenol was formed from 550°C to 900°C with a maximum yield of 1.5% at 700°C and benzene was observed around 650°C with a maximum yield of 9.4% at 900°C. At 700°C, substituted aromatic by-products were formed such as styrene,

indene, naphthalene, biphenylene and phenylethyne with the maximum yield of 15% at 850°C, 2.4% at 850°C, 2.1% at 920°C, 6.1% at 900°C, 1.6% at 950°C respectively. Dibenzofuran was detected in the narrow temperature range from 800°C to 900°C with maximum yield of 0.18% at 850°C.

3.1.1.1.2 Hydrogen-Lean Conditions

The temperature dependence and the percent yields of product formation from the pyrolysis of pure HQ (hydrogen-lean condition, without isopropyl alcohol) are presented in **Figure 3.2** and **Table 3.2**. Under these conditions, thermal degradation of HQ is again initiated at 250°C and slowly increases with temperature. The thermal degradation of HQ in the hydrogen-rich conditions was complete by 750°C, while decomposition of HQ in the hydrogen-lean conditions was not complete until 820°C. Other differences in the product distribution were also observed.

The formation of p-benzoquinone was observed at 250°C with a maximum yield of 15% at 500°C and was completely decomposed at 750°C. Also, p-benzoquinone was the only observable product below 700°C. The highest percent yield of phenol was 6.3% at 775°C and was detected in the range of 700°C to 950°C. Significant yield of dibenzofuran was detected from 725°C to 1000°C under hydrogen-lean condition with maximum yield of 1.1% at 775°C. Coincidently, dibenzo-p-dioxin achieved a maximum yield of 0.39% also at 775°C and was observed only for the hydrogen-lean condition over the temperature range of 725°C to 950°C. Benzene (maximum yield of 0.15% at 900°C) and substituted aromatic by-products (maximum yields of styrene, 0.36% at 900°C; indene, 0.14% at 850°C; naphthalene, 0.082% at 900°C; biphenylene, 0.18% at 850°C and phenylethyne, 0.043% at 900°C) were observed above 650°C under hydrogen-lean conditions.

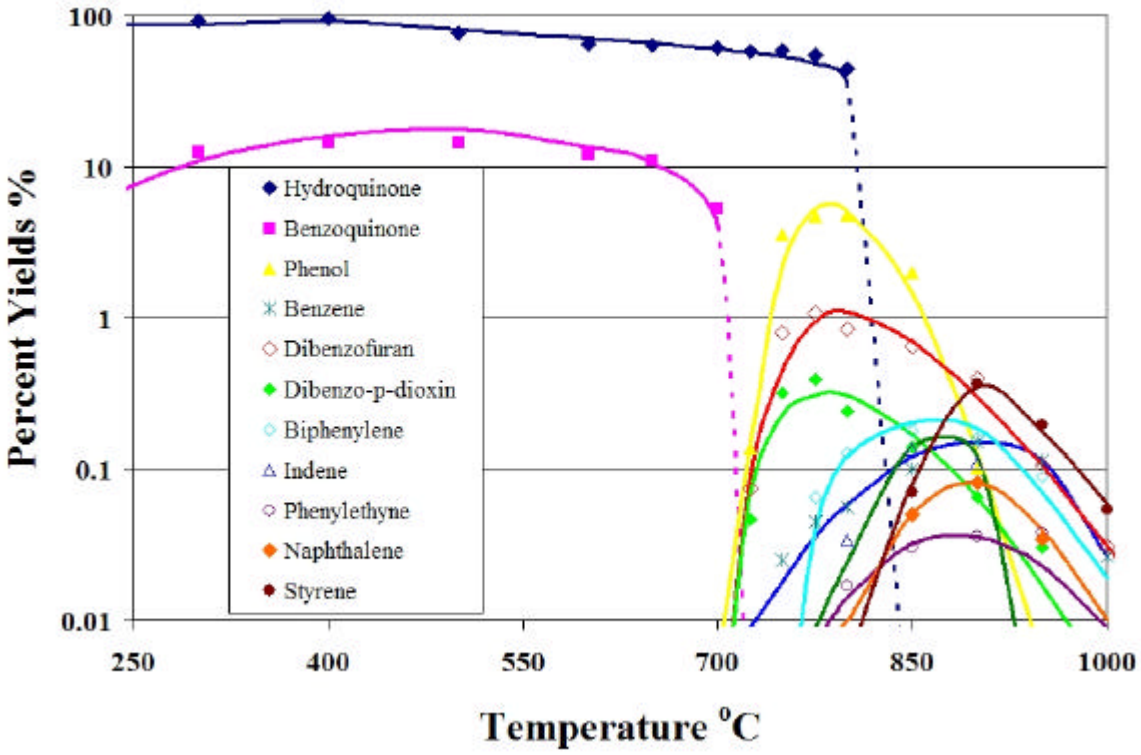

Figure 3.2: Percent Yield of Products from the Gas-phase Pyrolysis of HQ under Hydrogen-Lean Conditions

Table 3.1 Percent Yield of Products from the Gas-phase Pyrolysis of HQ under Hydrogen-Rich Conditions

Temperature °C	Hydro-quinone	p-Benzo-quinone	Phenol	Benzene	Phenylethyne	Styrene	Indene	Naphthalene	Biphenylene	Dibenzo-furan
250	94	0.24								
300	78	5.6								
350	73	6.4								
400	48	17								
450	46	28								
500	38	28								
550	35	33	0.051							
600	26	27	0.39							
650	29	19	0.82							
680	28	12	1.5	0.38						
700	22	7.6	1.5	0.58						
725	0.51	7.2	1.3	1.7		0.38	0.061	0.026		
750		1.2	0.86	3.4		1.1	0.21	0.067		
800			0.68	6.2		2.4	0.44	0.35	0.18	
825			0.27	7.5	0.23	9.7	1.8	0.81	0.87	0.042
850			0.26	7.7	0.48	14	2.4	1.1	1.5	0.18
875				9.1	1.2	12	1.9	1.5	3.9	0.15
900				9.5	1.6	14	1.7	2.1	6.1	0.11
925				9.5	1.5	7.2	0.99	2.2	5.5	
950				9.1	1.6	4.2	0.38	1.9	5.1	
1000				7.9	1.2	2.1	0.21	1.1	4.4	

Table 3.2 Percent Yield of Products from the Gas-phase Pyrolysis of HQ under Hydrogen-Lean Conditions

Temperature °C	Hydro-quinone	p-Benzo-quinone	Phenol	Benzene	Dibenzo-furan	Dibenzo-p-dioxin	Biphe-nylene	Indene	Phenyl-ethyne	Naph-thalene	Styrene
250	86	5.0									
300	88	12									
350	87	13									
400	85	14									
450	82	14									
500	77	15									
550	68	13									
600	65	12									
650	64	11									
700	62	5.3									
725	58		0.14		0.076	0.048					
750	59		3.6	0.026	0.81	0.32					
775	55		6.3	0.046	1.1	0.39	0.066		0.011		
800	45		4.8	0.058	0.85	0.24	0.13	0.034	0.024		
850			2.1	0.11	0.65	0.14	0.18	0.14	0.029	0.052	0.071
900			0.12	0.15	0.41	0.065	0.16	0.11	0.043	0.082	0.36
950			0.011	0.12	0.12	0.031	0.091		0.042	0.034	0.19
1000				0.027	0.033						0.054

3.1.1.2 Gas-Phase Oxidation of Hydroquinone

A mixture of 80% helium and 20% oxygen was used as a gas carrier for this experiment. The percent yields of product formation and temperature dependence of the oxidative thermal degradation of HQ are presented in **figure 3.3** and **table 3.3**. The reaction time was maintained at 2.0 seconds inside the flow-reactor for all operational temperature range of 200^{o}C to 1000^{o}C.

HQ was rapidly decomposed above 200^{o}C and completely degraded around 550^{o}C. Instantaneously, p-benzoquinone was observed upon degradation of HQ at 200^{o}C achieving a maximum yield of 36% at 250^{o}C. The formation of p-benzoquinone was decreased with increasing temperature and it was the only major product observed over the wide temperature range of 200^{o}C to 700^{o}C Phenol was not observed under this condition, but benzene was detected at low temperature of 250^{o}C and achieved a maximum yield of 1.2% at 350^{o}C in the range of temperature between 250^{o}C and 550^{o}C. Fewer products were observed under oxidative condition than under pyrolytic condition. No dioxin products were formed at any experimental temperatures. Above 400^{o}C, other products such as 4,4'-dihydroxydiphenyl ether and 4,4'-dihydroxybiphenyl were detected with a maximum yield of 0.031% at 450^{o}C and 0.44% at 450^{o}C respectively.

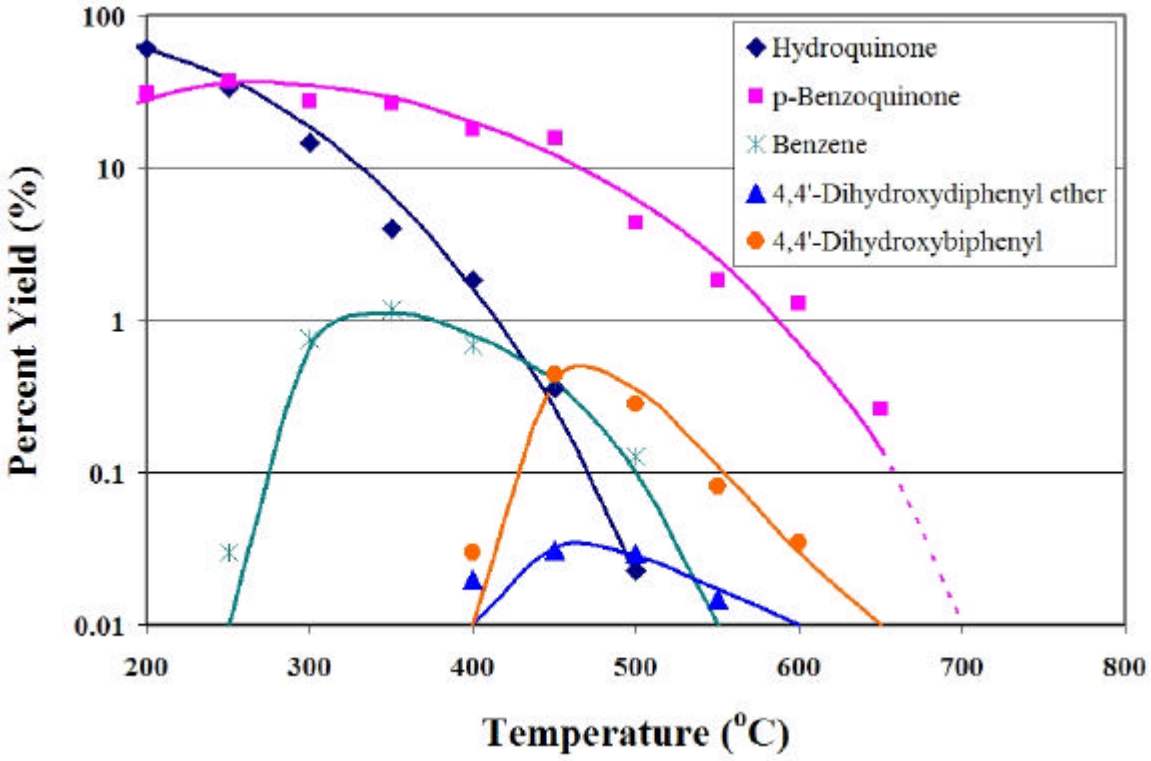

Figure 3.3: Percent Yield of Products from the Gas-phase Oxidation of Pure HQ

Table 3.3 Percent Yield of Products from the Gas-phase Oxidation of Pure HQ

Temperature °C	Hydroquinone	p-Benzo-quinone	Benzene	4,4'-dihydroxy-diphenyl ether	4,4'-dihydroxy-biphenyl
200	61	31			
250	33	36	0.031		
300	15	27	0.76		
350	3.9	26	1.2		
400	1.8	18	0.68	0.024	0.032
450	0.36	16	0.41	0.031	0.44
500	0.032	4.4	0.13	0.029	0.28
550		1.8	0.031	0.019	0.082
600		1.3			0.031
650		0.26			

3.2.1 Catechol

3.2.1.1 Pyrolysis of Catechol

Gas-phase pyrolysis of CT was performed in the temperature range of 250°C to 1000°C for a reaction time of 2.0 seconds for two reaction conditions:

- CT in the presence of isopropyl alcohol (hydrogen-rich source) in helium gas carrier.
- Pure CT (hydrogen-lean source) in helium gas carrier.

3.2.1.1.1 Hydrogen-Rich Conditions

Figure 3.4 and **table 3.4** present the temperature dependence and the percent yields of products formation from gas-phase pyrolysis of CT in the present of isopropyl alcohol (hydrogen-rich condition). The thermal degradation of CT was observed at 250°C and rapidly increased at 550°C. Around 750°C, CT decomposed to below the limit detectable concentration. In pyrolysis of HQ, a significant amount of HQ was converted into p-benzoquinone at low temperature and similar behavior was expected for CT; however, o-benzoquinone was not observed during the pyrolysis of CT.

Phenol was not detected until 600°C and achieved the maximum yield of 1.8% at 750°C and was observed in the temperature range of 600°C to 900°C. Benzene was formed in a wide temperature range between 650°C and 1000°C with a relatively constant high yield of 6.5% from 850°C to 950°C. At 650°C, dioxin-type products started to form. Dibenzo-p-dioxin was observed in the temperature range between 650°C and 800°C with a maximum yield of 0.65% at 700°C while dibenzofuran was detected in a wide temperature range from 650°C to 1000°C with a highest yield of 3.5% at 750°C.

Above 650°C, polycyclic aromatic hydrocarbons (PAHs) and substituted aromatic products were detected that are the result of fragmentation of CT into C2 and C4 products, followed by molecular growth. These by-products were styrene, indene, naphthalene, biphenylene and phenylethyne with the maximum yield of 8.2% at 900°C, 1.2% at 850°C, 1.4% at 950°C, 3.2% at 950°C, and 0.79% at 950°C, respectively.

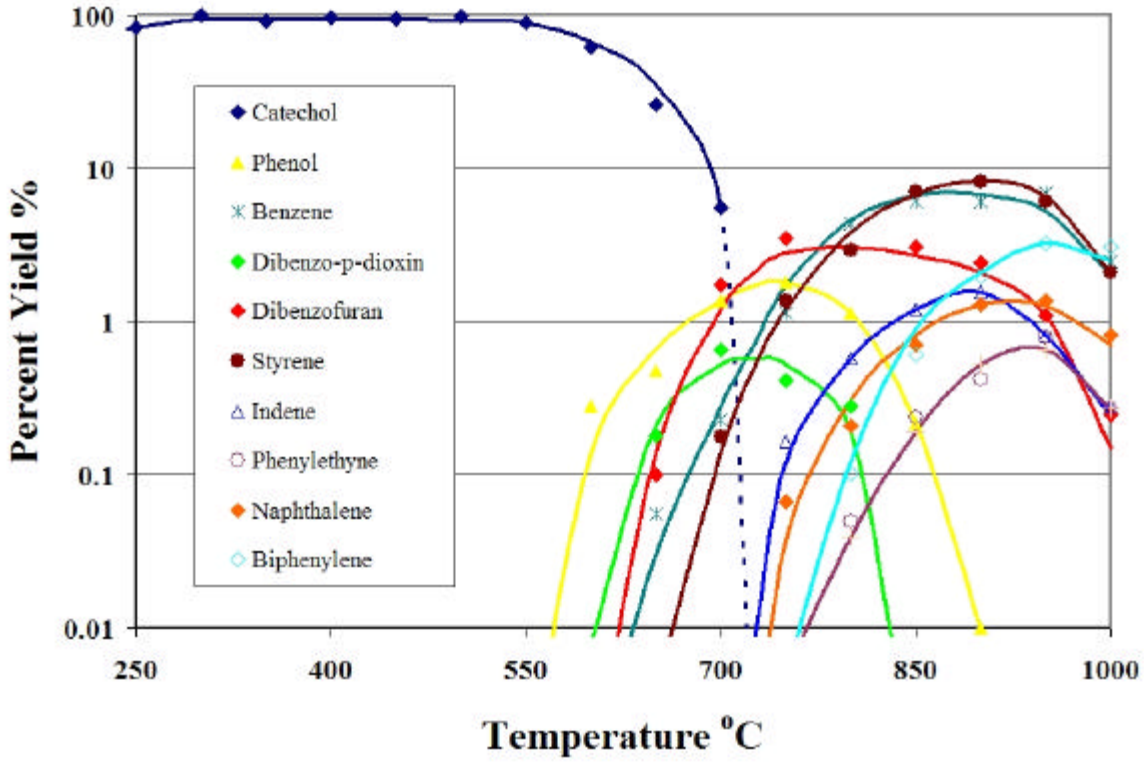

Figure 3.4: Percent Yield of Products from the Gas-phase Pyrolysis of CT under Hydrogen-Rich Condition

3.2.1.1.2 Hydrogen-Lean Conditions

The percent yields of products formation and temperature dependence of the pyrolysis of CT without the present of isopropyl alcohol (hydrogen-lean condition) are presented in **Figure 3.5** and **Table 3.5**. The decomposition of CT was initiated at 250°C and increased slightly with temperature until 800°C where it rapidly decomposed to below

detectable levels at 850°C. Similar to hydrogen-rich conditions, o-benzoquinone was not observed for the entire of temperature profile from the pyrolysis of CT under hydrogen-lean conditions.

The only observable product below 750°C was phenol and it achieved a maximum yield of 0.18% at 700°C. Dibenzofuran was the only observable dioxin-type product with maximum yield of 0.33% at 900°C. Benzene was not detected until 900°C with a maximum yield of 0.27% at 950°C. Aromatic products were detected at high temperature above 800°C including anthracene, naphthalene, biphenylene and phenylethyne achieved a maximum yield of 0.63% at 900°C, 1.6% at 950°C, 1.2% at 950°C, and 0.18% at 950°C, respectively.

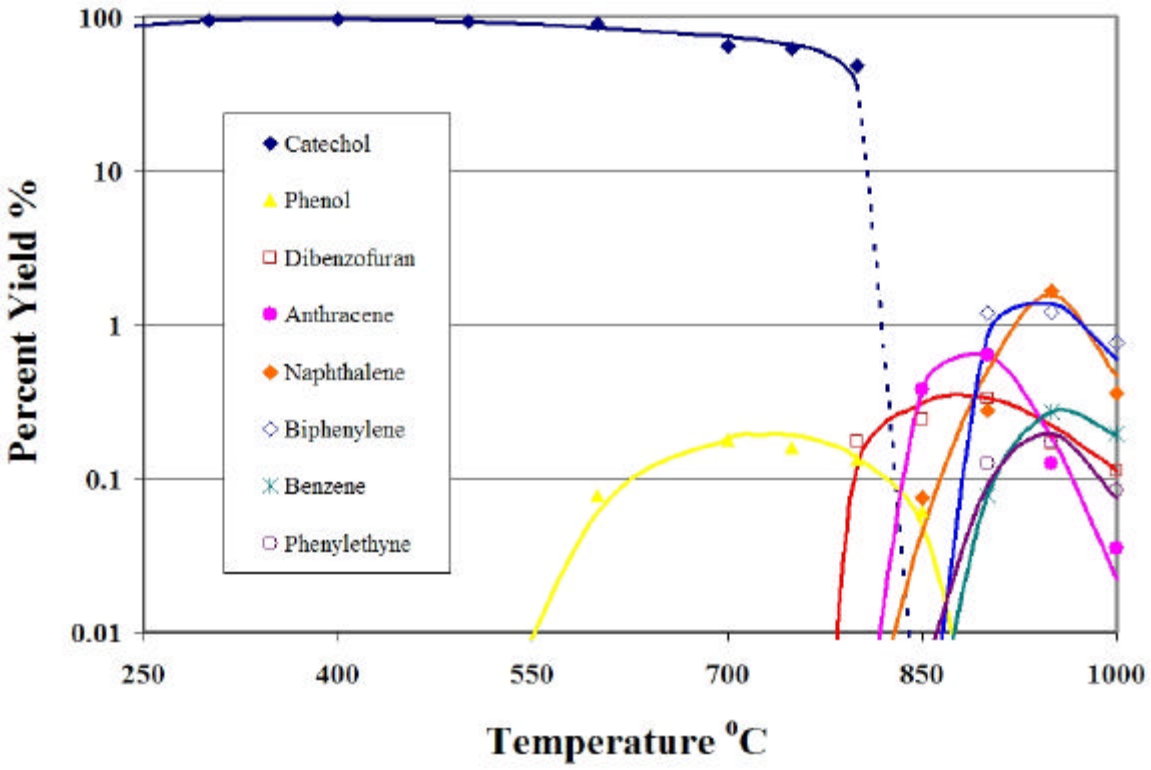

Figure 3.5: Percent Yield of Products from the Gas-phase Pyrolysis of CT under Hydrogen-lean Condition.

Table 3.4: Percent Yield of Products from the Gas-phase Pyrolysis of CT under Hydrogen-Rich Conditions

Temperature °C	Catechol	Phenol	Benzene	Dibenzo-dioxin	Dibenzo-furan	Styrene	Indene	Phenylethyne	Naphthalene	Biphenylene
250	93									
300	99									
350	92									
400	96									
450	95									
500	98									
550	91									
600	63	0.28								
650	26	0.48	0.056	0.18	0.11					
700	5.6	1.4	0.23	0.65	1.7	0.18				
750		1.8	1.1	0.41	3.5	1.4	0.17		0.068	
800		1.1	4.4	0.28	2.9	2.9	0.57	0.049	0.21	0.11
850		0.21	6.1		3.1	7.1	1.2	0.24	0.71	0.61
900			6.1		2.4	8.2	1.6	0.42	1.3	1.9
950			6.8		1.1	6.1	0.82	0.79	1.4	3.2
1000			3.5		0.25	2.1	0.28	0.27	0.81	3.2

Table 3.5: Percent Yield of Products from the Gas-phase Pyrolysis of CT under Hydrogen-lean Conditions

Temperature °C	Catechol	Phenol	Dibenzo-furan	Anthracene	Napthalene	Biphenylene	Benzene	Phenylethyne
250	95							
300	94							
350	96							
400	97							
450	94							
500	93							
550	91							
600	89	0.078						
650	823	0.12						
700	64	0.18						
750	63	0.16						
800	48	0.13	0.17					
850		0.062	0.24	0.37	0.076			
900			0.33	0.63	0.28	1.2	0.078	0.12
950			0.17	0.12	1.6	1.3	0.27	0.17
1000			0.11	0.036	0.36	0.76	0.19	0.083

3.2.1.2 Gas-Phase Oxidation of Catechol.

The gas carrier for this experiment was a mixture of 80% of helium gas and 20% of oxygen gas. The reaction time was maintained at 2.0 seconds inside the flow-reactor for the entire operational temperature range between 200°C and 1000°C. The temperature dependence and percent yields of product formation of the oxidative thermal degradation of CT are presented in **Figure 3.6** and **Table 3.6**. The decomposition of CT was initiated as low as 200°C and rapidly degraded when the temperature increased. CT totally decomposed to below the limit detectable concentration around 600°C.

Fewer products were observed under oxidative conditions. However, the formation of o-benzoquinone was detected instantaneously upon degradation of CT at 200°C. Between 200°C and 450°C, o-benzoquinone achieved a maximum yield of 6.5% and decreased rapidly above 500°C. From 400°C to 750°C, 2,2'-dihydroxydiphenyl ether was observed with a maximum yield of 0.46% at 450°C. 1,8-Dihydroxy-naphthalene was detected from 450°C to 700°C and achieved a maximum yield of 0.056% at 550°C.

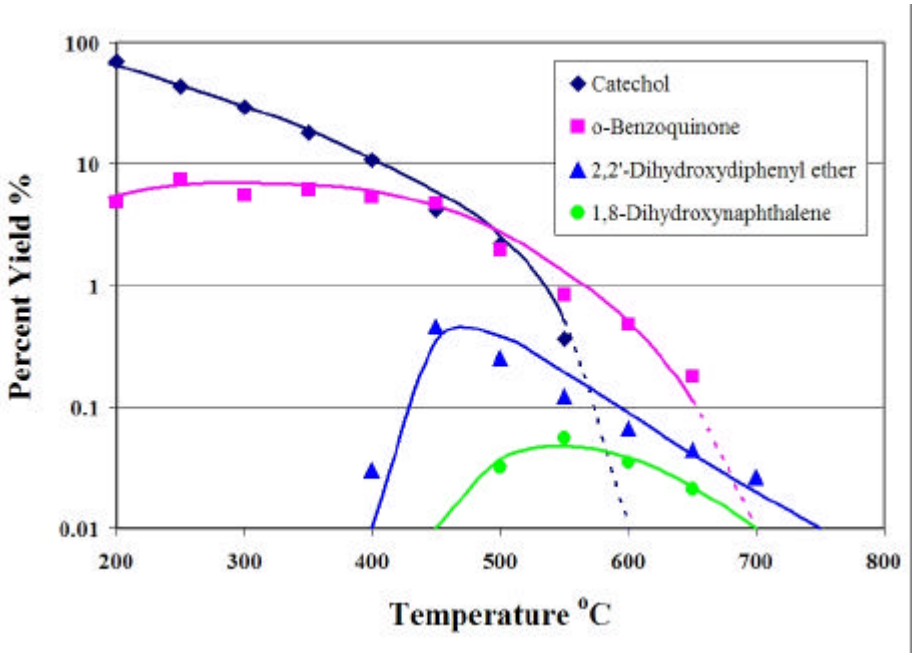

Figure 3.6: Percent Yield of Products from the Gas-phase Oxidation of Pure CT

Table 3.6 Percent Yield of Products from the Gas-phase Oxidation of Pure CT

Temperature °C	Catechol	o-Benzoquinone	2,2'-dihydroxyl-diphenyl ether	1,8-Dihydroxy-naphthalene
200	88	4.5		
250	69	4.8		
300	44	7.4		
350	29	5.6		
400	18	6.2	0.031	
450	11	5.3	0.46	
500	4.2	4.7	0.25	0.032
550	2.2	1.9	0.12	0.056
600	0.36	0.83	0.066	0.043
650		0.47	0.042	0.032
700		0.18	0.033	

3.2 Surface-Bound Radicals

Surface-bound radicals were formed during the adsorption of precursor organic molecules on metal oxides. Five percent copper oxide supported on silica oxide (CuO/SiO_2) was used as a surrogate for combustion-generated particulate matter. Precursors of phenoxyl and semiquinone type radicals were adsorbed on 5% CuO/SiO_2 and characterized using electron paramagnetic resonance (EPR) and gas chromatograph mass spectrometer (GC-MS) technique.

3.2.1 Formation and Stabilization of Surface-Bound Radicals

Using a vacuum system and thermoelectric furnace, six precursors of phenoxyl and semiquinone type radicals including monochlorobenzene (MCBz), 1,2-dichlorobenzene (1,2-DCBz), phenol (P), 2-monochlorophenol (2-MCP), hydroquinone (HQ), and catechol (CT) were adsorbed onto the 5% CuO/SiO_2 surface. **Figure 3.7** depicts the EPR spectra of the above precursors dosed onto CuO/SiO_2 surface at 200°C.

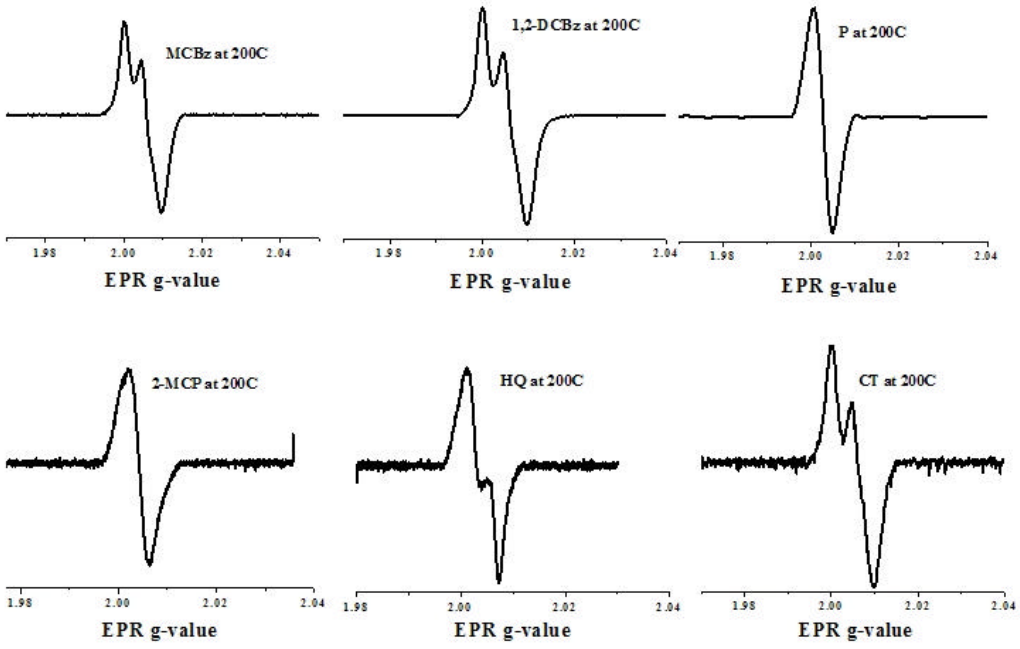

Figure 3.7: EPR Spectra of the Precursors Dosed onto CuO/SiO_2 Surface at 200°C

The best fit line of temperature dependence of EPR g-value for the surface-bound radicals from the precursors in the temperature range between 50°C and 300°C is presented in figure 3.8. Surface-bound radicals from HQ and CT formed as low as 50°C to 100°C and had nearly constant g-value when the temperature increased to 300°C. HQ exhibited a g-value in the range of 2.0061 - 2.0068 while CT exhibited a g-value in the range of 2.0054 - 2.0064. In contrast to HQ and CT, the other four precursors, MCBz, 1,2-DCBz, P, and 2-MCP did not form radicals until 150°C.

The behavior of the surface-bound radicals from MCBz, 1,2-DCBz, P, and 2-MCP fell into two different groups. The first group includes MCBz and 1,2-DCBz that generated bound-radicals with a high g-value at 150°C then decreased when the temperature increased. MCBz exhibited a g-value in the range of 2.0053 - 2.0071 and 1,2-DCBz exhibited a g-value in the range between 2.0052 - 2.0070. The second group contained P and 2-MCP and initially exhibited low g-values at 150°C that slightly increased as the temperature was raised to 300°C. The range of g-values for P and 2-MCP were 2.0033 - 2.0037 and 2.0047 - 2.0055, respectively. **Figure 3.8** presents the temperature dependence of EPR g-value of surface bound radicals generated from the precursors.

The yield of surface-bound radicals was also studied in the temperature range of 50°C-300°C. CT generated surface-bound radicals at relatively low concentration throughout the studied temperature range and achieved a maximum yield of 1.18×10^{18} spins/g of CuO/SiO_2 surface for adsorption at 200°C. Similar to CT, surface-bound radicals from HQ displayed very low yields at 50°C and slightly increased to 1.93×10^{18} spins/g of CuO/SiO_2 surface at 230°C.

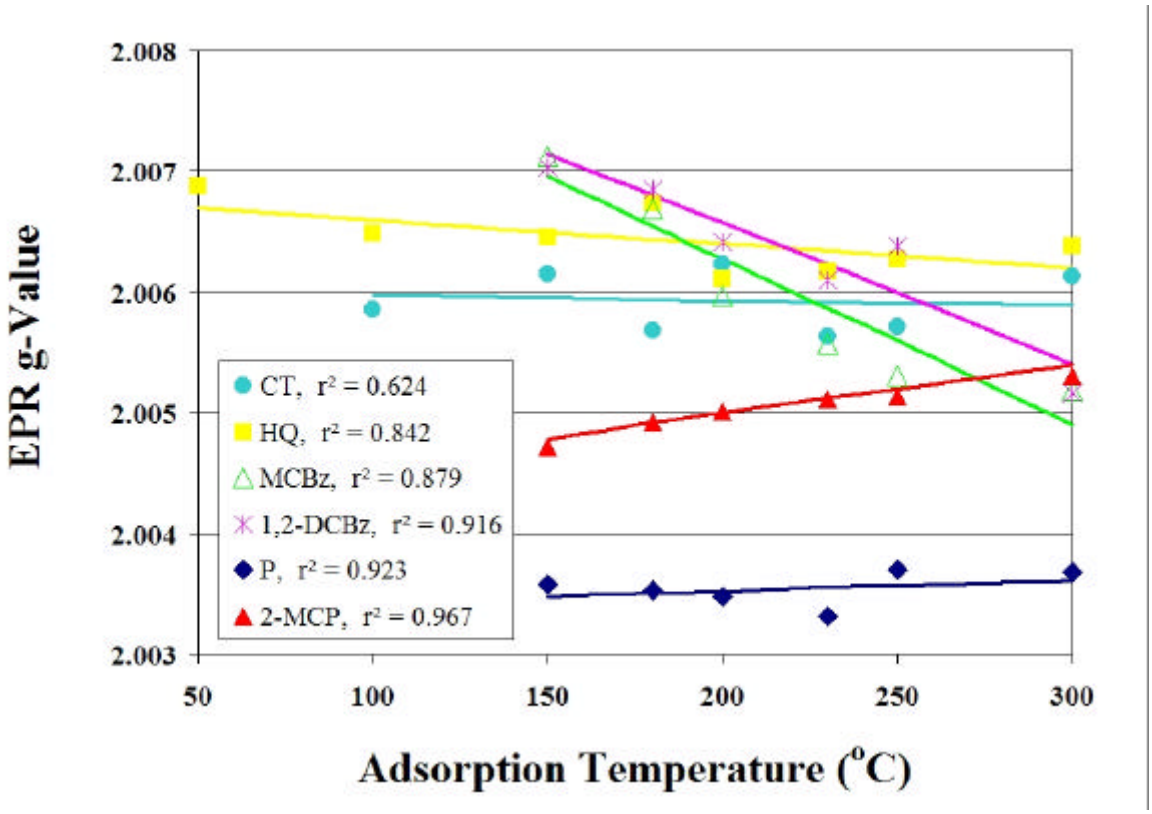

Figure 3.8: Temperature Dependence of EPR g-Value of Surface-Bound Radicals Generated from the Precursors

P and 2-MCP achieved a maximum yield of radicals at the same temperature of 230°C with a concentration of 5.70 x 10^{18} spins/g and 8.12 x 10^{18} spins/g of CuO/SiO_2 surface respectively. Bound-radicals from both P and 2-MCP precursors were initially formed at relatively low yields at 150°C and rapidly increased to the maximum yields at 230°C. MCBz generated bound-radicals achieved to the maximum yield of 3.70 x 10^{19} spins/g of surface fly-ash at 200°C and gradually decreased as the temperature increased. 1,2-DCBz achieved its maximum yield of radicals at of 6.72 x 10^{18} spins/g at 230°C of CuO/SiO_2 surface. **Figure 3.9** and **Table 3.7** display the concentration of surface-bound radicals from chemisorption of the precursors on 5% CuO/SiO_2 surface in the studied temperature range of 50°C - 300°C.

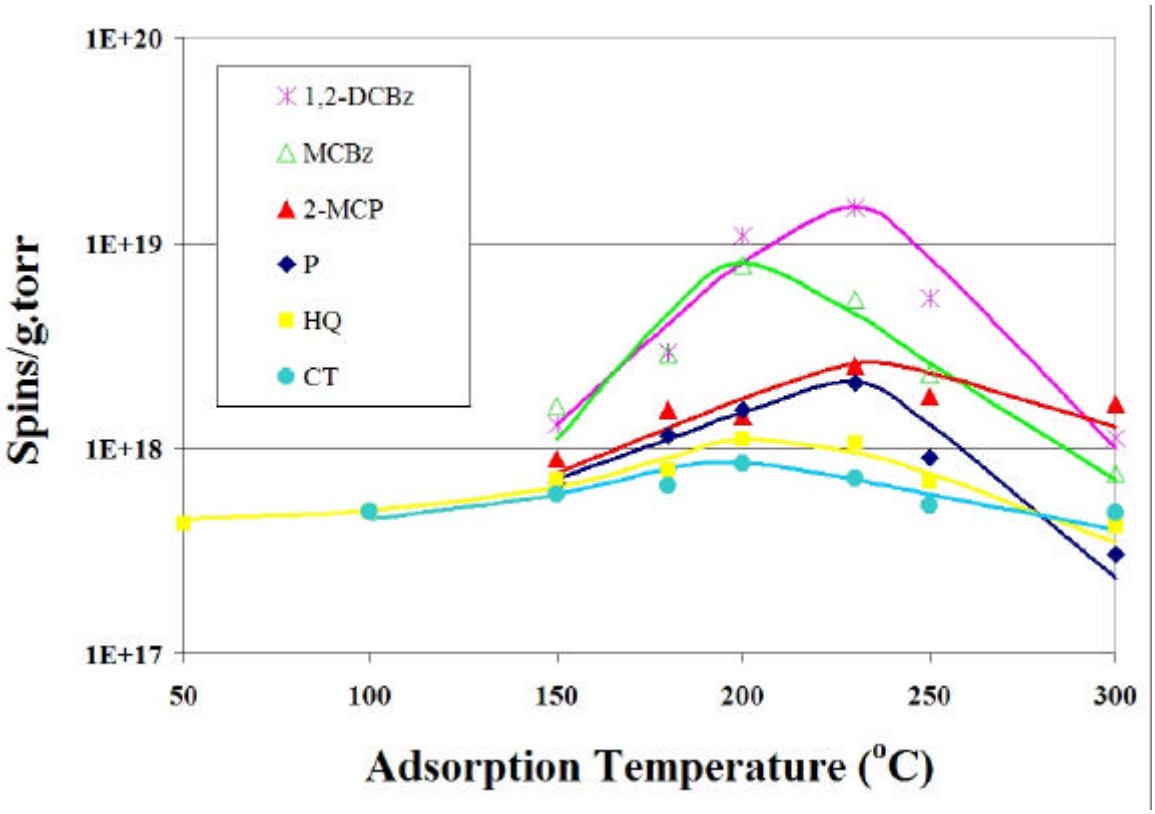

Figure 3.9 Temperature Dependence of Concentration of Surface-Bound Radicals Generated from the Precursors

Table 3.7: Temperature Dependence of Concentration (spins/g.torr) of Surface-Bound Radicals Generated from the Precursors

Temperature °C	Catechol	Hydroquinone	Mono-chlorobenzene	1,2-Dichloro-benzene	Phenol	2-Mono-chlorophenol
50		2.45E+17				
100	4.55E+17	3.51E+17				
150	6.78E+17	8.14E+17	5.96E+18	3.46E+18	6.19E+17	1.99E+18
180	7.96E+17	7.98E+17	9.40E+18	7.40E+18	2.74E+18	4.52E+18
200	1.45E+18	1.75E+18	3.70E+19	4.23E+19	3.53E+18	3.48E+18
230	1.18E+18	1.93E+18	2.64E+19	6.72E+19	5.70E+18	8.12E+18
250	1.01E+18	1.10E+18	1.19E+19	1.33E+19	2.57E+18	6.87E+18
300	1.20E+18	1.06E+18	4.33E+18	5.47E+18	9.04E+17	7.75E+18

3.2.2 Persistence of the Surface-Bound Radicals

The surface-bound radicals from the six precursors achieved their highest yields from 200°C - 230°C (c.f. **Figure 3.9**). Accordingly, these surface bound-radicals were generated at 230°C and their persistence was studied upon exposure to air. **Figure 3.10** presents the time dependence of EPR spectra of surface-bound radicals during exposure to the air for 2-MCP.

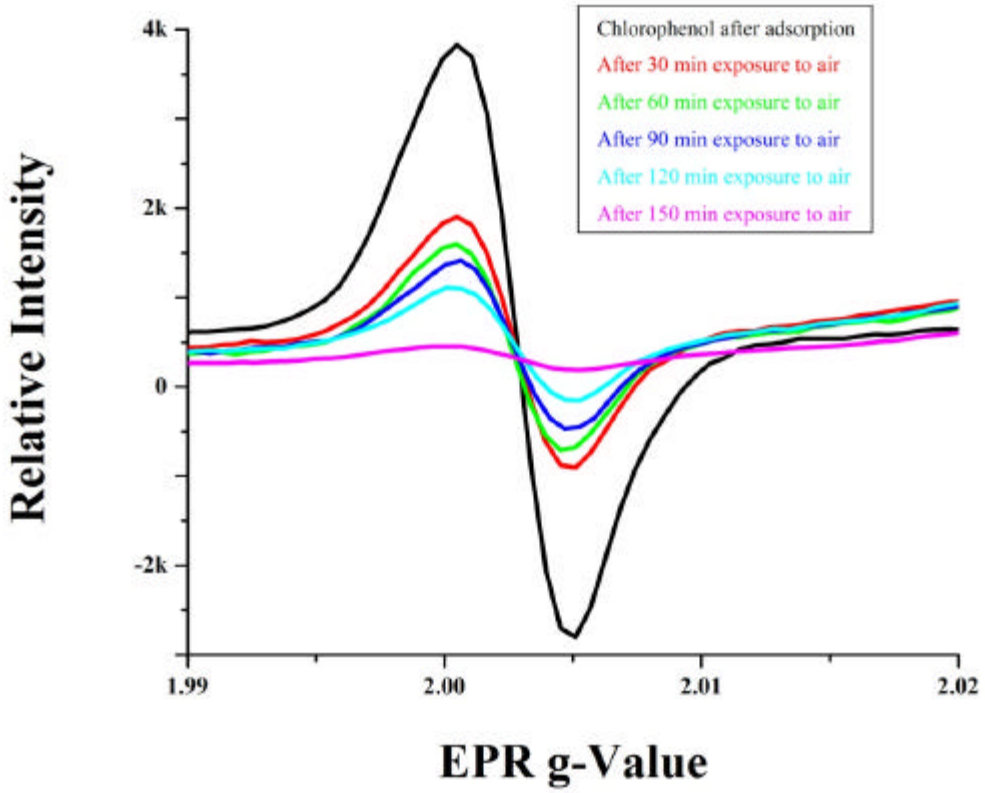

Figure 3.10: EPR Spectra of Bound Radicals from 2-Monochlorophenol Exposed to the Air in 30 Minute Time Intervals

Surface bound-radical decays fit first order decay kinetic when exposed to air. **Figure 3.11** displays the concentration of bound-radical versus time on a semi-logarithmic

scale. Bound-radicals from HQ decayed fastest with a lifetime of t = 27 min. The decay rate of bound-radical from CT was slightly lower than HQ with a lifetime of t = 36 min. The longest lifetime belonged to bound-radicals from P with a lifetime of t = 74 min. Radicals produced from 1,2-DCBz, MCBz, and 2-MCP also exhibited long lifetimes with t of 43 min, 56 min, and 64 min, respectively.

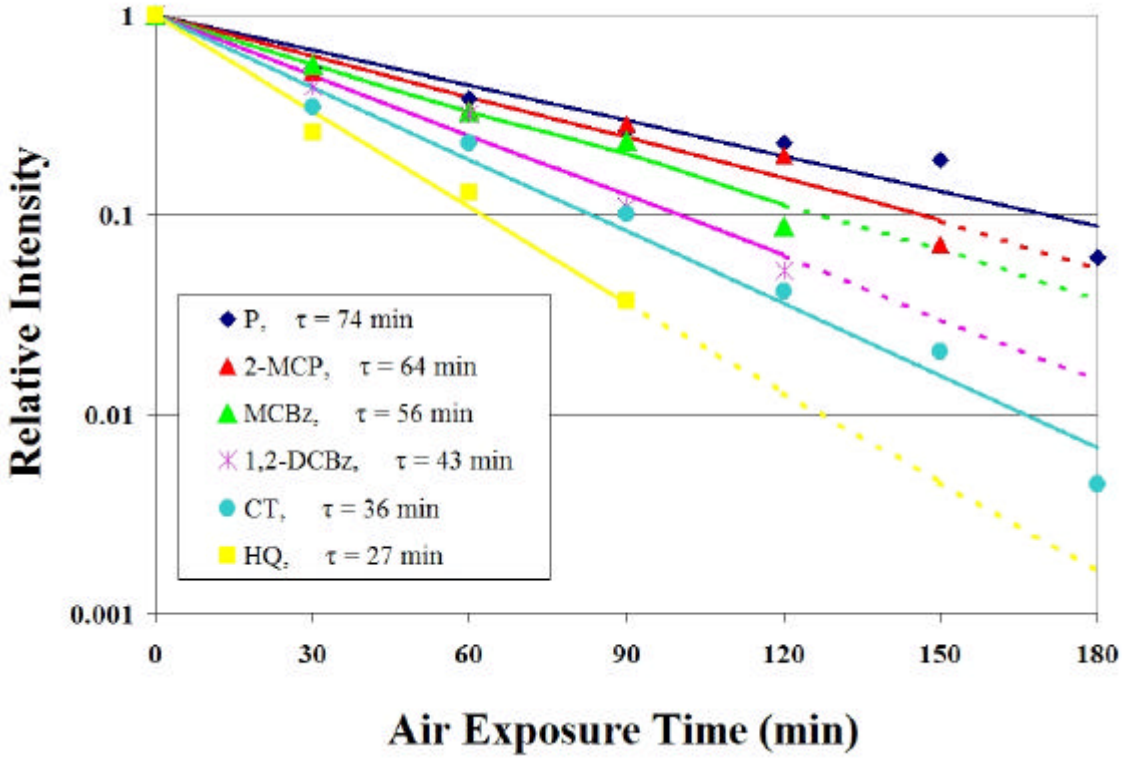

Figure 3.11: First Order Kinetic Decay of Surface-Bound Radicals

3.2.3 Extraction and Chemical Analysis of Surface-Bound Radicals

Surface bound-radicals were generated at 230°C from the six precursors then extracted from the matrix using several polar and non-polar solvents. Methyl alcohol (MEA) and isopropyl alcohol (IPA) were chosen as polar solvents while toluene (TOL) and

tert-butyl benzene (TBB) were chosen as non-polar solvents. Dichloromethane (DCM) was used as a solvent that had characteristic between polar and non-polar solvent.

Figure 3.12 illustrates the EPR radical signals from adsorbed phenol on 5% CuO/SiO_2 surface before and after extraction with IPA, polar solvent. A strong EPR signal (blue line) was observed before radical extraction (after adsorption of phenol molecule on the matrix) and a weak EPR signal (red line) was observed after radical extraction with IPA solvent. Both signals exhibit a g-value of 2.004. Before extraction, the EPR signal achieved a relative intensity peak-to-peak line-height of 2649 unit counts and the line-width of 6.2G. However, this EPR signal was reduced significantly to the relative intensity peak-to-peak line-height of 173 unit counts and line-width of 5.8G.

The EPR radical signals of the extract (using IPA as a solvent) from the adsorbed phenol matrix are presented in **Figure 3.13**. A weak EPR signal (red line) is exhibited in the original extract using isopropyl alcohol solvent and a strong signal (blue line) was exhibited with the addition of a few drops dilute sodium hydroxide (NaOH). The EPR radical signal intensity of the original extract achieved a relative peak-to-peak line-height of 46,000 unit counts and line-width of 3.0G. After adding a few drops of NaOH, this signal increases to the relative intensity peak-to-peak line-height of 89,000 unit counts with the same line-width. These signals exhibited a g-value of 2.005.

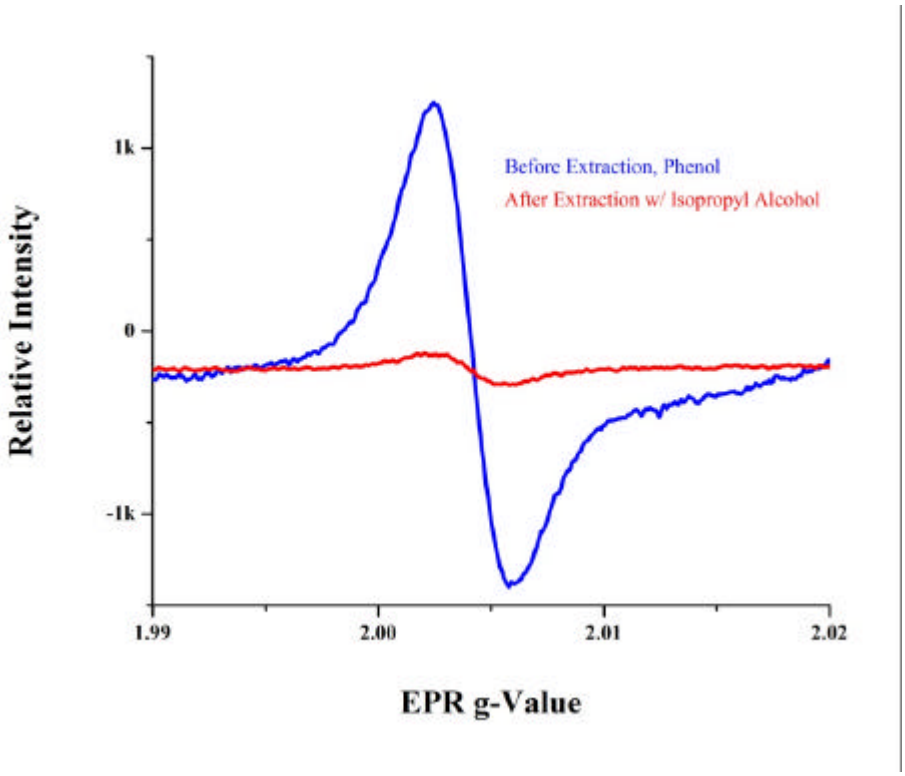

Figure 3.12: EPR Radical Signal of Residue from Chemisorbed Phenol on the Surface before and after Extraction Using Isopropyl Alcohol

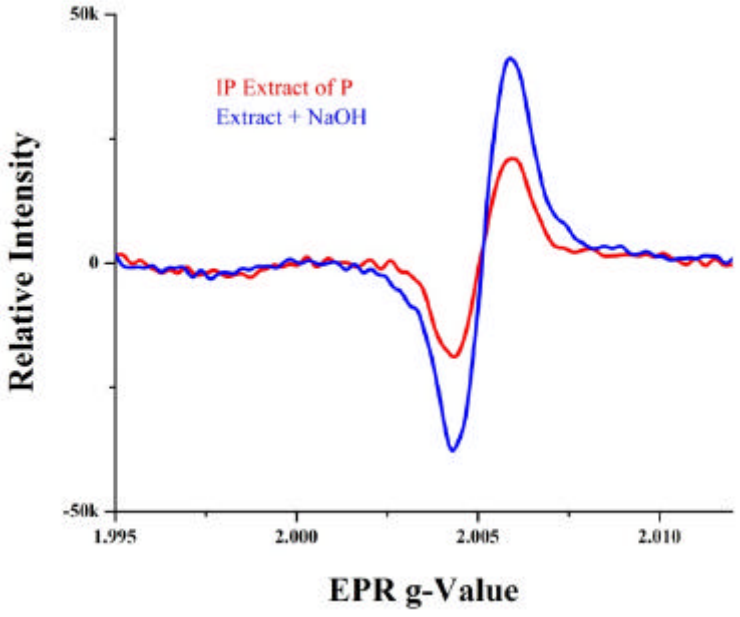

Figure 3.13: EPR Radical Signal of the Extract from Chemisorbed Phenol Matrix Using Isopropyl Alcohol as a Solvent

The EPR radical signals of the residue from the adsorbed phenol on the CuO/SiO_2 surface before and after extraction with toluene, non-polar solvent are presented in **figure 3.14**. These signals display a g-value of 2.004 and the line-width peak-to-peak of 5.1G. The EPR signal of bound radical before extraction exhibits the relative intensity peak-to-peak line-height of 14500 unit counts. After extraction with toluene, this signal only reduces by 12% to the relative intensity line-height of 12700 unit counts.

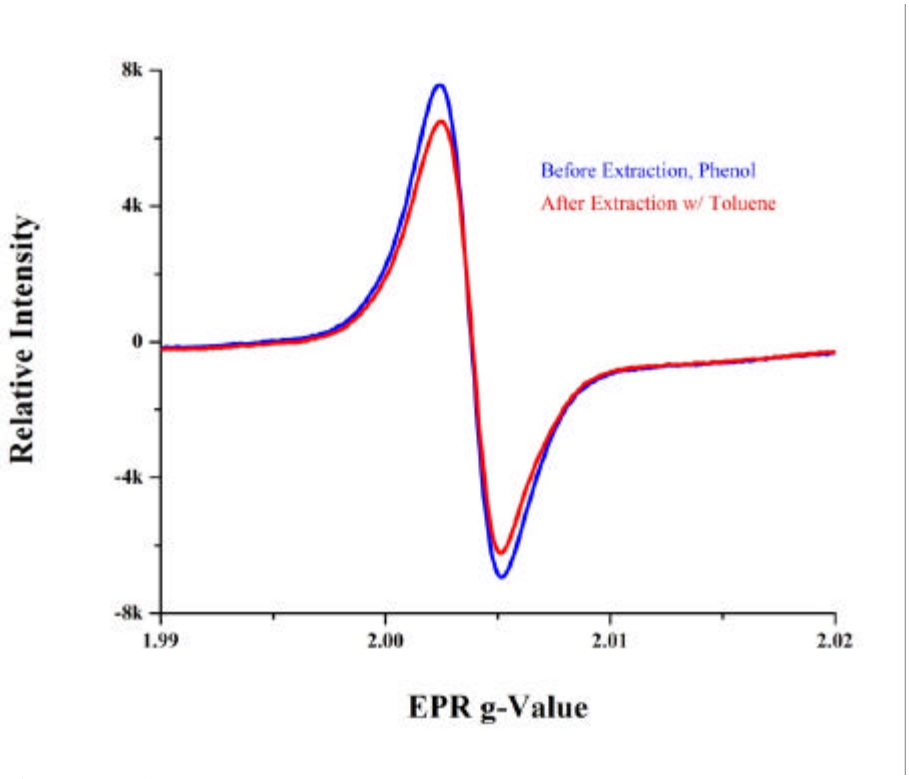

Figure 3.14: EPR Radical Signals of Residue from Chemisorbed Phenol on the Surface before and after Extraction with Toluene

The EPR spectra of the extract (using TOL as a solvent) from the adsorbed phenol matrix are presented in **Figure 3.15**. No EPR signal was observed in the original extract or after addition of a few drops dilutes NaOH. This observation was agreed with a previous observation of radical signals of the residue (c.f. **Figure 3.14**). Indeed, TOL did not extract radicals off the residue; therefore, no EPR signal was observed in the extract.

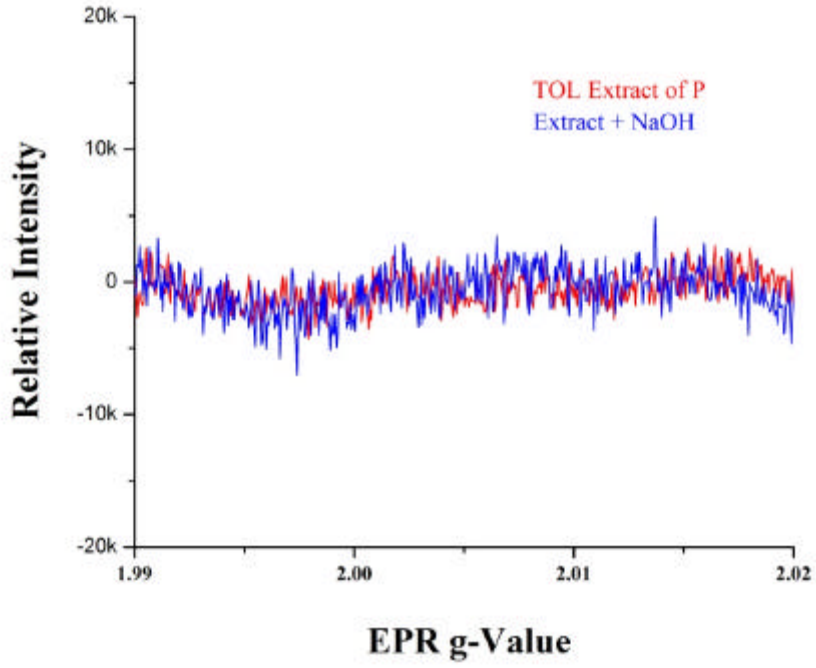

Figure 3.15: EPR Radical Signal of the Extract from Chemisorbed Phenol Matrix Using Toluene as a Solvent

Other precursors behaved similar to phenol that polar solvents (IPA and MEA) extracted more surface-bound radicals than non-polar solvents (TOL and TBB). In fact, EPR signal was reduced significantly after extraction with polar solvents and partially after extraction with non-polar solvents. Additionally, EPR signal was appeared in the extract polar solvents but not in the extract non-polar solvents.

Appendix 1 exhibits the EPR radical signal on the surface before and after extraction with different solvents and the EPR radical signal of the extract from other precursors including 2-MCP, MCBz, 1,2-DCBz, CT, and HQ. **Table 3.8** displays the summary the detection of EPR signal following solvent extraction from different precursors. **Table 3.9** summarizes the dielectric constants and pKa's of the solvents used in this study. **Figure**

3.16 presents dielectric constants versus percent reduction of EPR signal on the particle residue.

Table 3.8: Percent Reduction of EPR signal Following Solvent Extraction

Solvents	Phenol		2-MCP		MCBz		1,2-DCBz		CT		HQ	
	%R	Ext	%R	Ext	%R	Ext	%R	Ext	%R	Ext	%R	Ext
IPA	93	+	92	+	90	+	97	+	85	+	98	+
MEA	92	+	96	+	99	+	98	+	68	+	97	+
DCM	18	-	25	-	42	-	47	-	56	+	53	-
TOL	12	-	17	-	21	-	43	-	27	-	32	-
TBB	15	-	9	-	11	-	28	-	14	-	12	-

Where: %R is the percent reduction of EPR radical signal detected on the surface of residue after extraction, Ext (+) is EPR signal was detected in the extract, and Ext(-) is EPR signal was not detected in the extract.

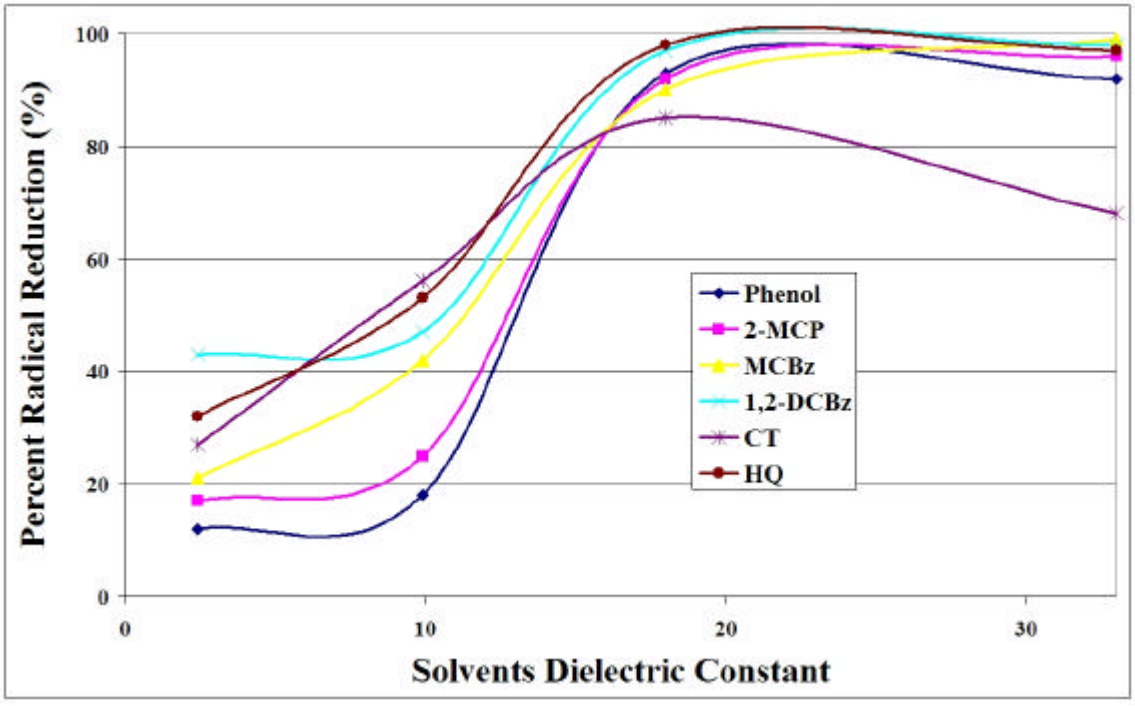

Figure 3.16: Solvents Dielectric Constants versus Radical Extractability

Table 3.9: Solvent Dielectric Constants and pKa's

Solvents	Dielectric Constant	pKa
TOL	2.4	40
TBB	2.3	>43[a]
MEA	33	16
IPA	18	19
DCM	9.9	~ 56[b]

[a.] From comparison with benzene (pKa = 43).
[b.] From comparison with methane (pKa = 56).

After injection of the original extract of chemisorbated phenol into GC-MS, many products were observed as shown in the **Table 3.10**. Only phenol was observed in non-polar solvents, while other products including dimer-type species were formed in polar solvents. **Table 4.10** also shows molecular products identify in solvent extracts from other precursors of 2-MCP, MCBz, DCBz, HQ, and CT.

Table 3.10: Observable Molecular Products in Solvent Extracts from Precursors

Absorbate	TOL	TBB	MEA	IPA	DCM
Phenol	Phenol (trace)	Phenol (trace)	Phenol, dibenzofuran, 2-phenoxyphenol	Phenol, dibenzofuran, 2-phenoxyphenol, dibenzo-p-dioxin	Phenol, dibenzofuran
2-MCP	2-MCP (trace)	2-MCP (trace)	Phenol, 2-MCP, dibenzo-p-dioxin, 2-chlorodibenzo-p-dioxin	2-MCP, phenol, dibenzo-p-dioxin, 2-chlorodibenzo-p-dioxin, 2,8-dichloro-dibenzofuran, 2,4'-dichloro-5-hydroxydiphenyl ether, 1,2-DCBz.	2-MCP
MCBz	None	None	1,2-DCBz, MCBz, 2-MCP, phenol, 2-chloro-diphenyl ether	MCBz 2-chloro-diphenyl ether,	MCBz, 1,2-DCBz, dibenzofuran
1,2-DCBz	1,2-DCBz (trace)	None	MCBz, 2-MCP, 1,2-DCBz	MCBz, 1,2-DCBz	1, 2-DCBz, 2-MCP, 1-chloro-naphthalene, CT
CT	CT (trace)	None	o-Benzoquinone, CT, phenol, 1, 2-DCBz, 2-phenoxyphenol	CT, phenol, 2- dibenzofuran, 2-phenoxyphenol	Phenol, CT
HQ	None	None	p-Benzoquinone	p-Benzoquinone	p-Benzoquinone

Figure 3.17 and **Figure 3.18** exhibit the products after extraction bound-radical generated from chemisorbed phenol molecule using non-polar and polar solvents respectively. Products after extraction with DCM solvent, which has characteristic between

polar and non-polar solvents, are presented in **Figure 3.19**. No dimers were observed after extraction with the non-polar TOL solvent; however, dibenzofuran was observed after extraction with DCM solvent. Dibenzofuran, 2-phenoxyphenol, and dibenzo-p-dioxin were also detected in the IPA extract.

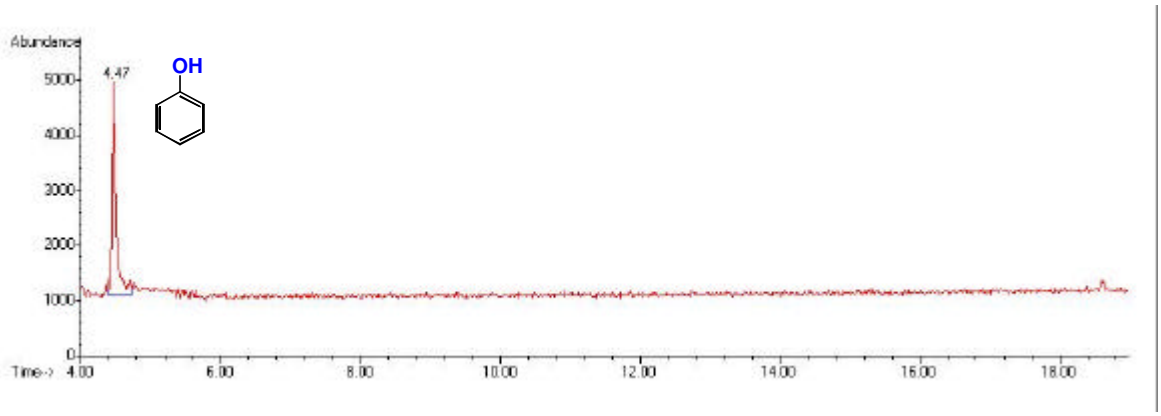

Figure 3.17: GC-MS Spectra of Product of Phenol after Extraction by Using TOL

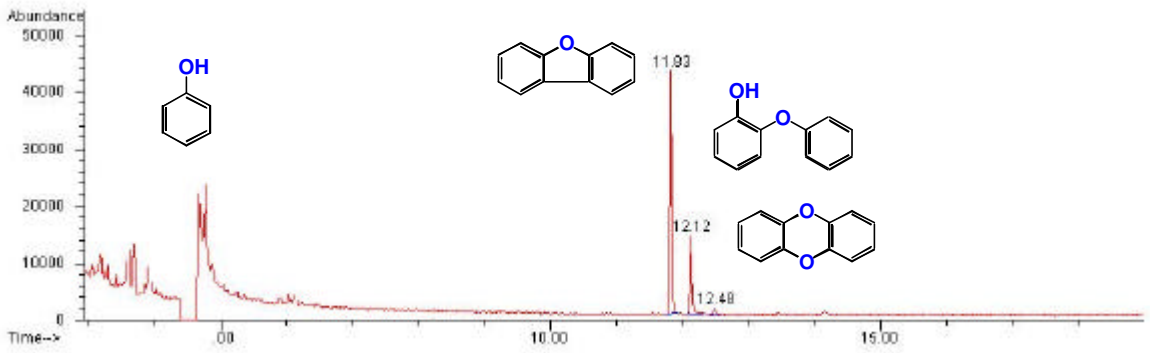

Figure 3.18: GC-MS Spectra of Products of Phenol after Extraction by Using IPA

Similar to phenol, many molecular products including dimer-type species were detected in the polar solvent extract and a few in non-polar extract from other adsorbated precursors. Appendix 1 displays the GC-MS analysis products of extracts of other

precursors including 2-MCP, MCBz, 1,2-DCBz, CT, and HQ. Appendix 2 exhibits the chromatogram of the extracts of precursors.

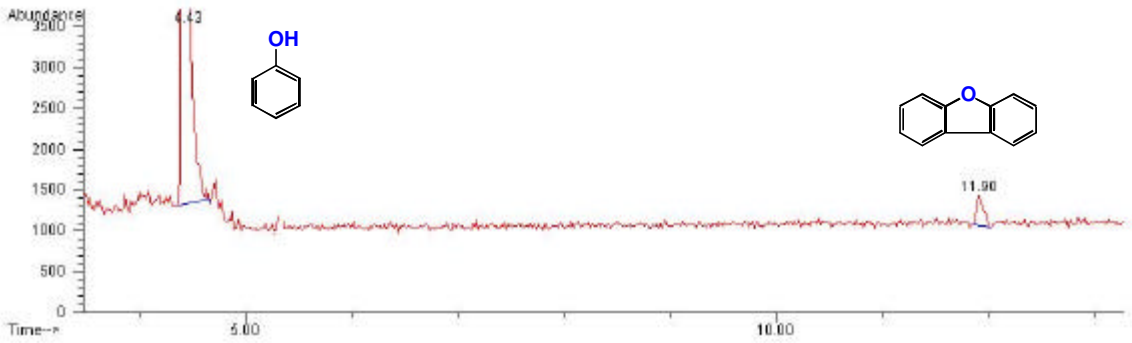

Figure 3.19: GC-MS Spectra of Products of Phenol after Extraction by Using DCM

3.2.4 Toxicology

Samples of radical-particle systems were prepared for Dr. Stephania Comier studied their toxicology toward human bronchia epithelial cells. Methyl cellulose was used as a media and a positive control while saponin was used as a negative control. Figure 3.20 exhibited the percent of survival cells after exposure to bound-radical from adsorbate 2-MCP on 5% CuO/SiO_2 surface for 24 hours. 300µg of particles resulted in only 80% cell viability while 3000µg of particles resulted in less than 10% cell viability.

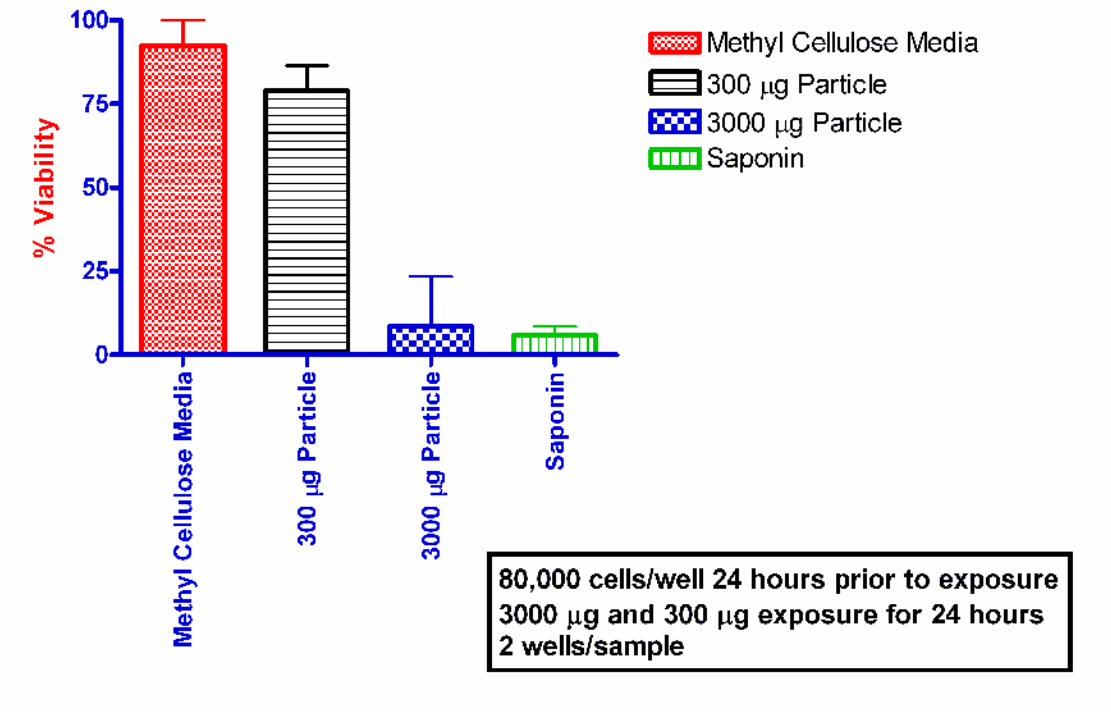

Figure 3.20: Percent of Viability of Cells after Exposure to Particle Containing Surface-Bound Radicals

CHAPTER 4: DISCUSSION

4.1 Thermal Degradation of Hydroquinone and Catechol in Gas-Phase

The study of the degradation of hydroquinone (HQ) and catechol (CT) helps to identify which persistent radical is formed during the thermal process. Although structurally similar, HQ and CT displayed different reaction pathways because of significant differences in their product distribution from thermal decomposition. Oxidation versus pyrolysis of HQ and CT also resulted in unusual changes in the product distribution.

4.1.1 Hydroquinone

In thermal degradation of HQ, the dominant product is *para*-benzoquinone (p-benzoquinone) at low temperature. At high temperatures above 650^{o}C other products such as phenol, benzene, styrene, indene, naphthalene, biphenylene, phenylethyne, dibenzofuran (DF), and dibenzo-p-doxin (DD) are formed during pyrolytic condition. Under oxidative condition, benzene, 4,4'-dihydroxybiphenyl, 4,4'-dihydroxydiphenyl ether, and cinnamaldehyde were formed in addition to the major product p-benzoquinone. Hydrogen-rich conditions initially inhibited HQ decomposition (below 500^{o}C) but promoted product formation at higher temperatures. The decomposition process apparently proceeds via formation of a resonance stabilized p-semiquinone radical.

4.1.1.2 Pyrolysis of HQ

Comprehensive product yield determinations from the high-temperature, gas-phase pyrolysis of hydroquinone in two operational modes (hydrogen rich and lean conditions) are studied at a reaction time of 2.0 seconds over a temperature range of 250^{o}C to 1000^{o}C. The

presence of an additional source of hydrogen had a significant impact on the pyrolysis of hydroquinone. Indeed, substantial differences in thermal stability of HQ at moderate temperatures (250°C - 550°C) are readily apparent. Over this temperature range, p-benzoquinone is the principal product of thermal degradation of HQ under both hydrogen rich and lean conditions.

Under hydrogen-lean conditions, the yield of p-benzoquinone remained constant at the level of 15% (c.f. **Figure 3.2**) while the presence of excess hydrogen seems to initially inhibit this process (below 1% yield at 250°C – c.f. **Figure 3.1**) with a gradual increase of the yield to 32% at 550°C. As demonstrated in the mechanistic discussion presented below, the addition of a hydrogen source promotes the back reaction of the initially-formed semiquinone radicals to convert back to molecular HQ.

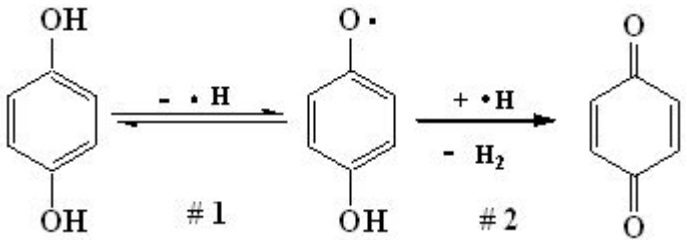

Scheme 4.1: Formation of p-Semiquinone Radical and p-Benzoquinone

p-Benzoquinone formation is initiated through the endothermic dissociation (ΔH_{rxn} = 80.8 kcal/mol) [1] of a phenoxyl-hydrogen bond to form p-semiquinone radical (rxn 1, **Scheme 4.1**). Dissociation of the second phenoxyl-hydrogen bond forms the observed p-benzoquinone. The presence of excess hydrogen from the solvent facilitates the reverse reaction through hydrogen addition, resulting in the obvious inhibition of semiquinone radical formation. However, as the temperature is increased, p-benzoquinone yield increases

in the presence of the excess of hydrogen atoms indicating of abstraction of the second phenoxyl hydrogen by hydrogen atom (rxn 2, **Scheme 4.1**).

The concentration of hydrogen atoms also impacts the phenol yield (c.f. **Figure 3.1** and **figure 3.2**). Phenol appears at 550°C under the hydrogen-rich condition while did not observe until 700°C under hydrogen-lean condition. This is attributable to the displacement of hydroxyl radical from HQ by hydrogen atoms (c.f. **Scheme 4.2**). Subsequent loss of the phenoxyl-hydrogen in phenol by unimolecular decomposition ($? H_{rxn}$ = 86 kcal/mol) [2] or abstraction (ΔH_{rxn} = 40 kcal/mol) [3] by hydrogen atoms forms phenoxyl radical (c.f. **Scheme 4.2**).

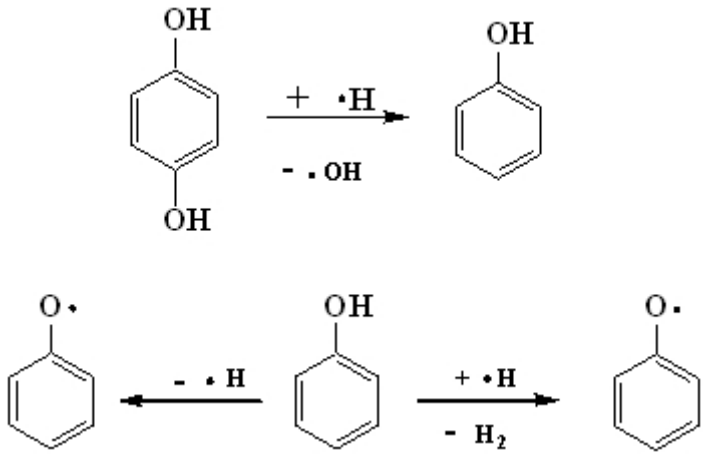

Scheme 4.2: Formation of Phenol and Phenoxyl Radical

The formation of dibenzo-p-dioxin (DD) and dibenzofuran (DF) are significantly affected by the presence of a hydrogen source. Under hydrogen-lean conditions, the appearance of the DF and DD coincide with phenol formation. This is in contrast to hydrogen-rich conditions, where only trace quantities of DF were detected above 800°C and DD was not detected at all (c.f. **Figure 3.1** and **Figure 3.2**).

The formation of polychlorinated dibenzo-p-dioxin/dibenzofuran PCDD/F in gas-phase [3-5] as well as on the surface[6-8] from chlorinated phenols have been studied extensively. It has been suggested that PCDD/F formation is mainly due to radical-radical reactions. **Schemes 4.3** and **Scheme 4.4** are proposed as the DF and DD formation pathways involving phenoxyl radical-radical recombination and phenoxyl-phenol radical-molecule reactions. In the radical-radical pathway of DF formation, two phenoxyl radicals in their keto-form recombine to form a dimer intermediate (? H_{rxn} = -13.8 kcal/mol) [9]. The latter intermediate can either tautomerize to 2,2-dihydroxybiphenyl (? H_{rx} = 18.3 kcal/mol) [9] followed by an intra-molecular water elimination process to form DF (? H_{rxn} = 64.7 kcal/mol) [9] (upper pathway in scheme 4.3) or undergo a hydrogen abstraction followed by intra-molecular inter-ring displacement of hydroxyl radical to form DF (lower pathway in **Scheme 4.3**).

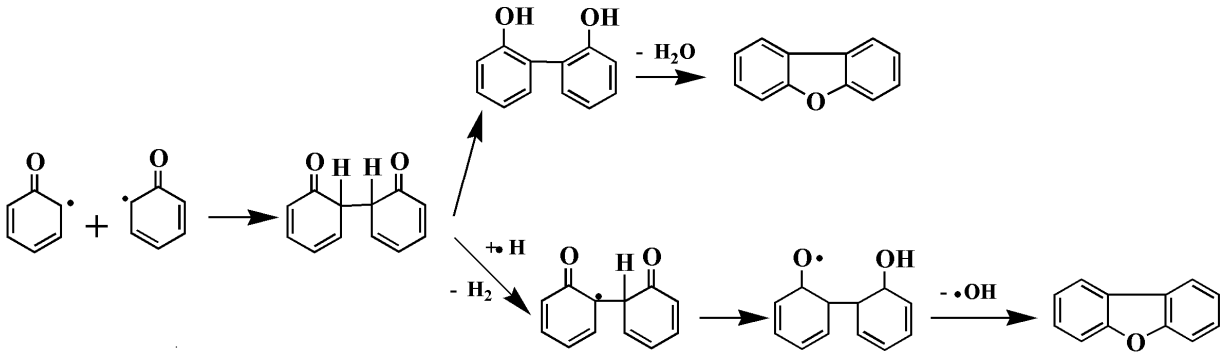

Scheme 4.3: Formation of DF from Radical-Radical Recombination Reactions [10]

The enol form of the phenoxyl radical displaces a ring hydrogen of the phenol molecule to form a hydroxy-biphenyl ether intermediate which is followed by a ring closure process via intra-molecular inter-ring displacement of hydrogen. Non-chlorinated phenoxyl radicals have been studied and DF formation is preferred over DD formation through the radical-radical pathway [3].

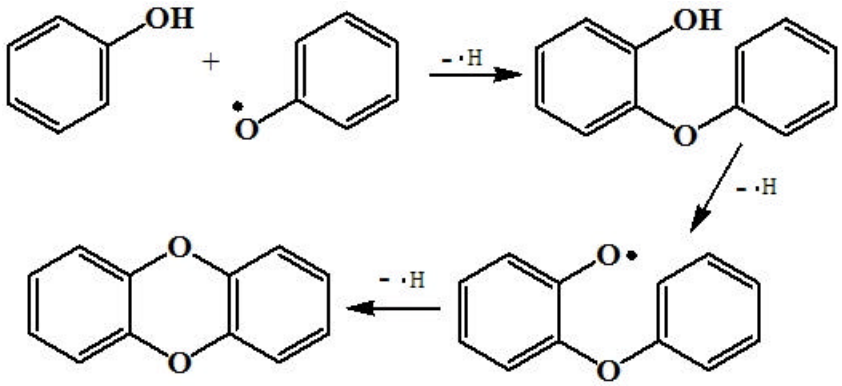

Scheme 4.4: DD formation from the radical-molecule reactions

Increases in benzene concentration correspond to the reduction of DD and DF yields under hydrogen-rich conditions. The mechanism for benzene formation via displacement of hydroxyl by a hydrogen atom in phenol is presented in **Scheme 4.5** ($?H_{rxn}$ = 4.0 kcal/mol) [10]. Both DD or DF formation and benzene formation require phenol or phenoxyl radicals as a reactant; thus they compete for phenol. The reduction of DD and DF yields in the presence of a hydrogen-rich source is attributable to an increase in the rate of benzene formation. Consequently, the increase in benzene yield results in reducing the concentration of phenoxyl radicals that is required for the formation of DD and DF.

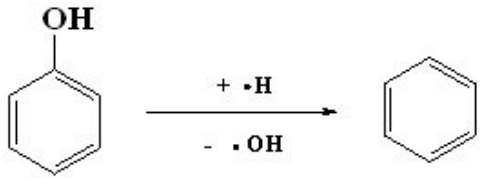

Scheme 4.5: Benzene formation from phenol

The substituted aromatic species such as styrene, indene, naphthalene, biphenylene, and phenylethyne do not form until above 700°C. They correspond to the complete destruction of HQ into smaller C2, C3, and C4 fragments that can undergo molecular growth

to form the observed species. These types of products are consistently observed from pyrolysis of hydrocarbon species and their mechanisms of formation are well established [11-13]. However, HQ may promote formation of substituted aromatic species through formation of cyclopentadienyl radical by elimination of CO from phenoxyl radical [11, 14] (c.f. **Scheme 4.6**).

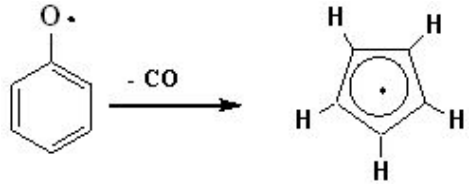

Scheme 4.6: Cyclopentadienyl Radical Formation

The activation energy for this unimolecular decomposition reaction is about 52 kcal/mol which is significantly higher than its enthalpy, ? H = 20 kcal/mol [15, 16], but still low enough to result in significant product formation. Homogeneous radical-radical recombination of cyclopentadienyl radicals is known to form naphthalene as depicted in **Scheme 4.7** [17].

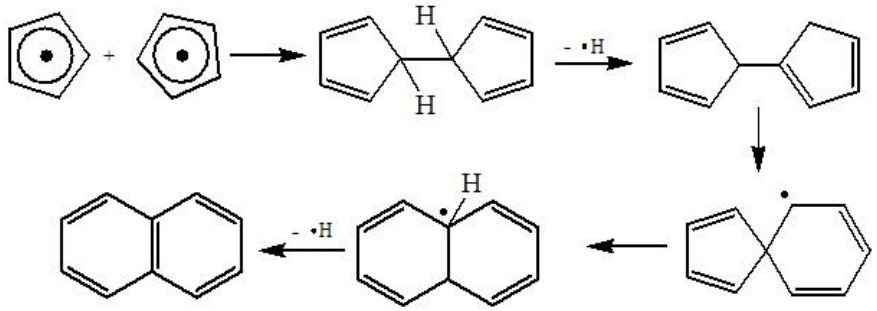

Scheme 4.7: Naphthalene Formation

Although not directly observable in this study, pyrolysis of HQ forms persistent free radicals including p-semiquinone, phenoxyl, and cyclopentadienyl that are strongly reducing

agents and suspect causative agents of cancer, heart disease and lung disease [18-28]. The formation of p-semiquinone radical is strongly implied because of the observation of p-benzoquinone as the only molecular product over the temperature range of 250°C to 700°C. Formation of phenoxyl is implied by the detection of molecular phenol over the temperature range of 550°C to 900°C. Also, formation of cyclopentadienyl is implied by the formation of naphthalene above the temperature of 700°C.

4.1.1.2 Oxidation of HQ

From oxidation of HQ, p-benzoquinone was a major product at all temperature; however, phenol was not observed. Under oxidative conditions, hydroxyl radical abstracted a hydrogen atom from hydroxyl group in HQ to form p-semiquinone radical (c.f. **Scheme 4.8**). Subsequent loss of the second hydroxyl-hydrogen from semiquinone radical results in p-benzoquinone formation (c.f. **Scheme 4.8**).

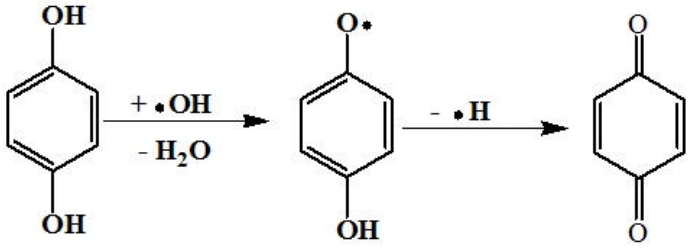

Scheme 4.8: p-Semiquinone Radical and p-Benzoquinone Formation

Difference from pyrolysis, oxygen enhances the rate of thermal decomposition of HQ under oxidation extensively. The formation of 4,4'-hydroxybiphenyl can be readily accounted for by the recombination reaction of two p-hydroxy-phenyl radicals or the radical-molecule reaction of p-hydroxy-phenyl radical with HQ as depicted in **Scheme 4.9.** Their formation could be attributed to the tautomerization of phenoxyl radicals formed from

phenol as was observed in the pyrolysis of HQ. However, phenol was not observed in the oxidation studies.

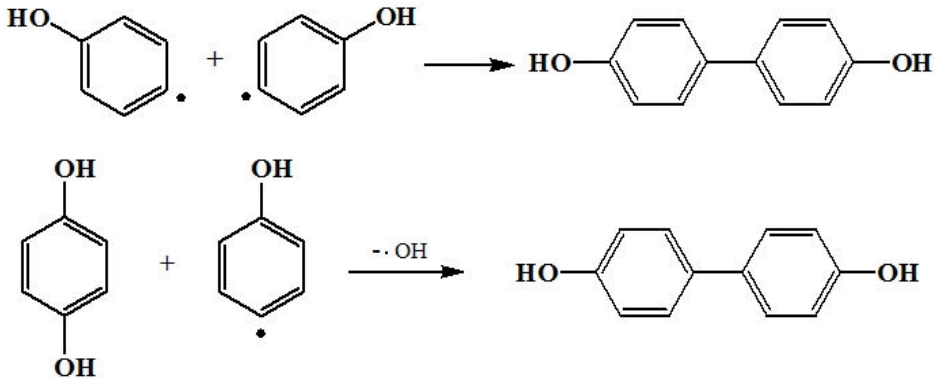

Scheme 4.9: Formation of 4,4' hydroxylbiphenyl

However, purely gas-phase pathways to p-hydroxy-phenyl radicals appear improbable, and a surface-assisted pathway is suspected. Substituted phenols may chemisorb to silica to form surface-associated phenolates as depicted in **Scheme 4.10**. Subsequent rupture of the phenyl-oxygen bond results in the formation of the p-hydroxy-phenyl radical which then reacts via the gas-phase reactions depicted in **Scheme 4.9**.

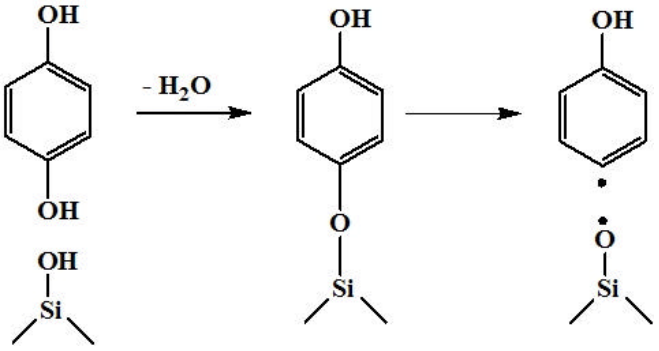

Scheme 4.10: Silica Surface-Mediated Formation of p-Hydroxy-Phenyl Radical

Conversion of HQ to benzene would appear to involve displacement of two hydroxyl groups which should form phenol as an intermediate. Although phenol was observed during

pyrolysis studies, it was not observed under oxidation conditions; therefore, the gas-phase pathway appears improbable. **Scheme 4.11** is proposed a surface-mediated loss of both hydroxyl substituents from HQ. The resulting phenyl diradical can abstract phenoxyl-hydrogens from HQ to form benzene and p-BQ if a single HQ is involved (or p-SQ if two HQ are involved).

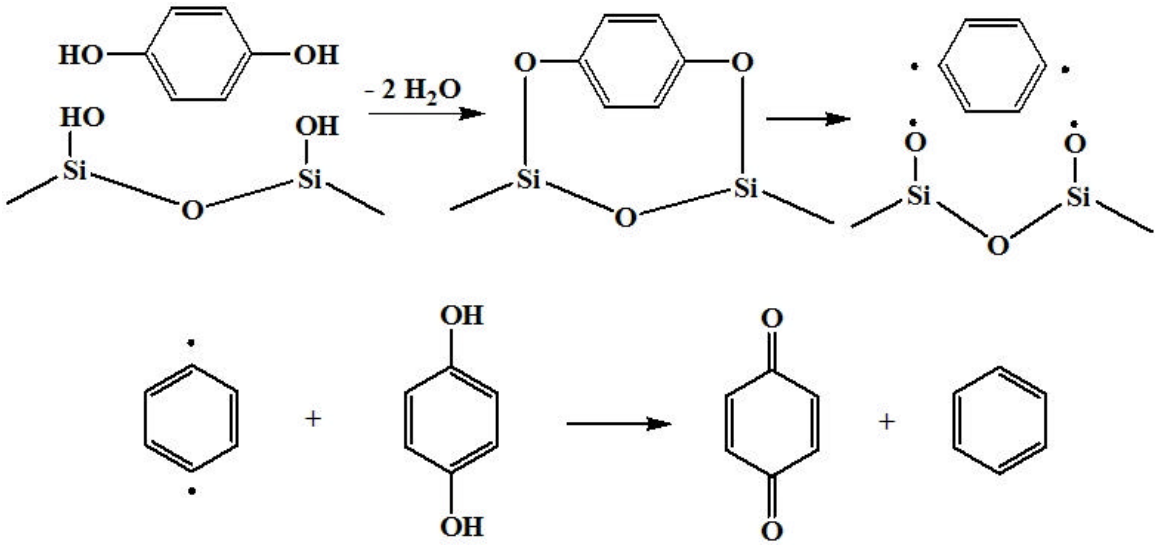

Scheme 4.11: The formation of benzene via a surface-mediated reaction of HQ

Over the same temperature range, traces of 4,4'-dihydroxydiphenyl ether begins to form as well as 4,4' hydroxylbiphenyl. The proposed mechanism is presented in **Scheme 4.12**. The oxygen-centered radical or enol-form of semiquinone radical displaces one hydroxyl group of hydroquinone to form 4,4'-dihydroxydiphenyl ether. This agrees with the reduction of both hydroquinone and p-benzoquinone over the same temperature range that 4,4'-dihydroxydiphenyl ether is formed.

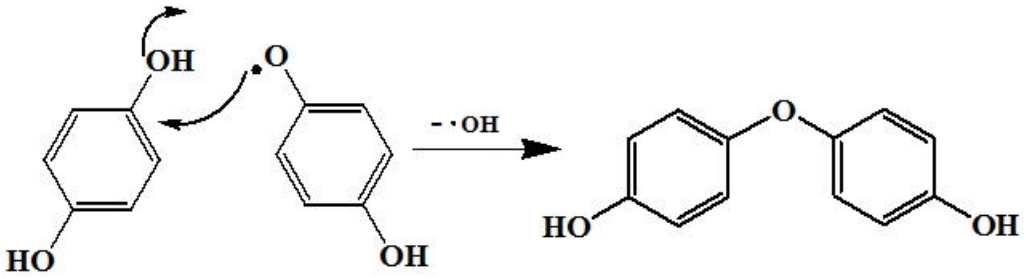

Scheme 4.12: 4,4'-Dihydroxydiphenyl Ether Formation from Semiquinone Radical

The formation of p-semiquinone radical is strongly implied because of the observation of p-benzoquinone over a wide temperature range of 200°C to 700°C under oxidative condition. The significant difference in the oxidation and pyrolysis of HQ is the presence of hydroxyl radicals that can readily abstract hydroxyl-hydrogen of HQ under oxidative condition. Consequently, this increases the yield of p-semiquinone radicals as evidenced by the formation of p-benzoquinone. This difference in oxidative and pyrolytic degradation behavior is even more apparent for CT.

4.1.2 Catechol

Thermal degradation of CT yielded a variety of products similar to thermal degradation of HQ. However, ortho-benzoquinone (o-benzoquinone) was not observed in pyrolysis of CT. Other products from pyrolysis of CT are phenol, benzene, dibenzofuran (DF), dibenzo-p-dioxin (DD), phenylethyne, styrene, indene, anthracene, naphthalene, and biphenylene. The absence of o-benzoquinone in the products of pyrolysis of CT is a result of an intra-molecular water elimination reaction between two ortho hydroxyl groups in CT molecule. In contrast to pyrolytic condition, o-benzoquinone was detected instantaneously upon degradation of CT under oxidative conditions because oxygen facilitated hydrogen abstraction at low temperature before water elimination was eventually feasible. Fewer

products were observed from the oxidation of CT; however, the additional products including 2,2'-dihydroxydiphenyl ether and 1,2-dihydroxy-naphthalene were observed above 400°C.

4.1.2.1 Pyrolysis of CT

CT and HQ are both dihydroxyl benzenes, with the hydroxyl groups located in *ortho* and *para* positions, respectively. Based on their structural similarities, similar products of their thermal degradation were expected. However, the lack of o-benzoquinone in the products of CT thermal degradation was unexpected and led to a conclusion that the mechanisms of initial decomposition of CT and HQ are very different despite to the structural similarities. The hydroxyl bond dissociation energy is required ΔH_{rxn} = 79.3 kcal/mol for CT and ΔH_{rxn} = 80.8 kcal/mol for hydroquinone [1]. However, the close proximity of the two otho-hydroxyl groups in CT enables an intra-molecular water elimination process that is thermodynamically much for favorable (ΔH_{rxn} = 22.5-38.5 kcal/mol) [29], even though concerted processes can have activation energies considerably higher than their endothermicity. **Scheme 4.13** presents the intra-molecular elimination of water in CT that result in the formation of an epoxide. Epoxides are difficult to detect by GC because they readily react with the column stationary phase.

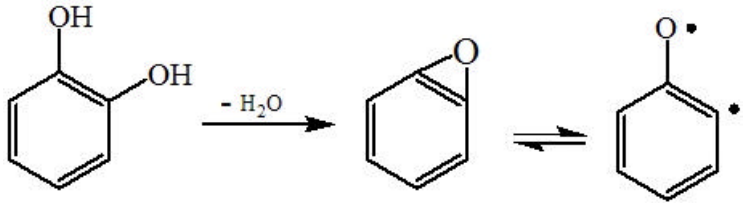

Scheme 4.13: Internal Water Elimination Reaction in CT Pyrolysis

Phenol was the first observable product at 600°C. The epoxy-benzene (or alternate diradical form) reacts rapidly with hydrogen atom (probably via extraction from CT or the isopropyl alcohol with some contribution from recombination with hydrogen atoms) to form phenol. Indeed, the percent yield of phenol in hydrogen-rich condition is 10 times higher than the percent yield of phenol under hydrogen-lean condition. **Scheme 4.14** presents the phenol formation through a hydrogen addition to epoxy-benzene. This reaction is exothermic with the enthalpy in the range of ΔH = -46.6 to -51.9 kcal/mol [29]. As the temperature increases, the yield of phenol increases with increasing CT decomposition (and probably increasing epoxy-benzene formation as an intermediate).

Benzene was detected at higher temperatures than phenol and appeared as phenol decomposed, indicating it is formed by displacement of the hydroxyl group by hydrogen atom in phenol molecule (c.f. **Scheme 4.5**). Benzene is formed at much higher yield and in wider range of temperatures under hydrogen-rich conditions than under hydrogen-lean condition confirming the role of hydrogen atoms in its formation.

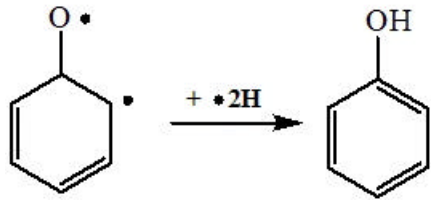

Scheme 4.14: Phenol Formation from Di-Radical

The majority of products are formed above the temperature of 700°C under hydrogen-rich and 800°C under hydrogen lean conditions (c.f. **Figure 3.4** and **Figure 3.5**). Much higher yields of the poly-aromatic products were observed under hydrogen-rich

conditions which are attributable to formation of the molecular poly-aromatic by recombination of the analogous radical with hydrogen atoms.

Elimination of CO from phenoxyl radical yields cyclopentadienyl radical (c.f. **Scheme 4.6**), and cyclopentadienyl radicals have been strongly implicated in the formation of naphthalene (c.f. **Scheme 4.7**). The formation of anthracene is believed from the combination of three cyclopentadienyl radicals according to its structure formula is similar to naphthalene (c.f. **Scheme 4.15**).

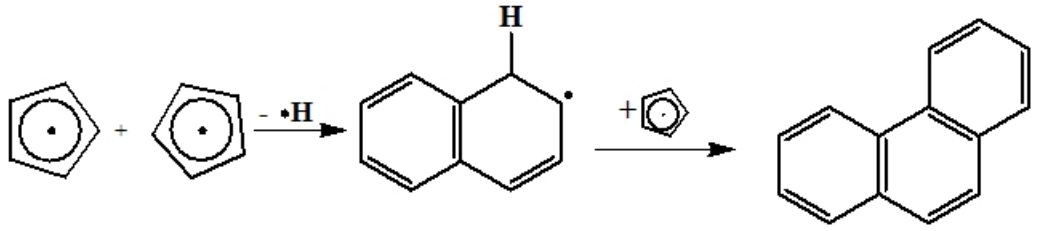

Scheme 4.15: Anthracene Formation

During thermal degradation of CT under hydrogen-rich conditions, significant levels of Dibenzofuran (DF) and dibenzo-p-dioxin (DD) were detected. However, only low levels of DF and no DD were formed under hydrogen-lean conditions. The formation of DF and DD is most likely a result of reactions involving the epoxy species that can exist as relatively stable diradical resonance form. Interaction of the epoxy-benzene with a molecular CT results in DF formation (c.f. **Scheme 4.16**). In the di-radical resonance form, the oxygen-centered radial displaces one of hydroxyl groups from CT to form hydroxyl-biphenyl ether intermediate followed by the ring closure via the displacement of hydroxyl by the carbon-centered radical to form DF (c.f. **Scheme 4.16**).

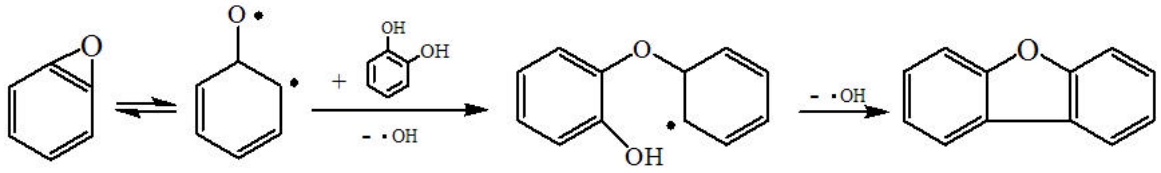

Scheme 4.16: DF Formation from Epoxy-benzene

Recombination of two epoxy-benzenes or diradicals forms DD as prososed in **Scheme 4.17**. The higher yield of DF compared to DD is consistent with the low concentration of epoxide or diradicals that favors the DF radical-molecule formation pathway over the radical-radical recombination pathway that leads to DD.

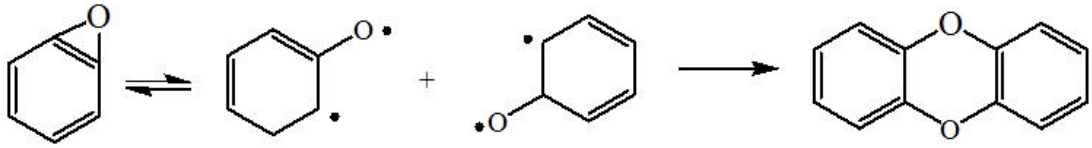

Scheme 4.17: DD Formation from Recombination of Two Epoxy-benzenes

Under hydrogen-rich conditions, complete decomposition of CT shifts about 100°C lower than under hydrogen-lean conditions. This phenomenon suggests involvement of hydrogen atoms in the formation of phenol. The yield of phenol increases drastically from 600°C to 800°C when excess hydrogen source is available in the reaction feed (c.f. **Scheme 4.14**). The formation of phenoxyl radical is in the intermediate steps of phenol formation. In fact, addition of one hydrogen atom to epoxy-benzene or diradical species yields phenoxyl radicals (c.f. **Scheme 4.18**).

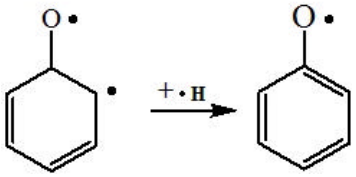

Scheme 4.18: Phenoxyl Radical Formation

The formation of phenoxyl radical significantly contributes to DD and DF formation. The combination of two keto form of phenoxyl radicals yields DF (c.f. **Scheme 4.3**) and the interaction of enol form of phenoxyl radicals with molecular phenol yields DD (c.f. **Scheme 4.4**). Also, keto form of phenoxyl radicals interacts with epoxy-benzene will yields DF as proposing in **Scheme 4.19** bellow.

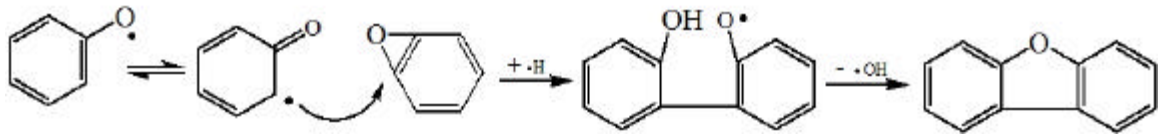

Scheme 4.19: DF Formation from Phenoxyl Radical and Epoxy-Benzene

The keto form of phenoxyl radical displaces a hydroxyl-hydrogen of phenol to form dimer radical intermediate and followed by the ring closure process through intra-molecular inter-ring displacement of hydrogen to form DD. **Scheme 4.20** presents the formation of DD from phenoxyl radical and phenol.

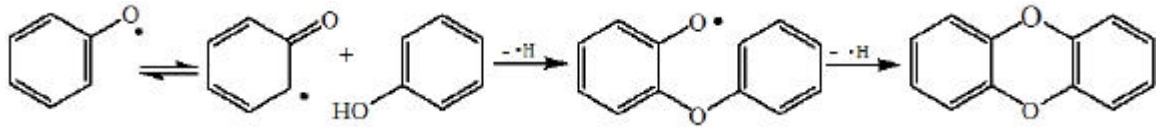

Scheme 4.20: DD Formation from Phenoxyl Radical and Phenol

The lack of o-benzoquinone formation in the products of pyrolysis of CT led to a conclusion that CT initially decomposed through intra-molecular elimination of water due to the close proximity of the two hydroxyl group in CT. Detection of molecular phenol over the temperature range of 550^{o}C to 900^{o}C indirectly infers of diradical and phenoxyl radcial

formation. The formation of cyclopentadienyl is implied by the formation of naphthalene above the temperature of 750°C.

4.1.2.2 Oxidation of CT

In contrast to pyrolysis of CT, the formation of o-benzoquinone was detected instantaneously upon degradation of CT at 200°C for oxidation of CT. Under oxidative condition, the presence of hydroxyl radical in the system increases the rate of reaction of CT at lower temperatures through promotion of the abstraction of the phenolic hydrogens in CT.

Under pyrolytic conditions, the principal decomposition pathway for CT was the elimination of water from the ortho-hydroxy groups to form the epoxide. This pathway was not available in HQ, which instead formed *p*-benzoquinone. Under pyrolytic conditions, formation of either *o*- benzoquinone or *p*- benzoquinone from CT or HQ, respectively, would require the abstraction of a hydroxyl-hydrogen by hydrogen atom. This reaction cannot compete with the more rapid elimination of water for CT under pyrolytic conditions. However, under oxidative conditions, hydroxyl radicals are now present in sufficient concentration for hydrogen abstraction to occur that results in the formation of an *o*-semiquinone radical.

o-Semiquinone radical may decompose by unimolecular decomposition of the second oxygen-hydrogen bond to form o-BQ. Abstraction of the second hydroxyl hydrogen by hydroxyl radical may also contribute because of the possibly unusually high concentration of *o*-semiquinone due to its reported stability and resistance to reaction with oxygen [30, 31]. **Scheme 4.21** displays the formation of *o*-semiquinone and *o*-benzoquinone from decomposition of CT.

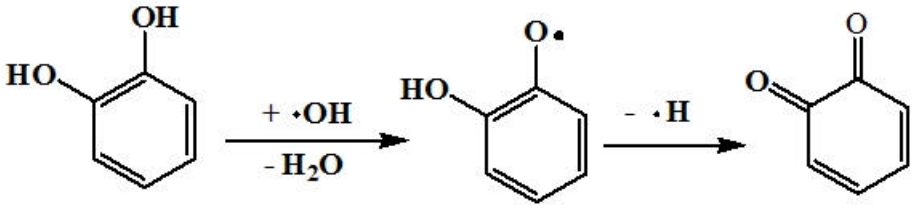

Scheme 4.21: *o*-Semiquinone and *o*-Benzoquinone Formation

CT rapidly degraded as the temperature increased and completely decomposed at 600°C while o-benzoquinone was still observed until 700°C. Decomposition of CT produced 1, 8-dihydroxynaphthalene below 700 C in trace quantities. Naphthalene is known to be formed by recombination of cyclopentadienyl radicals that formed by the elimination of CO from phenoxyl radical (c.f. **Scheme 4.6** and **Scheme 4.7**). Hydroxy-cyclopentadienyl radicals can be formed by elimination of CO from *o*-semiquinone. Recombination of two hydroxy- cyclopentadienyl radicals result in the formation of the 1, 8-dihydroxynaphthalene by a mechanism analogous to that of formation of naphthalene from cyclopentadienyl. **Scheme 4.21** displays the formation of 1, 8-dihydroxynaphthalene from o-semiquinone radical. Hydroxy-naphthalenes likely do not form from the thermal oxidation of HQ (*vide infra)* because of the high rate of the conversion of the intermediate *p*-semiquinone radical to *p*-benzoquinone rather than hydroxy- cyclopentadienyl.

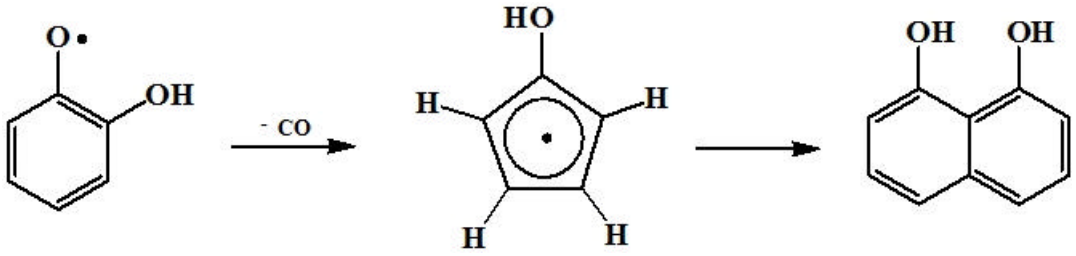

Scheme 4.21: 1,8-Dihydroxynaphalene Formation from *o*-semiquinone radical

The yield of CT and *o*-benzoquinone drastically decreased as the yield of 2,2'-dihydroxydiphenyl ether increased. The enol form of *o*-semiquinone displaces one of hydroxyl groups of CT to form 2,2'-dihydroxydiphenyl ether. **Scheme 4.22** presents the formation of 2,2'-dihydroxydiphenyl ether.

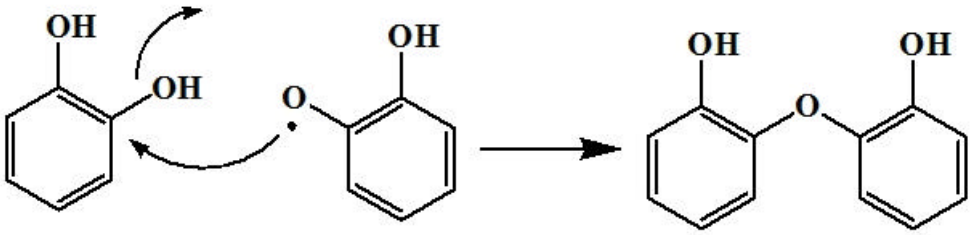

Scheme 4.22: 2,2'-Dihydroxydiphenyl Ether Formation

Formation of semiquinone-type radical is implied due to observation of *o*-benzoquinone under oxidative condition. Although oxygen facilitated the decomposition of CT as well as the products, *o*-benzoquinone still existed over a wide range of temperature and interacted with CT to form dimers. Hydroxy- cyclopentadienyl radicals may also imply because of the formation of 1,8- dihydroxynaphalene. Phenoxyl-type radical may not implied under oxidative condition; however, phenol was detected under pyrolytic condition that suggests possible formation of semiquinone-type and phenoxyl-type radicals over some reactive surfaces

4.2 Surface-Bound Radicals

Our group and other researchers have previously suggested that surface-bound radicals are formed during the adsorption of organic molecules on metal oxides[6, 32-37]. This is hypothesis to be theory chemisorption of organic molecules onto a metal surface followed by reduction of the metal to form surface-bound radicals. **Figure 4.1** presents the general formation of surface-bound radicals from interaction of organic molecules and metal

surface. In order to prove this hypothesis, the nature of semiquinone-type and phenoxyl-type radicals was studied by using transition metal copper oxide supported on silica as a surrogate of combustion generated fly-ash.

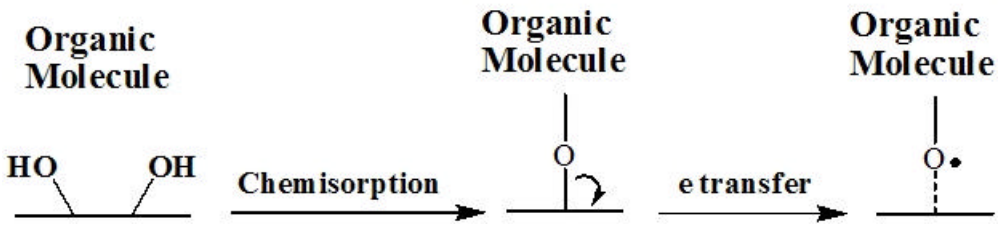

Figure 4.1: Formation of Surface-Bound Radicals

4.2.1 Formation and Stabilization of Surface-Bound Radicals

HQ and CT are chosen as potential precursors for semiquinone radicals due to their molecular structures are very similar to semiquinone radicals; 2-MCP may also form semiquinone radical. MCBz and phenol are chosen as potential precursors for phenoxyl radicals; 1,2-DCBz and 2-MCP are chosen as potential precursors for 2-chlorophenoxyl radicals. MCBz and 1,2-DCBz may chemisorb with the surface and form surface- bound radicals through the elimination of hydrogen chloride (c.f. **Scheme 4.23a and Scheme 4.23b**).

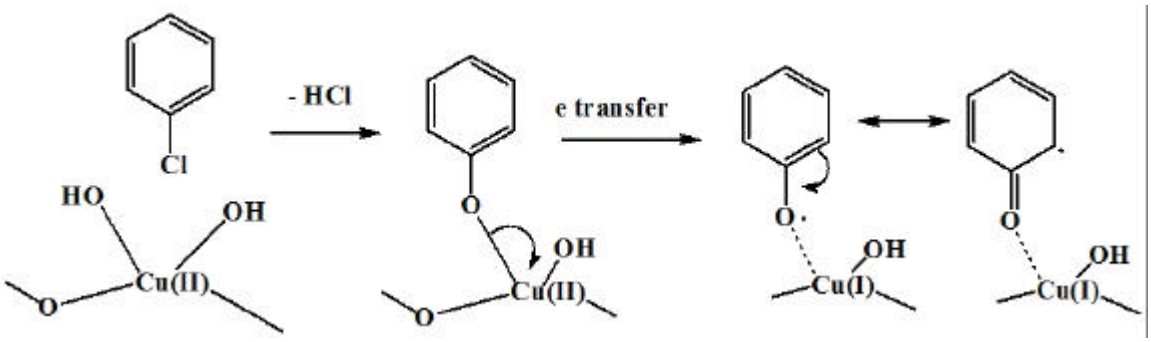

Scheme 4.23a: Surface-Bound Radical Formation from MCBz

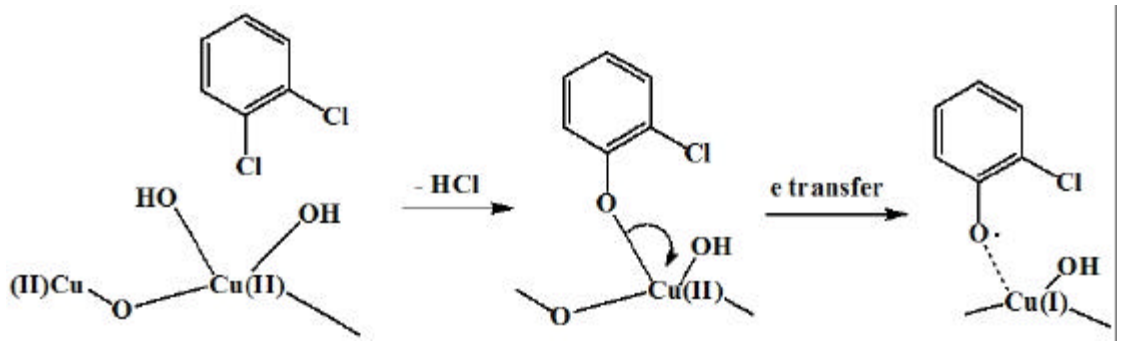

Scheme 4.23b: Surface-Bound Radical Formation from 1,2-DCBz

Chlorinated benzene binds to the surface at chlorine site and induces hydrogen to release hydrogen chloride due to weak bond between chlorine and benzene ring. Electrons transfer and reduction of the copper in chemisorption result in formation of surface-bound radicals.

HQ, CT, and P form surface-bound radicals through water elimination when they associate with CuO/SiO_2 surface (c.f. **Scheme 4.24a and Scheme 4.24b**). Hydroxylated benzenes bind to the surface at hydroxyl site and interact with hydroxyl group from the surface to release water. Again, electrons transfer and reduction of the copper in chemisorption from the surface generate surface-bound radicals.

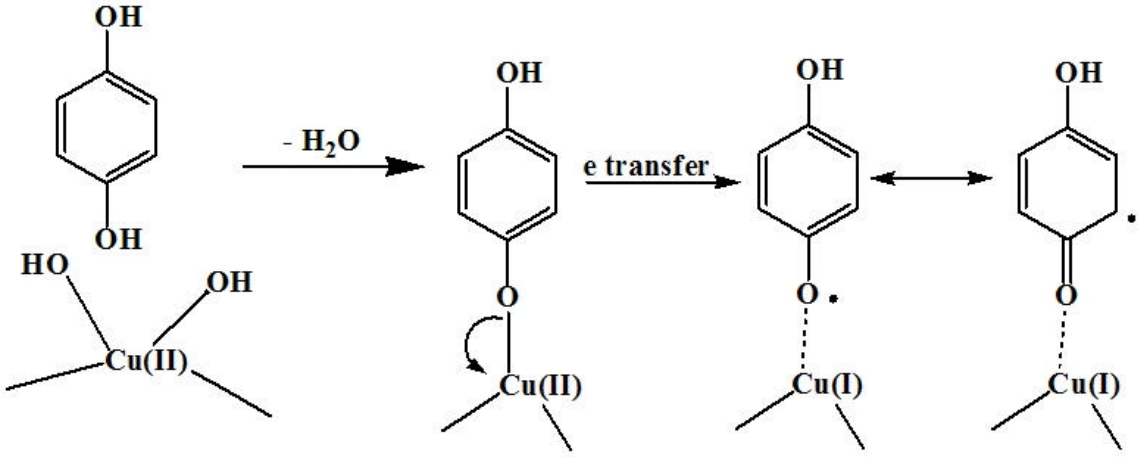

Scheme 4.24a: Surface-Bound Radical Formation from HQ

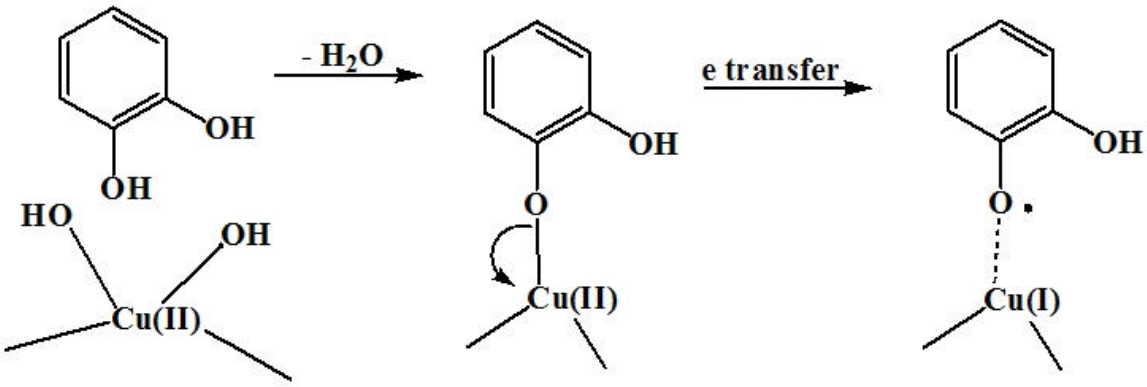

Scheme 4.24b: Surface-Bound Radical Formation from CT

However, 2-MCP can form radicals initially through either hydrogen chloride or water elimination route because it contains both chlorine and hydroxyl substitutents. **Scheme 4.25** displays the formation of bound-radical from 2-MCP.

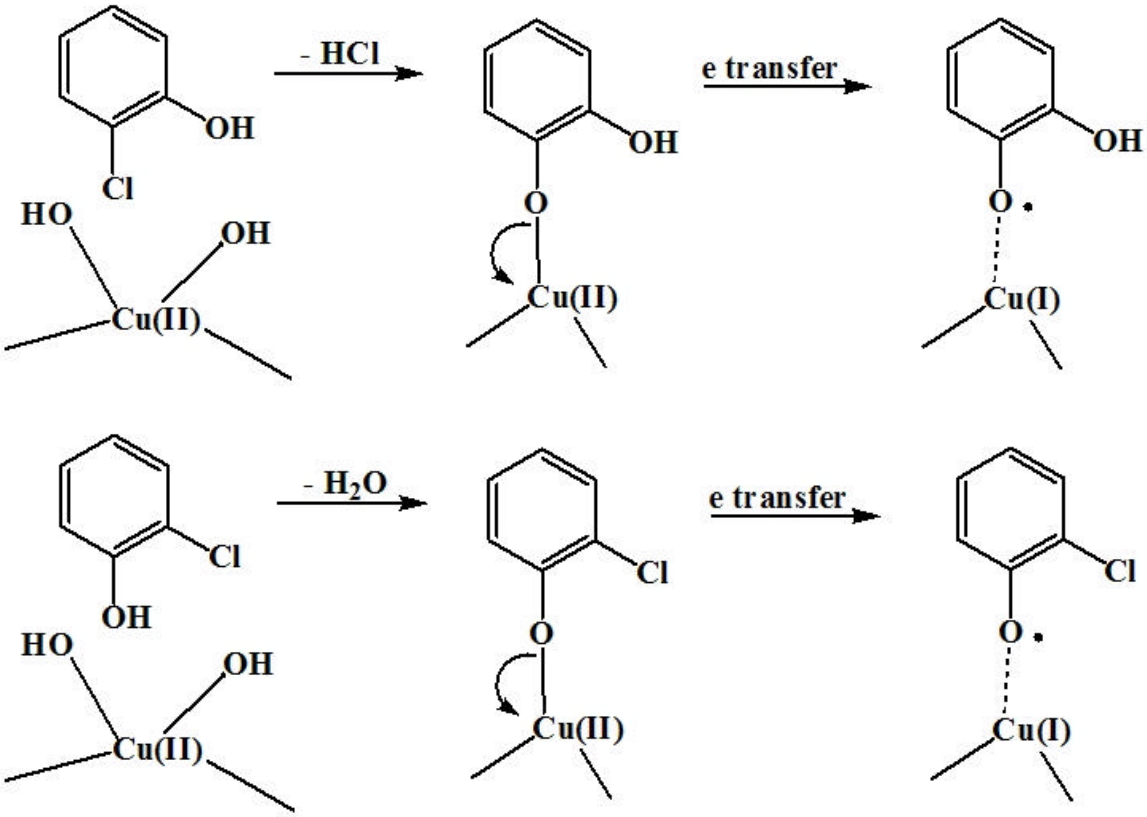

Scheme 4.25: Surface-Bound Radical Formation from 2-MCP

Semiquinone-type and phenoxyl-type radicals have been proven that they form on the surface of particles containing copper oxide. The next study will investigate their characteristic as surface-bound radicals.

4.2.2 Temperature Dependence of EPR g-Value and Concentration of Surface-Bound Radicals on CuO/SiO_2 Surface

Surface-bound radicals of chemisorbed precursors on the copper oxide surface exhibited absorption spectra with two peaks that were assigned to the two EPR g-values g_1 and g_2 (c.f. **Figure 4.2**). The first peak was always at the same place for any precursor or chemisorbed temperature while the second peak was vary with precursor or chemisorbed temperature. The first peak had a low EPR g-value associate with an unpaired electron transferred from the chemisorbed precursor and trapped in the metal oxide matrix. This is the point defect or oxygen vacancy which is often called F-center due to its specific optical absorption [38-40]. The dotted line displays an EPR g-value of g_1= 2.0016 for the first peak of all precursors, which is in the range of the formation of F-center (g=2.001-2.002). The second peak had a high EPR g-value and was the actual EPR signal for an unpaired electron of surface-bound radicals.

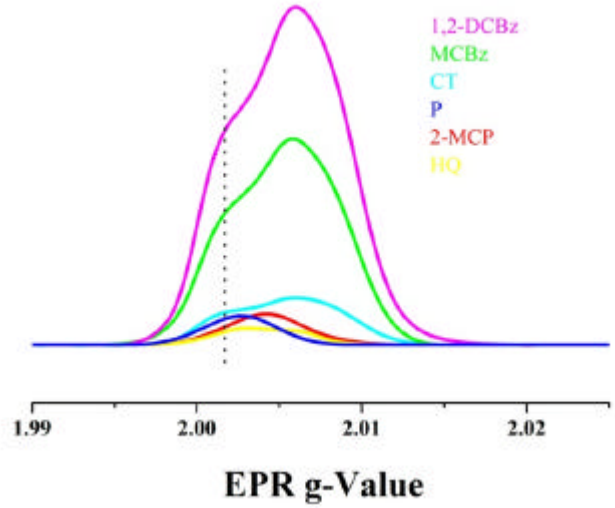

Figure 4.2: F-Center of Precursor Absorption Spectra at 230°C

The Origin 7.0 software with peak fitting was used to calculate the g-value of all surface-bound radicals using gaussian peak type with very small deviation range of +/- 0.0002. **Figure 4.3** displays derivative spectra or EPR spectra (left) and absorption spectra (right) of MCBz at 200°C. This demonstrates a perfect match of the overall peak fitting and the original EPR spectra of a precursor, MCBz.

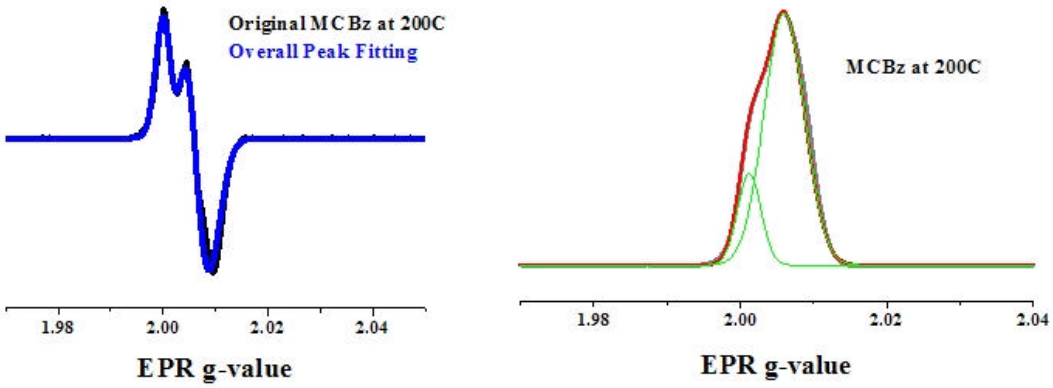

Figure 4.3: Derivative (left) and Absorption (right) Spectra of MCBz at 200°C

It appears that the rate of surface-bound radicals' formation correlates with the rate of chemisorption of the precursors. Based on the yield of radicals (c.f. **Figure 3.9**), the hydroxyl subtituent-containing precursors HQ, CT, 2-MCP, and phenol exhibited lower yields of radical formation than chlorine subtituent-containing precursors MCBz and 1,2-DCBz. The reason for this phenomenon may be the strong hydrogen bonding inhibits chemisorption process. In fact that HQ, CT, 2-MCP, and phenol generated surface-bound radicals through water elimination pathway, which involves hydrogen bonding. On the other hand, MCBz and 1,2-DCBz generated surface-bound radicals through hydrogen chloride elimination, which involves weaker hydrogen bonding. 2-MCP displayed an

intermediate radical yield between chlorinated benzene and hydroxylated benzene groups because it has both chlorine and hydroxyl substitution. HQ and CT generated nearly constant low yield throughout the temperatures studies while substituted benzenes such as MCBz and 1,2-DCBz increased significantly at 200^{o}C and rapidly reduced in yield with increasing the temperature. This is due to the fact that these precursors de-chlorinated with increasing temperature and they cannot chemisorb onto the surface through hydrogen chloride elimination.

Chlorinated benzenes exhibit a higher g-value than non-chlorinated benzene precursors [41]. MCBz and 1,2-DCBz initially generated radicals with high g-value at low temperature around 150^{o}C and gradually decreased g-value as increasing temperature. This is due to the fact that these molecules de-chlorinated with increasing temperature [7]. Phenol generated radical with constant low g-value; however, 2-MCP generated radicals with higher g-value than phenol due to chlorine substitution. At low temperature, the hydrogen chloride elimination pathway is favored while water elimination pathway is favored at high temperature. Therefore, one observes g-value of 2-MCP slightly increased with increasing temperature. Similarly, HQ and CT exhibited a constant g-value, but they have higher g-value than phenol because they have an extra hydroxyl group causing high resonance stabilized. These radicals localize on the oxygen atom which increases spin-orbit coupling; consequently, they have higher g-value.

4.2.3 Persistence of Surface-Bound Radicals

Most radicals have very short lifetimes of pico-mili-seconds [42-45]. Only a few radicals are known to have lifetimes longer that is 10 seconds[46, 47]. Lifetime of phenoxyl

radical achieves in 10 ns in solution[48] while the lifetime of semiquinone radical is from 0.2-10 ms [49-51].

Radicals exhibit longer-lived on surfaces than in solution [52] and particularly they can exist for very long period of time on silica surface [53]. In fact, phenoxyl and semiquinone-type radicals are very stable on CuO/SiO_2 surface because they still were detected after 2 to 3 hours exposure to the air (c.f. **Figure 3.11**). The reason for this phenomenon due to the unpaired electron is associated with the surface of the particle or metal, and it is apparently protected from reaction with oxygen in the air causing the radicals being environmentally persistent. Experimentally, the decay of bound-radicals followed first order kinetic because the plot of concentration of radicals with respect to the air exposure time formed more straight line in logarithmic scale than the plot of inverse concentration of radicals with respect to air exposure time.

Normally, radicals are very active in gas-phase or in solution because they are easily converted into molecular species or reacted to other radicals to form new products. Phenol generated bound-radicals, which is the most persist among six precursors that has the lifetime t around 74min. Semiquinone-type radicals are less stable on the surface than phynoxyl radical due to semiquinone radicals are more reactive with oxygen in the air than phenoxyl radicals. **Figure 4.4** presents the relative persistence of the radicals.

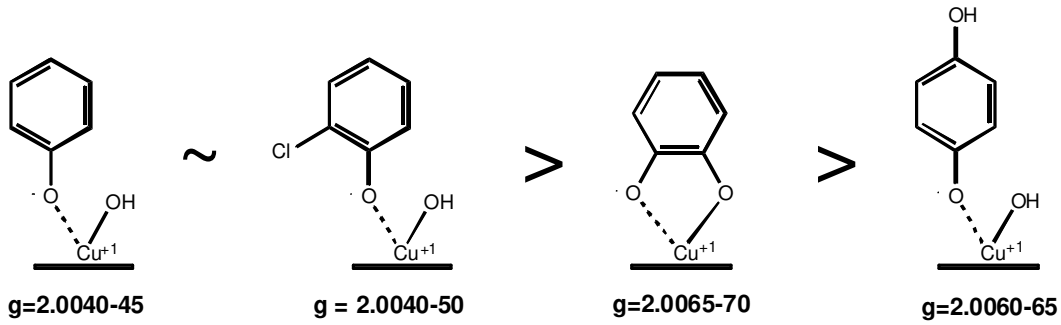

Figure 4.4: Relative Persistence of Surface-Bound Radical

This order follows the general trend observed for calculated reactivity of gas-phase radical with oxygen [54]. Semiquinone-type and phenoxyl-type radical persist on CuO/SiO_2 surface; however, can they be extracted off the surface by some types of solvent?

4.2.4 Mechanism of Products Formation in the Extract

In order to test the extractability of the bound-radical on the surface, several polar and non-polar solvents were used as the extract. Phenol generated very strong radical signal on the CuO/SiO_2 surface through chemisorption; however, this signal was reduced by 93% after extraction with polar solvent such as methyl alcohol (MEA) or isopropyl alcohol (IPA) for one hour (c.f. **Figure 3.12**). Accordingly, polar solvents have ability to extract radicals well.

As a result of the lifetime of radical being very short in the solution, the extract was subjected to EPR measurement immediately after separation of residue and the extract. The EPR radical signal was observed at the g-value of 2.005; however, this signal was increased significantly after introduction of a few drops of dilute sodium hydroxide into the original extract (c.f. **Figure 3.13**). This phenomenon is due to the fact that basic solution converts molecular species to radical anion [55, 56]. **Scheme 4.26** is presents p-semiquinone radical converts to radical anion.

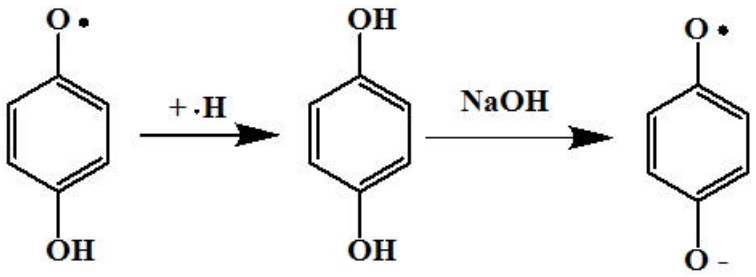

Scheme 4.26: Conversion of Molecular Species to Anion Radical

In the extract, semiquinone radicals scavenge a hydrogen atom and quickly convert to molecular species. On the other hand, HQ or CT molecular may form anion radical in the presence of base. The study of pulse radiolysis suggested that in alkaline solutions, phenol interacts with negative ion hydroxide to form semiquinone anion radical [57-60]. Neta and Fessenden proposed the following mechanism of HQ and CT formation from phenoxyl radical (c.f. **Scheme 4.27**)

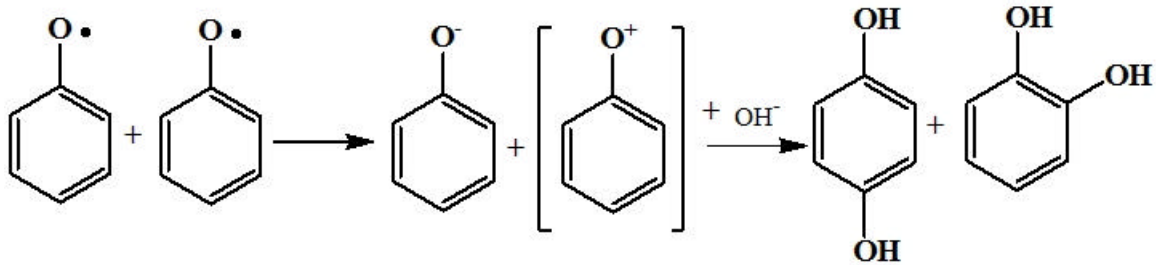

Scheme 4.27: HQ and CT formation from phenoxyl radical

Non-polar solvents did not extract or hardly extracted radicals from the surface. The radical signal on the residue was reduced only around 12% after extraction of adsorbed phenol bound-radical using non-polar toluene solvent (c.f. **Figure 3.14**). No EPR signal was detected from the original extract and the mixture of the original extract with addition of dilute sodium hydroxide (NaOH) (c.f. **Figure 3.15**) that also proved toluene did not extract radicals.

The polar, alcoholic solvents, MEA and IPA, have a high dielectric constant, contain slightly acidic hydrogen, and efficiently extract the radicals. The non-polar, hydrocarbon solvents, TOL and TBB, have a low dielectric constant no measurable acidity, and poorly

extract the radicals. DCM with a moderately high dielectric constant and no acidic hydrogen extracts radicals with modest efficiency (c.f. **Table 3.9** and **Figure 3.16**).

Three extraction scenarios can be envisioned: 1) the chemisorbed species is extracted as a radical via the solvated forces of the solvent as expressed by the solvent dielectric constant (c.f. **Scheme 4.27a**), 2) the chemisorbed species is extracted as an anion and possibly stabilized by hydrogen-bonding as well as the dispersion forces of the solvent as expressed by both the dielectric constant and the pKa of the solvent (c.f. **Scheme 4.27b**), and 3) the chemisorbed species is extracted as molecular species via donation of an acidic hydrogen from the solvent as expressed by the pKa of the solvent (c.f. **Scheme 4.27c**).

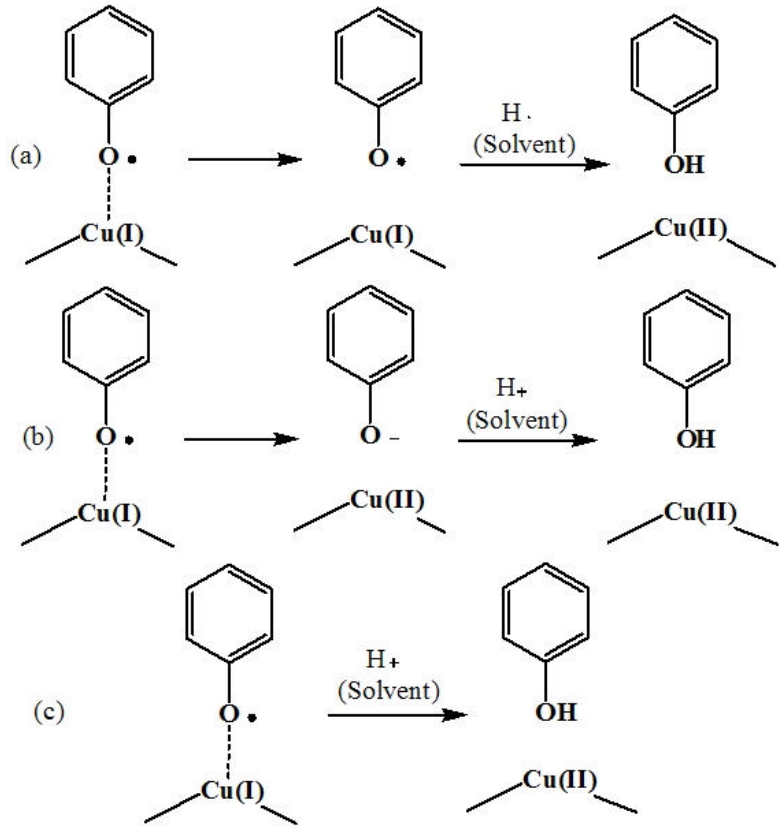

Scheme 4.27: a) Extraction of the chemisorbed species as a radical due to simple solvated effects, b) extraction as an anion assisted by H-bonding with the solvent, and c) extraction as a molecular species using the solvent as a proton donor.

It is not clear which extraction scheme is dominant. The detection of a weak radical signal in solution indicates that pathway **a** proceeds to some extent. The presence of the parent molecular species of the adsorbate suggests that either pathway **c** is occurring or the extracted radical/anion is reacting with the solvent to abstract a hydrogen atom or a proton as illustrated in second reactions in pathways **b** and **c.** Pathway **c** is attractive in that it readily explains the increased extraction efficiency of the alcohol solvents, IPA and MEA, by their providing a proton to facilitate formation of a stable molecular species upon extraction. However, the molecular products observed in the extract are the result of reactions of extracted radicals in solution.

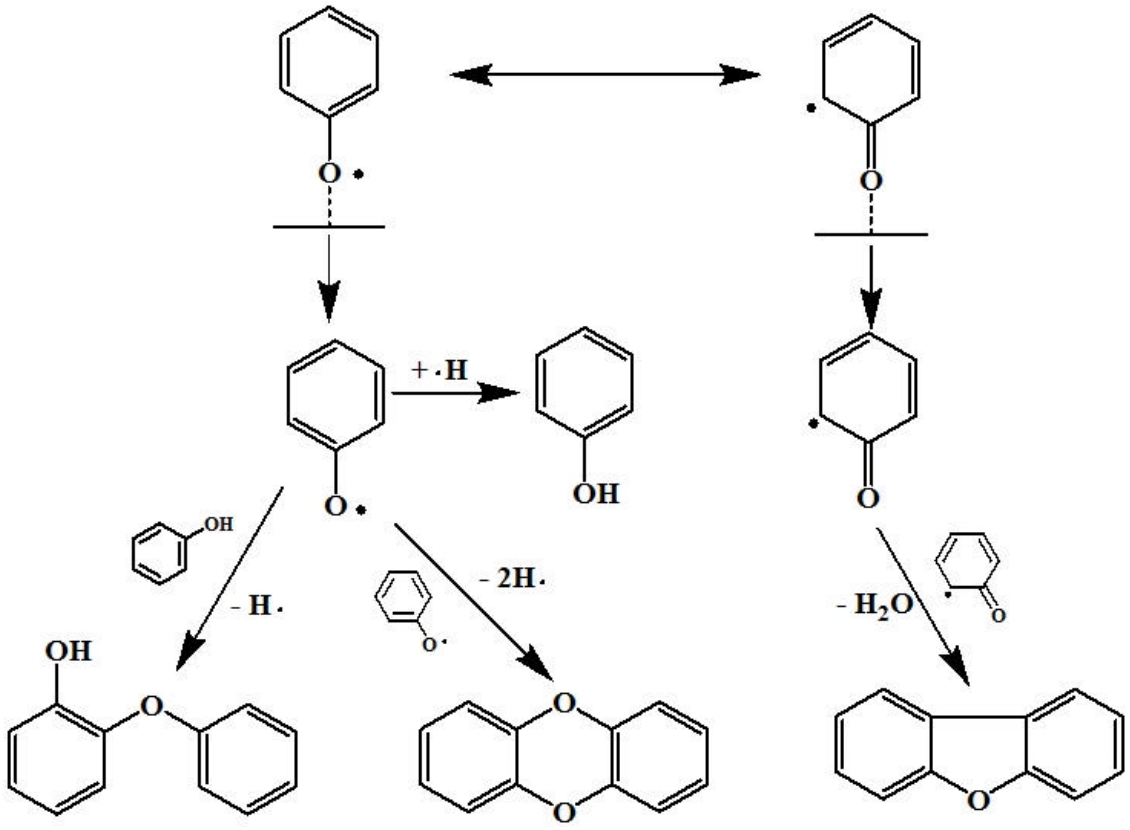

Scheme 4.28: Products of Radicals Interaction of Chemisorbed Phenol

Parallel to EPR analysis of the extract, GC-MS was used to identify the products of radical-radical interaction if radicals were in the extract. Indeed, GC-MS detected dioxin products in the extract include dibenzofuran, 2-phenoxyphenol, and dibenzo-p-dioxin (c.f. **Table 3.10**) in the extract using polar solvents. Only small amounts of phenol were observed in the extract using non-polar solvents due to very small amount of radical being extracted into the solvent and quickly converted to phenol. **Scheme 4.28** proposes possible mechanism of product formation from the interaction of adsorbed phenoxyl bound-radicals

Abstraction of a solvent hydrogen by phenoxyl forms phenol. The Enol-form of the phenoxyl radical displaces a ring hydrogen atom of another enol-form of phenoxyl radical followed by ring closure to form DD. Additionally, the enol-form of the phenoxyl radical displaces an ortho-hydrogen of phenol to form 2-phenoxylphenol. Two keto-form of phenoxyl radical combine through elimination of water to form DF.

Many dimers were observed from GC-MS analysis of the extract of adsorbed 2-MCP including dibenzo-p-dioxin, 2-chlorodibenzo-p-dioxin, 2,8-dichlorodibenzofuran, 2,4'-dichloro-5-hydroxydiphenyl ether. The proposed mechanism of the products formation from the radical-radical interaction in the extract of adsorbed 2-MCP is presented in following **Scheme 4.29**.

Two keto-form of 2-chlorophenoxyl radicals combine through elimination of water to form 2,8-dibenzofuran while two enol-form of 2-chlorophenoxyl radical combine through elimination of hydrogen chloride to form 2-chlorodibenzo-p-dioxin. The enol-form of 2-chlorophenoxyl radical displaces chlorine of the keto-form of phenoxyl radical followed by ring closure to form DD formation, or it may displace a ring hydrogen of 2-chlorophenol to form 2,4'-dichloro-5-hydroxydiphenyl ether.

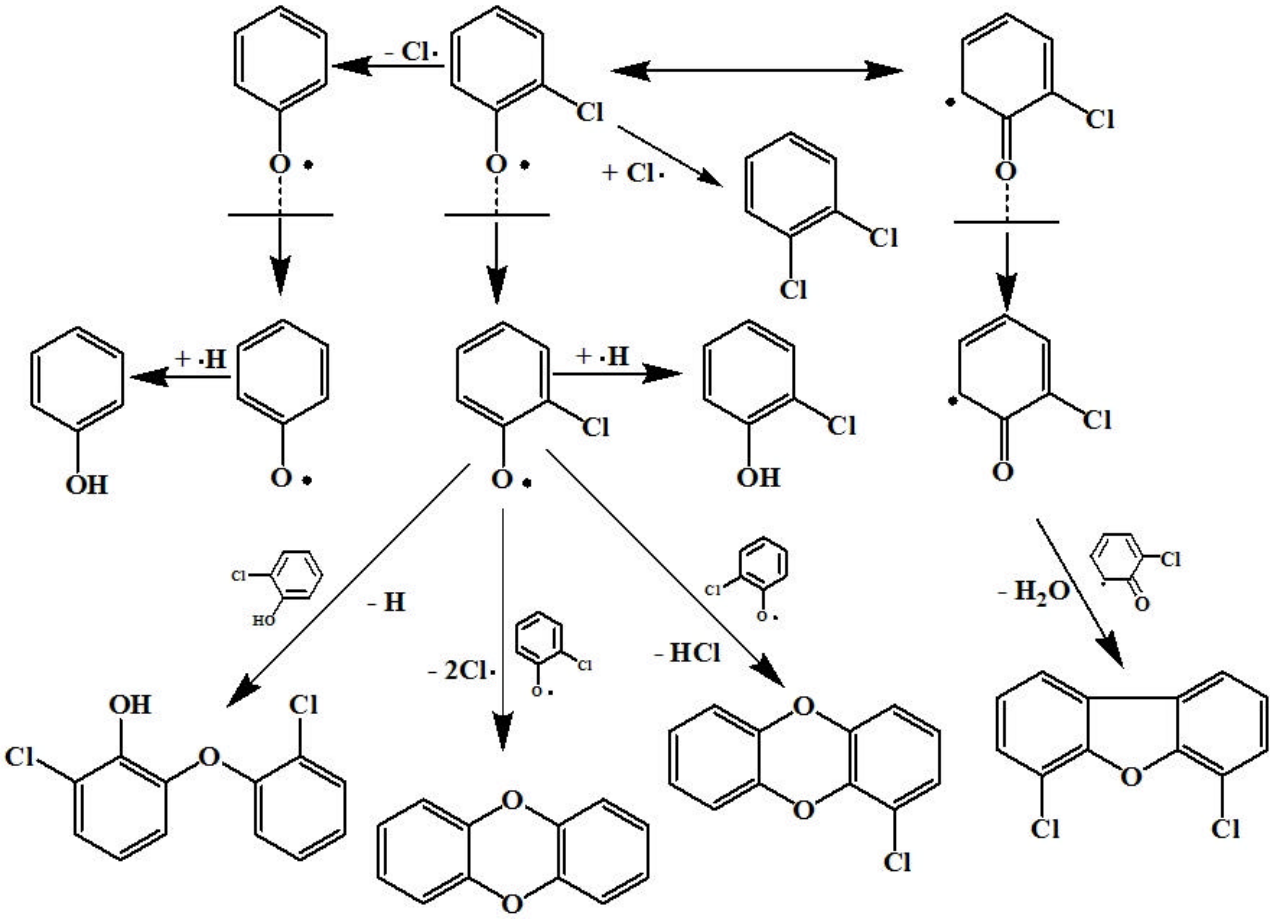

Scheme 4.29: Products of Radicals Interaction of Chemisorbed 2-MCP

MCBz reacts with the particle surface to form primarily chemisorbed phenoxyl radicals that form most of the same products observed from phenol. Surface-mediated chlorination, followed by phenoxyl-surface or phenoxyl-oxygen bond scission (with subsequent abstraction of a solvent hydrogen) form 2-MCP and 1,2-DCBz, respectively. **Scheme 4.30** display possible mechanism of products formation from radical-radical interaction in the extract of chemisorbed MCBz.

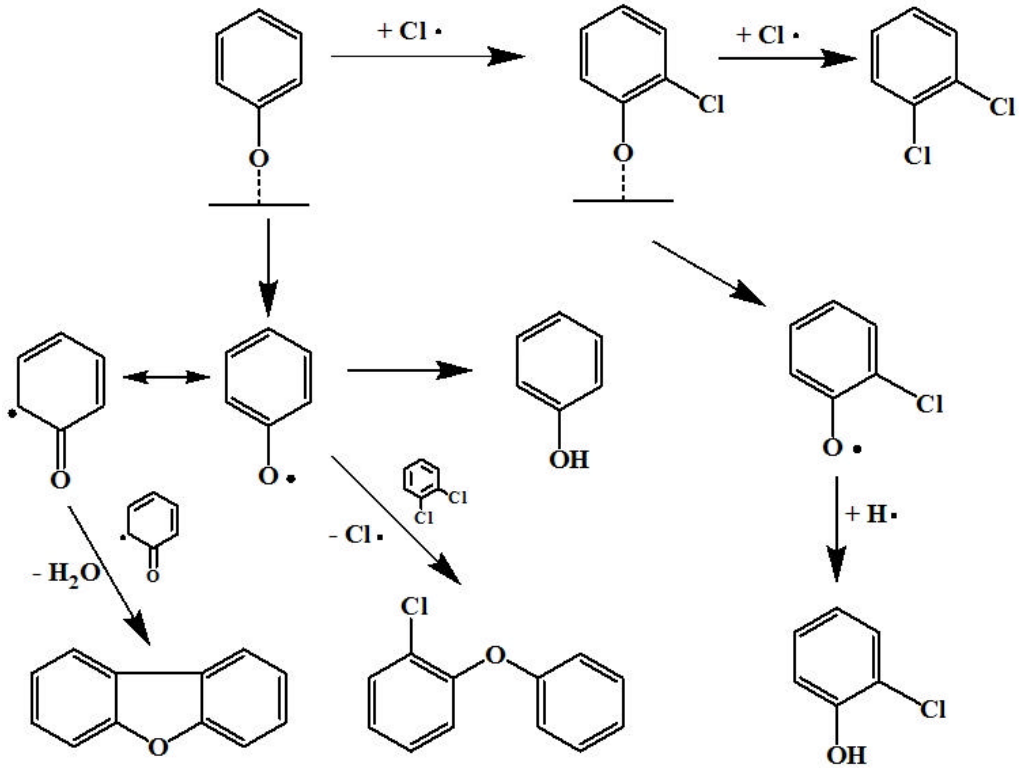

Scheme 4.30: Products of Radicals Interaction of Chemisorbed MCBz

Chemisorption of 1,2 DCBz forms both 2-monochlorophenoxyl radical (via chemisorption at one site by HCl elimination) and a doubly-surface –bound o-benzoquinone radical (via chemisorption at two sites by double HCl elimination). CT and 2-MCP are formed by hydrogen abstraction from the solvent by the o-semiquinone radical and 2-chlorophenoxyl radical, respectively. Chloronaphthalene is formed from recombination and rearrangement of chlorocyclopentadienyl radicals (formed by expulsion of CO from the 2-chlorophenoxyl radicals) in a pathway analogous to the gas-phase formation of naphthalene from recombination of cyclopentadienyl radicals [10, 17]. MCBz is formed by phenyl-oxygen bond scission and abstraction of hydrogen from the solvent. **Scheme 4.31** displays products of solution reaction of radicals extracted from chemisorbed 1,2-DCBz

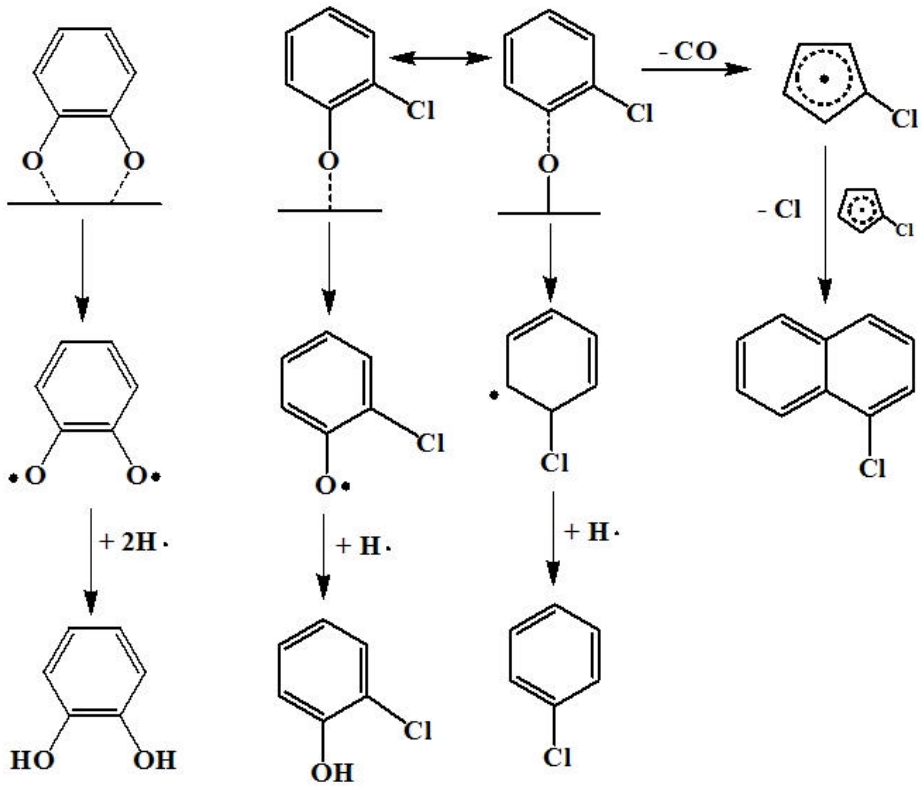

Scheme 4.31: Products of Radicals Interaction of Chemisorbed 1,2-DCBz

Similarly to 1,2-DCBz, CT can also chemisorb at one or two sites via elimination of one or two H_2O's, respectively. In the case of CT, the chemisorpion is primarily via the doubly-bonded species and solvent extraction of the surface associated o-benzoquinone radical is expectedly difficult, resulting in a very low yield of *o*-benzoquinone. CT is again formed from the extracted *o*-semiquinone radical via abstraction of a solvent hydrogen. Phenol is formed via an epoxide, formed be scission of one phenyl-oxygen bond and one oxygen-surface bond and hydrogen abstraction from the solvent. The singly-bound o-semiquinone extracted radical reacts with phenol to form hydroxydiphenyl ether. Product formation is proposed in the following **Scheme 4.32**.

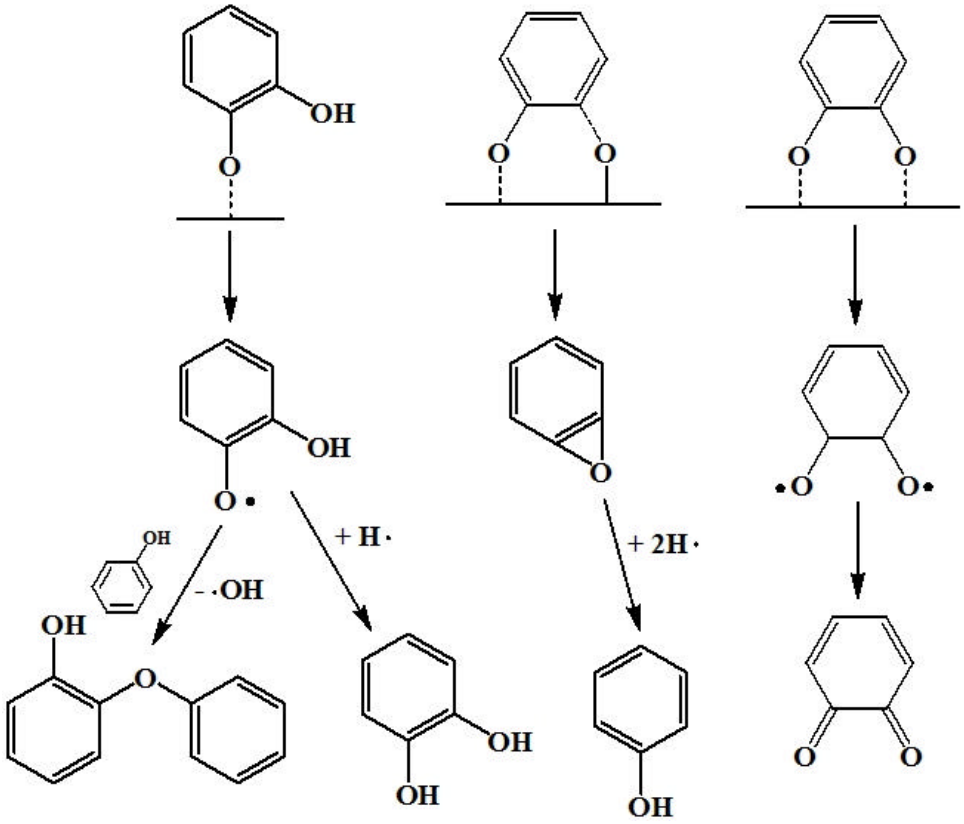

Scheme 4.32: Products of Radicals Interaction of Chemisorbed CT

HQ chemisorbs via elimination of H_2O to form a surface-associated *p*-semiquinone radical. Upon extraction, it loses the second hydroxyl hydrogen to form exclusively *p*-benzoquinone. Because of its rapid conversion to *p*-benzoquinone, dimerization products were not observed as was the case for the other extracted radicals. **Scheme 4.33** summarizes possible path-way of products formation.

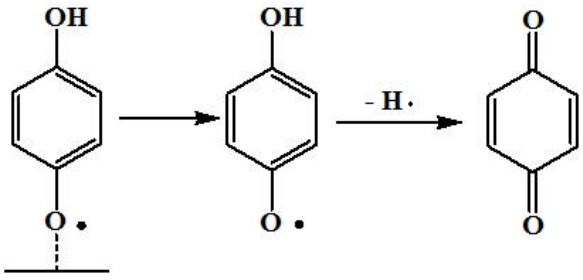

Scheme 4.32: Products of Radicals Interaction of Chemisorbed HQ

Surface-bound radicals are extractable in polar alcoholic solvent that can serve as a hydrogen donor. Aging of the samples may result in loss or decomposition of the more labile radicals. This study suggests that once extracted into solution, radicals that were environmentally persistent when associated with particulate matter will form molecular products in solution. The radical-radical interaction in the extract results in the formation of molecular dimers species. Solvent extraction converts semiquinone-type and phenoxyl-type radicals to molecular species that may result in misidentification in the literature as molecules rather than radicals.

4.3 References

1. Lucarini, M.; Mugnaini, V.; Pedulli, G. F., Bond dissociation enthalpies of polyphenols: The importance of cooperative effects. *Journal of Organic Chemistry* **2002,** 67, (3), 928-931.

2. Mulder, P.; Korth, H. G.; Pratt, D. A.; DiLabio, G. A.; Valgimigli, L.; Pedulli, G. F.; Ingold, K. U., Critical re-evaluation of the O-H bond dissociation enthalpy in phenol. *Journal of Physical Chemistry A* **2005,** 109, (11), 2647-2655.

3. Wiater, I.; Born, J. G. P.; Louw, R., Products, rates, and mechanism of the gas-phase condensation of phenoxy radicals between 500-840 K. *European Journal of Organic Chemistry* **2000**, (6), 921-928.

4. Evans, C. S.; Dellinger, B., Mechanisms of dioxin formation from the high-temperature oxidation of 2-bromophenol. *Environmental Science & Technology* **2005,** 39, (7), 2128-2134.

5. Addink, R.; Olie, K., Mechanisms of Formation and Destruction of Polychlorinated Dibenzo-P-Dioxins and Dibenzofurans in Heterogeneous Systems. *Environmental Science & Technology* **1995,** 29, (6), 1425-1435.

6. Alderman, S. L.; Farquar, G. R.; Poliakoff, E. D.; Dellinger, B., Reaction of 2-chlorophenol with CuO: XANES and SEM analysis. *Proceedings of the Combustion Institute* **2005,** 30, 1255-1261.

7. Cains, P. W.; McCausland, L. J.; Fernandes, A. R.; Dyke, P., Polychlorinated dibenzo-p-dioxins and dibenzofurans formation in incineration: Effects of fly ash and carbon source. *Environmental Science & Technology* **1997,** 31, (3), 776-785.

8. Lomnicki, S.; Dellinger, B., A detailed mechanism of the surface-mediated formation of PCDD/F from the oxidation of 2-chlorophenol on a CuO/silica surface. *Journal of Physical Chemistry A* **2003,** 107, (22), 4387-4395.

9. Asatryan, R.; Davtyan, A.; Khachatryan, L.; Dellinger, B., Molecular modeling studies of the reactions of phenoxy radical dimers: Pathways to dibenzofurans. *Journal of Physical Chemistry A* **2005,** 109, (49), 11198-11205.

10. Evans, C. S.; Dellinger, B., Mechanisms of dioxin formation from the high-temperature pyrolysis of 2-chlorophenol. *Environmental Science & Technology* **2003,** 37, (7), 1325-1330.

11. Marsh, N. D.; Ledesma, E. B.; Sandrowitz, A. K.; Wornat, M. J., Yields of polycyclic aromatic hydrocarbons from the pyrolysis of catechol [ortho-dihydroxybenzene]: Temperature and residence time effects. *Energy & Fuels* **2004,** 18, (1), 209-217.

12. Appel, J.; Bockhorn, H.; Frenklach, M., Kinetic modeling of soot formation with detailed chemistry and physics: Laminar premixed flames of C-2 hydrocarbons. *Combustion and Flame* **2000,** 121, (1-2), 122-136.

13. Richter, H.; Howard, J. B., Formation of polycyclic aromatic hydrocarbons and their growth to soot - a review of chemical reaction pathways. *Progress in Energy and Combustion Science* **2000,** 26, (4-6), 565-608.

14. Khachatryan, L.; Adounkpe, J.; Maskos, Z.; Dellinger, B., Formation of cyclopentadienyl radical from the gas-phase pyrolysis of hydroquinone, catechol, and phenol. *Environmental Science & Technology* **2006,** 40, (16), 5071-5076.

15. Colussi, A. J.; Zabel, F.; Benson, S. W., Very Low-Pressure Pyrolysis of Phenyl Ethyl Ether, Phenyl Allyl Ether, and Benzyl Methyl-Ether and Enthalpy of Formation of Phenoxy Radical. *International Journal of Chemical Kinetics* **1977,** 9, (2), 161-178.

16. Lin, C. Y.; Lin, M. C., Thermal-Decomposition of Methyl Phenyl Ether in Shock-Waves - the Kinetics of Phenoxy Radical Reactions. *Journal of Physical Chemistry* **1986,** 90, (3), 425-431.

17. Melius, C. F.; Colvin, M. E.; Marinov, N. M.; Pitz, W. J.; Senkan, S. M., Reaction mechanisms in aromatic hydrocarbon formation involving the C5H5 cyclopentadienyl moiety. *Symposium (International) on Combustion, [Proceedings]* **1996,** 26th, (Vol. 1), 685-692.

18. Leanderson, P.; Tagesson, C., Cigarette Smoke-Induced DNA Damage in Cultured Human Lung-Cells - Role of Hydroxyl Radicals and Endonuclease Activation. *Chemico-Biological Interactions* **1992,** 81, (1-2), 197-208.

19. Pryor, W. A., Mechanisms of Radical Formation from Reactions of Ozone with Target Molecules in the Lung. *Free Radical Biology and Medicine* **1994,** 17, (5), 451-465.
20. Pryor, W. A.; Hales, B. J.; Premovic, P. I.; Church, D. F., The Radicals in Cigarette Tar - Their Nature and Suggested Physiological Implications. *Science* **1983,** 220, (4595), 425-427.

21. Pryor, W. A., Cigarette smoke and the involvement of free radical reactions in chemical carcinogenesis. *The British journal of cancer. Supplement* **1987,** 8, 19-23.

22. Dellinger, B.; Pryor, W. A.; Cueto, R.; Squadrito, G. L.; Hegde, V.; Deutsch, W. A., Role of free radicals in the toxicity of airborne fine particulate matter. *Chemical Research in Toxicology* **2001,** 14, (10), 1371-1377.

23. Li, Y. B.; Trush, M. A., Reactive Oxygen-Dependent DNA-Damage Resulting from the Oxidation of Phenolic-Compounds by a Copper-Redox Cycle Mechanism. *Cancer Research* **1994,** 54, (7), S1895-S1898.

24. Borish, E. T.; Cosgrove, J. P.; Church, D. F.; Deutsch, W. A.; Pryor, W. A., Cigarette Tar Causes Single-Strand Breaks in DNA. *Biochemical and Biophysical Research Communications* **1985,** 133, (2), 780-786.

25. Pryor, W. A.; Prier, D. G.; Church, D. F., Electron-Spin Resonance Study of Mainstream and Sidestream Cigarette-Smoke - Nature of the Free-Radicals in Gas-Phase Smoke and in Cigarette Tar. *Environmental Health Perspectives* **1983,** 47, (Jan), 345-355.

26. Hirakawa, K.; Oikawa, S.; Hiraku, Y.; Hirosawa, I.; Kawanishi, S., Catechol and hydroquinone have different redox properties responsible for their differential DNA-damaging ability. *Chemical Research in Toxicology* **2002,** 15, (1), 76-82.

27. Pryor, W. A.; Stone, K.; Zang, L. Y.; Bermudez, E., Fractionation of aqueous cigarette tar extracts: Fractions that contain the tar radical cause DNA damage. *Chemical Research in Toxicology* **1998,** 11, (5), 441-448.

28. Squadrito, G. L.; Cueto, R.; Dellinger, B.; Pryor, W. A., Quinoid redox cycling as a mechanism for sustained free radical generation by inhaled airborne particulate matter. *Free Radical Biology and Medicine* **2001,** 31, (9), 1132-1138.

29. Borosky, G. L., Theoretical study related to the carcinogenic activity of polycyclic aromatic hydrocarbon derivatives. *Journal of Organic Chemistry* **1999,** 64, (21), 7738-7744.

30. Cooksey, C. J.; Land, E. J.; Riley, P. A.; Sarna, T.; Truscott, T. G., On the Interaction of Anisyl-3,4-Semiquinone with Oxygen. *International Journal of Radiation Biology* **1988,** 53, (6), 999-999.

31. Forquer, I.; Covian, R.; Bowman, M. K.; Trumpower, B. L.; Kramer, D. M., Similar transition states mediate the Q-cycle and superoxide production by the cytochrome bc(1) complex. *Journal of Biological Chemistry* **2006,** 281, (50), 38459-38465.

32. Farquar, G. R.; Alderman, S. L.; Poliakoff, E. D.; Dellinger, B., X-ray spectroscopic studies of the high temperature reduction of Cu(II)0 by 2-chlorophenol on a simulated fly ash surface. *Environmental Science & Technology* **2003,** 37, (5), 931-935.

33. Alderman, S. L.; Farquar, G. R.; Poliakoff, E. D.; Dellinger, B., An infrared and X-ray spectroscopic study of the reactions of 2-chlorophenol, 1,2-dichlorobenzene, and chlorobenzene with model CuO/silica fly ash surfaces. *Environmental Science & Technology* **2005,** 39, (19), 7396-7401.

34. Balbuena, P. B.; Calvo, S. R.; Lamas, E. J.; Salazar, P. F.; Seminario, J. M., Adsorption and dissociation of H2O2 on Pt and Pt-alloy clusters and surfaces. *Journal of Physical Chemistry B* **2006,** 110, (35), 17452-17459.

35. Thomson, J., Generation of radical species in surface reactions of chlorohydrocarbons and chlorocarbons with fluorinated gallium(III) oxide or indium(III) oxide. *Journal of the Chemical Society-Faraday Transactions* **1998,** 94, (13), 1881-1885.

36. Lee, J.; Dougherty, D. B.; Yates, J. T., Chemisorbed benzoate-to-benzene conversion via phenyl radicals on Cu(110): Kinetic observation of conformational effects. *Journal of the American Chemical Society* **2006,** 128, (18), 6008-6009.

37. Kucherov, A. V.; Slinkin, A. A., Formation of Radicals in the Adsorption of Olefins on H-Mordenite .2. Conversions of Radical Particles at Increased Temperatures on Hm and Other Zeolites. *Kinetics and Catalysis* **1983,** 24, (4), 804-810.

38. Henderso.B; Wertz, J. E., Defects in Alkaline Earth Oxides. *Advances in Physics* **1968,** 17, (70), 749-&.

39. Sterrer, M.; Fischbach, E.; Risse, T.; Freund, H. J., Geometric characterization of a singly charged oxygen vacancy on a single-crystalline MgO(001) film by electron paramagnetic resonance spectroscopy. *Physical Review Letters* **2005,** 94, (18), -.

40. Di Valentin, C.; Neyman, K. M.; Risse, T.; Sterrer, M.; Fischbach, E.; Freund, H. J.; Nasluzov, V. A.; Pacchioni, G.; Rosch, N., Density-functional model cluster studies of EPR g tensors of F-s(+) centers on the surface of MgO. *Journal of Chemical Physics* **2006,** 124, (4), -.

41. Bersohn, M. a. B., J., *An Introduction to Electron Paramagnetic Resonance*. W.A. Benfamin, Inc.: New York, 1966.

42. Black, G.; Jusinski, L. E., Radiative Lifetimes of the V'3 = 0, 1, and 2 Levels of Ch3s(A2a1). *Journal of Chemical Physics* **1986,** 85, (9), 5379-5380.

43. Falvey, D. E.; Schuster, G. B., Picosecond Time Scale Dynamics of Perester Photodecomposition - Evidence for an Acyloxy Radical Intermediate in the Photolysis of Tert-Butyl 9-Methylfluorene-9-Percarboxylate. *Journal of the American Chemical Society* **1986,** 108, (23), 7419-7420.

44. Okamura, T.; Tanaka, I., Radiative Lifetimes of Benzyl, Deuterated Benzyl, and Methyl-Substituted Benzyl Radicals. *Journal of Physical Chemistry* **1975,** 79, (25), 2728-2731.

45. Regis, A.; Hapiot, P.; Servagent-Noinville, S., Detection of short-lived electrogenerated species by Raman microspectrometry. *Analytical Chemistry* **2000,** 72, (10), 2216-2221.

46. Tennyson, P. H.; Fontijn, A.; Clyne, M. A. A., Radiative Lifetimes of Metastable States of Free-Radicals .1. Nfb-Sigma-1+. *Chemical Physics* **1981,** 62, (1-2), 171-177.

47. Porter, G.; Wright, F. J., Primary Photochemical Processes in Aromatic Molecules .3. Absorption Spectra of Benzyl, Anilino, Phenoxy and Related Free Radicals. *Transactions of the Faraday Society* **1955,** 51, (11), 1469-&.

48. Johnson, C. R.; Ludwig, M.; Asher, S. A., Ultraviolet Resonance Raman Characterization of Photochemical Transients of Phenol, Tyrosine, and Tryptophan. *Journal of the American Chemical Society* **1986,** 108, (5), 905-912.

49. Smith, I.; Testa, A. C., Flash photolysis of molecules implicated in 9-nitroanthracene photochemistry. *Journal of Photochemistry and Photobiology, A: Chemistry* **1989,** 47, (2), 167-72.

50. Gindt, Y. M.; Vollenbroek, E.; Westphal, K.; Sackett, H.; Sancar, A.; Babcock, G. T., Origin of the transient electron paramagnetic resonance signals in DNA photolyase. *Biochemistry* **1999,** 38, (13), 3857-3866.

51. Al-Kazwini, A. T.; O'Neill, P.; Adams, G. E.; Cundall, R. B.; Lang, G.; Junino, A., Reactions of indolic radicals produced upon one-electron oxidation of 5,6-dihydroxyindole and its N(1)-methylated analog. *Journal of the Chemical Society, Perkin Transactions 2: Physical Organic Chemistry (1972-1999)* **1991**, (12), 1941-5.

52. Rodrigues, M. A.; Bemquerer, M. P.; Tada, D. B.; Bastos, E. L.; Baptista, M. S.; Politi, M. J., Synthesis and characterization of silica gel particles functionalized with bioactive materials. *Adsorption* **2005,** 11, (5/6), 595-602.

53. Hurrell, L.; Johnston, L. J.; Mathivanan, N.; Vong, D., Photochemistry of Lignin Model Compounds on Solid Supports. *Canadian Journal of Chemistry-Revue Canadienne De Chimie* **1993,** 71, (9), 1340-1348.

54. Dellinger, B.; Lomnicki, S.; Khachatryan, L.; Maskos, Z.; Hall, R. W.; Adounkpe, J.; McFerrin, C.; Truong, H., Formation and stabilization of persistent free radicals. *Proceedings of the Combustion Institute* **2007,** 31, (Pt. 1), 521-528.

55. Maskos, Z.; Khachatryan, L.; Cueto, R.; Pryor, W. A.; Dellinger, B., Radicals from the pyrolysis of tobacco. *Energy & Fuels* **2005,** 19, (3), 791-799.

56. Pedersen, J. A., On the application of electron paramagnetic resonance in the study of naturally occurring quinones and quinols. *Spectrochimica Acta Part a-Molecular and Biomolecular Spectroscopy* **2002,** 58, (6), 1257-1270.

57. Neta, P.; Fessende.Rw, Hydroxyl Radical Reactions with Phenols and Anilines as Studied by Electron-Spin Resonance. *Journal of Physical Chemistry* **1974,** 78, (5), 523-529.

58. Micic, O. I.; Nenadovic, M. T., Pulse Radiolytic Investigations of Some Peroxyhydroxycyclohexadienyl Radicals. *Journal of Physical Chemistry* **1976,** 80, (9), 940-944.

59. Land, E. J.; Ebert, M., Pulse Radiolysis Studies of Aqueous Phenol - Water Elimination from Dihydroxycyclohexadienyl Radicals to Form Phenoxyl. *Transactions of the Faraday Society* **1967,** 63, (533P), 1181-&.

60. Adams, G. E.; Michael, B. D., Pulse Radiolysis of Benzoquinone and Hydroquinone - Semiquinone Formation by Water Elimination from Trihydroxycyclohexadienyl Radicals. *Transactions of the Faraday Society* **1967,** 63, (533P), 1171-&.

CHAPTER 5: SUMMARY

Persistent free radicals (PFR) including semiquinone and phenoxyl radicals are highly resonance stabilized that can be formed in any combustion system or thermal processes. On the other hand, hydroquinone (HQ) and catechol (CT) are well documented products of combustion of many type of biomass including tobacco[1-3]; thus, HQ and CT are suspected biologically damaging semiquinone-type radicals. Semiquinone radicals are extremely active in oxidative stress that can lead to cancer, mutations, and alter DNA [4-6]. All hydrocarbon fuels will form phenol and substituted phenol that can form substituted phenoxyl radicals. Phenoxyl radicals may combine to form polychlorinated dibenzo-p-dioxin/ dibenzofuran (PCDD/F) which is the most toxic known environmental pollutant [7]. They are persistent when associate with combustion generated fly-ash that they can exist very long period of time and transport over considerable atmospheric distances [8-12]. This work is focused on the study of the nature and origin of PFR associated with combustion generated fine particles.

5.1 Thermal Degradation of Hydroquinone and Catechol in Gas-Phase

The study of thermal degradation of HQ and CT helps to identify which persistent radicals are formed and which conditions that radicals are formed during the decomposition processing. It also helps to understand the mechanism of dioxins products as well as other polycyclic aromatic hydrocarbon (PAH) products.

5.1.1 Products Formation from Gas-Phase Pyrolysis of HQ and CT

Since both HQ and CT are isomers, the only structural difference between those two is a position of the second hydroxyl group, that is *para* or *ortho* position, respectively. *p*-

Benzoquinone was formed instantly upon the degradation of HQ at 250°C due to the dissociation of a hydroxyl-hydrogen bond followed by the abstraction of a second hydroxyl-hydrogen by hydrogen atom. However, the lack of *o*-benzoquinone in the products of pyrolysis of CT was unexpected and led to a conclusion that an intra-molecular elimination of water is occurred for the initial step of CT decomposition because of the close proximity of the two hydroxyl groups in CT. This results in the formation of epoxy-benzene that may also exist as a diradical intermediate.

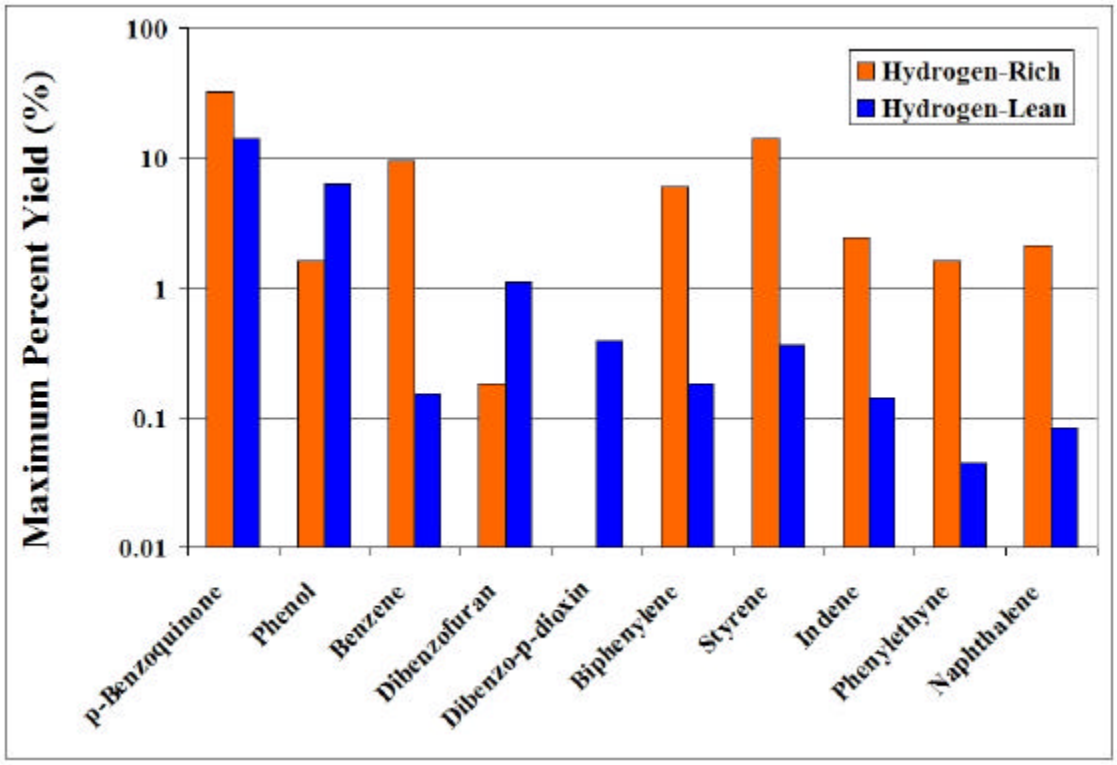

Figure 5.1: The Maximum Yield of Product Formation from Pyrolysis of HQ

The presence of an additional source of hydrogen had a significant impact on the pyrolysis of HQ and CT. Although in typical combustion or pyrolysis processes, hydrogen is in abundance, comparison between the reaction with and without additional hydrogen can

provide critical mechanistic information on the high-temperature chemistry of HQ and CT. Under hydrogen-rich conditions, the formation of products from pyrolysis of HQ and CT were formed at lower temperature and higher yield than under hydrogen-lean conditions. The differences in the maximum product yields from pyrolysis of HQ and CT were also observed as shown in **Figure 5.1** and **Figure 5.2**.

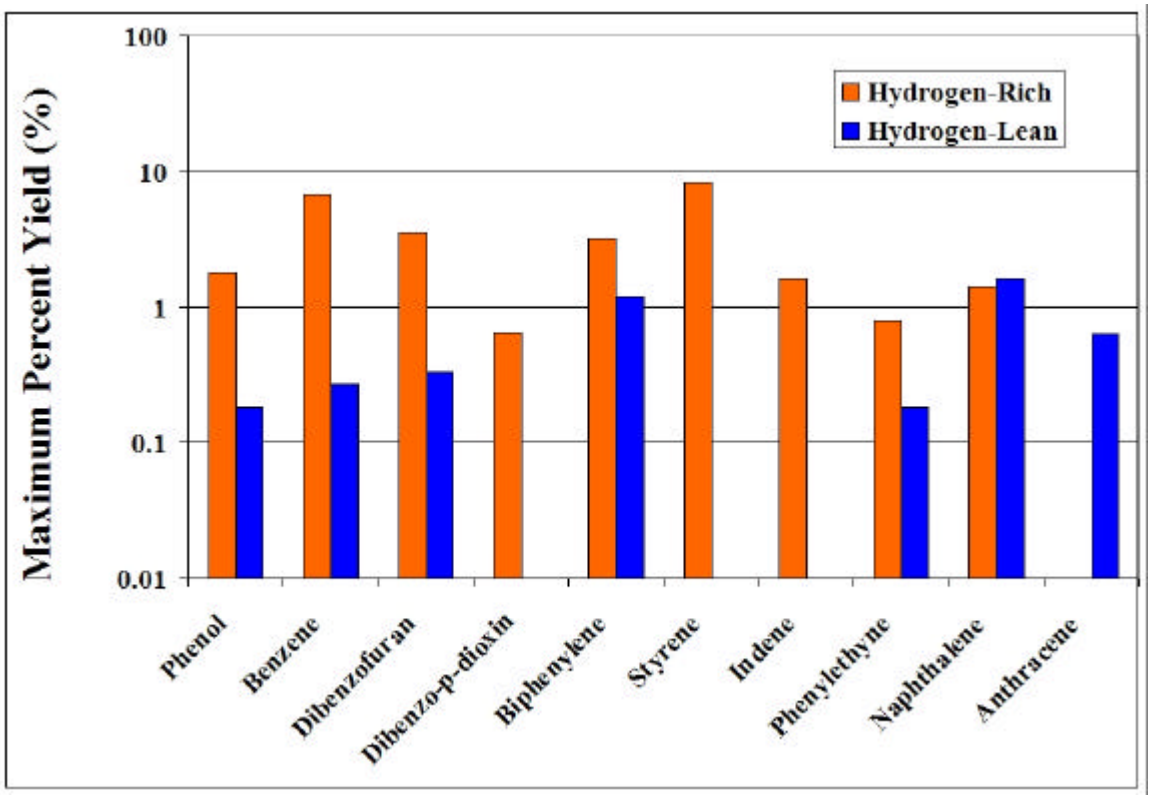

Figure 5.2: The Maximum Yield of Product Formation from Pyrolysis of CT

The formation of *p*-semiquinone radical is strongly implied because of the observation of p-benzoquinone as the only major molecular product in pyrolysis of HQ. Phenoxyl and cyclopentadienyl radical is also implied due to the observation of phenol, naphthalene and polycyclic aromatic hydrocarbon during the thermal decomposition of HQ

process. The interaction of phenoxyl radicals results in DD and DF formation while the reaction of other radicals and fragments yield substituted benzene and PAH product. **Scheme 5.1** displays overall mechanism of products formation from pyrolysis thermal degradation of HQ.

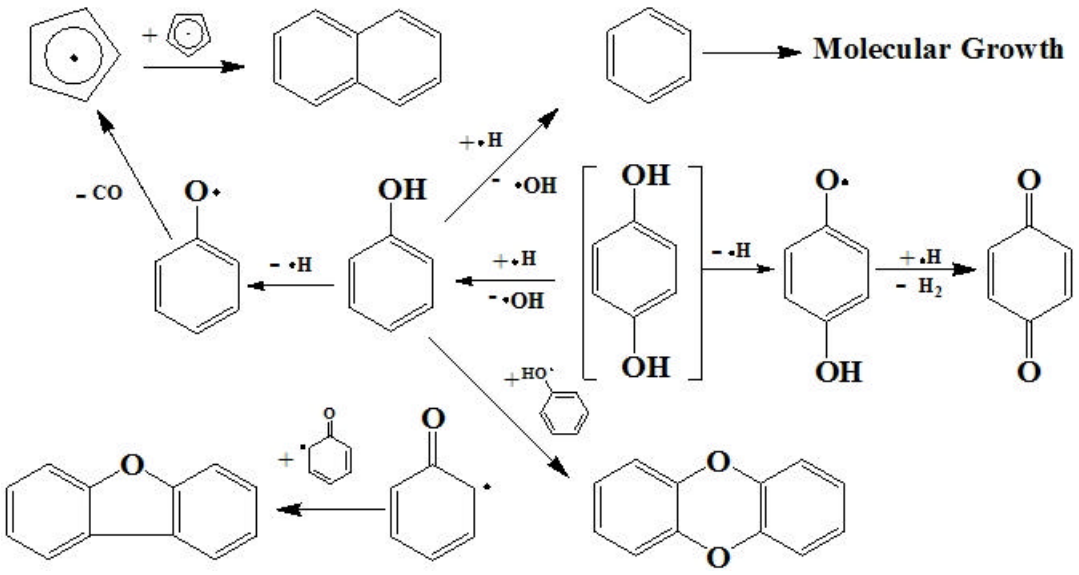

Scheme 5.1: Overall Product Formation from Pyrolysis of HQ

Although not directly observable in this study, the decomposition behavior of CT suggests the formation of persistent free radicals. The formation of epoxy-benzene from internal water elimination of CT as well as the detection of molecular phenol indirectly infers of diradical and phenoxyl radcial formation. The formation of cyclopentadienyl radical is implied by the formation of naphthalene product. The formation of DF and DD is most likely a result of reactions involving the epoxy-benzene that can exist as relatively stable diradical. Interaction of the epoxy-benzene with a molecular CT results in DF formation while recombination of two epoxy-benzene or diradicals forms DD. Scheme 5.2 exhibits the overall product formation of pyrolysis of CT.

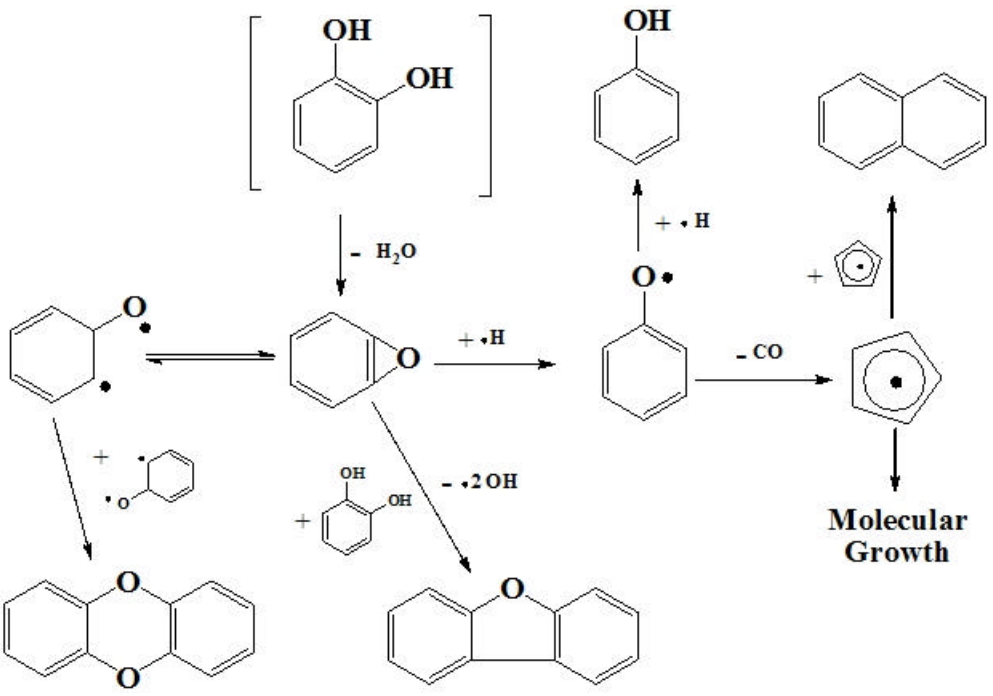

Scheme 5.2: Overall Product Formation from pyrolysis of CT

5.1.2 Products Formation from Gas Phase Oxidation of HQ and CT

Pyrolysis of HQ yielded *p*-benzoquinone, but *o*- benzoquinone was not observed in the pyrolysis of CT. In contrast, oxidation of HQ and CT yielded *p*-benzoquinone and *o*-benzoquinone, respectively as major products at all temperatures. There was fewer products formation under oxidative conditions than pyrolystic conditions. Figure 5.3 displays the maximum yield of product formation from oxidation of HQ and CT.

Under pyrolytic conditions, the principal decomposition pathway for CT was the elimination of water to form epoxy-benzene. However, under oxidative conditions, hydrogen abstraction pathway to form *o*- benzoquinone favored over the internal water elimination because hydroxyl radical abstracts hydroxyl-hydrogen atoms from HQ or CT much more efficiently than hydrogen. **Scheme 5.3** and **Scheme 5.4** depict the overall product formation of oxidation of HQ and CT, respectively.

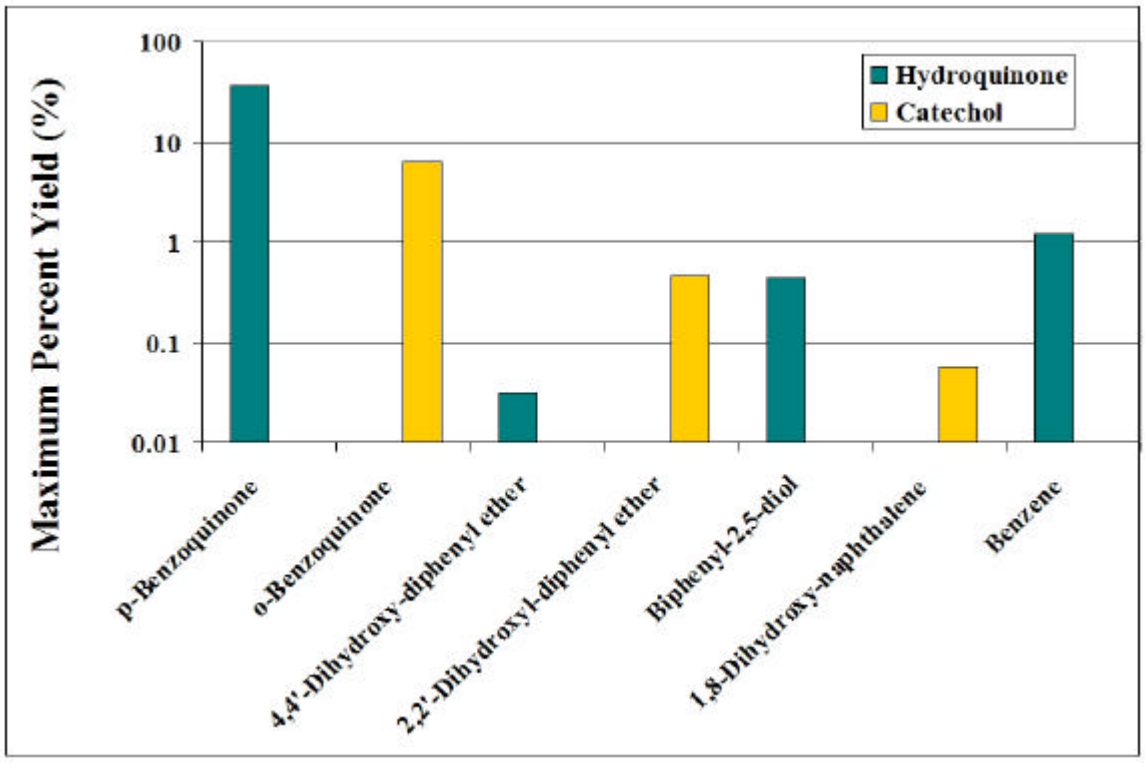

Figure 5.3: The Maximum Yield of Product Formation from Oxidation of HQ and CT

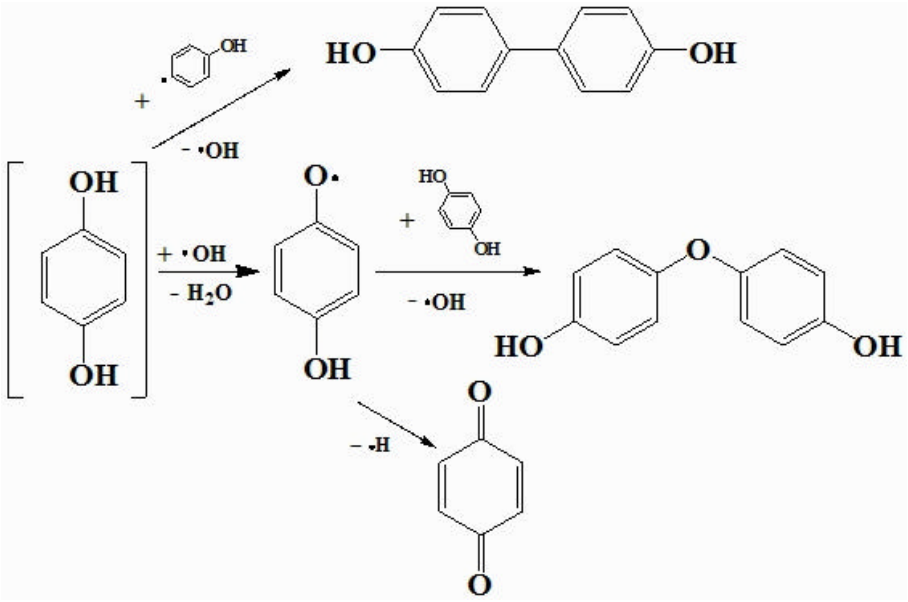

Scheme 5.3: Overall Product Formation from Oxidation of HQ

Oxygen facilitated the decomposition of HQ and CT as well as the products, but *p*-benzoquinone and *o*-benzoquinone still existed in a wide range of temperature. Additionally, the thermal oxidation behavior of HQ and CT suggests the formation of persistent free radicals although they are not directly observable in this study. Formation of biological damaging semiquinone-type radical is implied due to observation of *p*-benzoquinone and *o*-benzoquinone from 200°C to 700°C.

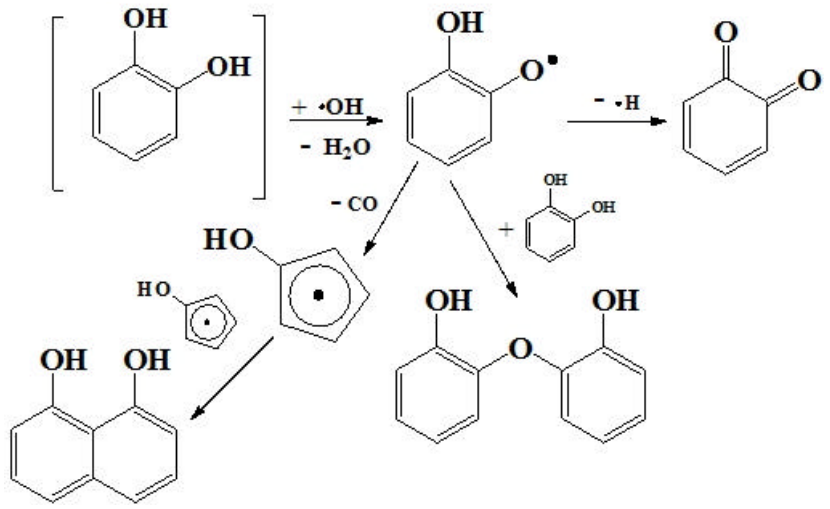

Scheme 5.4: Overall Product Formation from Oxidation of CT

The study of the thermal degradation of HQ and CT indirectly suggests the formation of semiquinone-type and phenoxyl-type radicals in the gas-phase. They may also exist on the surface of particles containing transition metal that is summarized in the next study.

5.2 Metal Mediated Formation of Persistent Free Radicals

Semiquinone-type and phenoxyl-type radicals have potential to be environmentally persistent and biologically active toward the concern of human health. Consequently, their formation and stabilization from various molecular precursors were studied with the focus

on metal mediated surface-bound radicals formed in association with combustion-generated particles. We have characterized these radicals by investigating the EPR g-value, intensity, lifetime, and formative conditions. HQ and CT are suggested primary precursors for semiquinone-type radicals while phenol (P), 2-chlorophenol (2-MCP), mono-chlorobenzene (MCBz), 1,2-dichlorobenzene (1,2-DCBz) are suggested as precursors for phenoxyl-type radicals.

5.2.1 Formation of Surface-Bound Radicals on CuO/SiO_2 Particles

Copper was chosen as a metal mediated surface because it is easy to reduce to copper (I) and oxidize back to copper (II). Hydroxylated benzenes (HQ, CT and P) bind to the metal surface particles, (5% copper oxide supported on silica dioxide CuO/SiO_2) at hydroxyl site and interact with hydroxyl group from the surface to release water. Electrons transfer and reduction of the copper in chemisorption from the surface generate surface-bound radicals. **Scheme 5.5** is presented the surface-bound radicals formation from phenol through water elimination pathway.

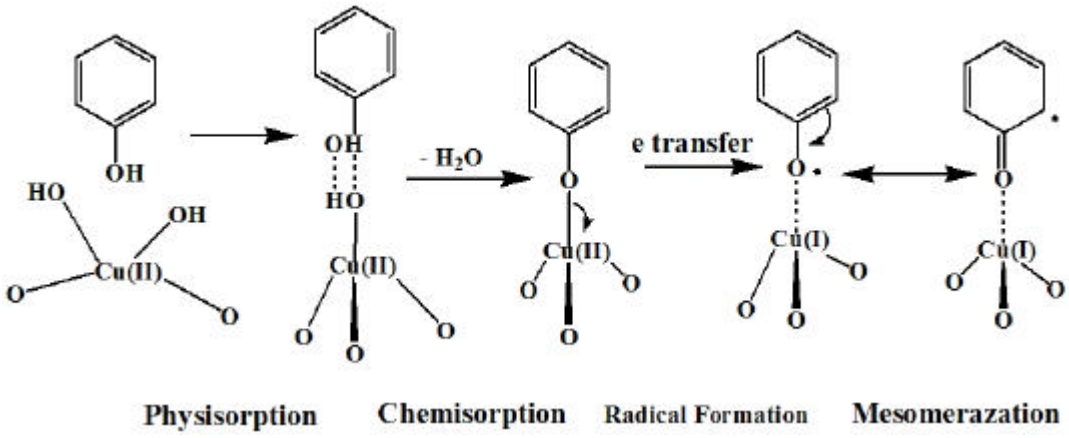

Scheme 5.5: Radicals Formation through Water Elimination Pathway

Chlorinated benzene (MCBz and 1,2-DCBz) binds to the metal surface at chlorine site and induces hydrogen to release hydrogen chloride due to a weak bond between chlorine and benzene ring. Again, electrons transfer and reduction of the copper in chemisorption process lead to the formation of surface-bound radicals. **Scheme 5.6** is exhibited the radical formation from chemisorption of MCBz through hydrogen chloride elimination pathway.

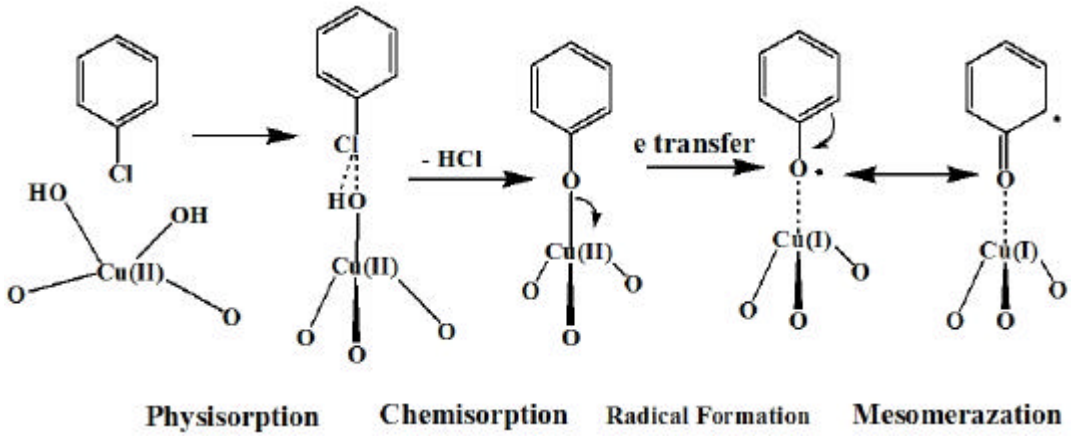

Scheme 5.6: Radicals Formation through Hydrogen Chloride Elimination Pathway

2-MCP contains both chlorine and hydroxyl substitutents; therefore, it can generate surface-bound radicals through either hydrogen chloride or water elimination route. In general, semiquinone-type and phenoxyl-type radicals all exist on the surface of particles, so what are their characteristics and which conditions that help them persist in the environment? The next study will explain these questions.

5.2.2 Temperature Dependence of EPR g-Value and Concentration of Surface-Bound Radicals on CuO/SiO_2 Surface

In this study, the precursors of phenoxyl radicals and semiquinone-type radicals chemisorbed onto CuO/SiO_2 surface at vary temperature range of 50°C to 300°C to investigate the temperature dependence of EPR g-value and concentration of surface-bound

radicals. The rate of surface-bound radicals' formation correlates with the rate of chemisorption of the precursors. All of precursors generate bound-radicals display the maximum yield in the temperature range between 200°C and 230°C. **Figure 5.4** and **Figure 5.5** are exhibited the radical maximum yield of precursors and the EPR g-value of precursors at that maximum yield.

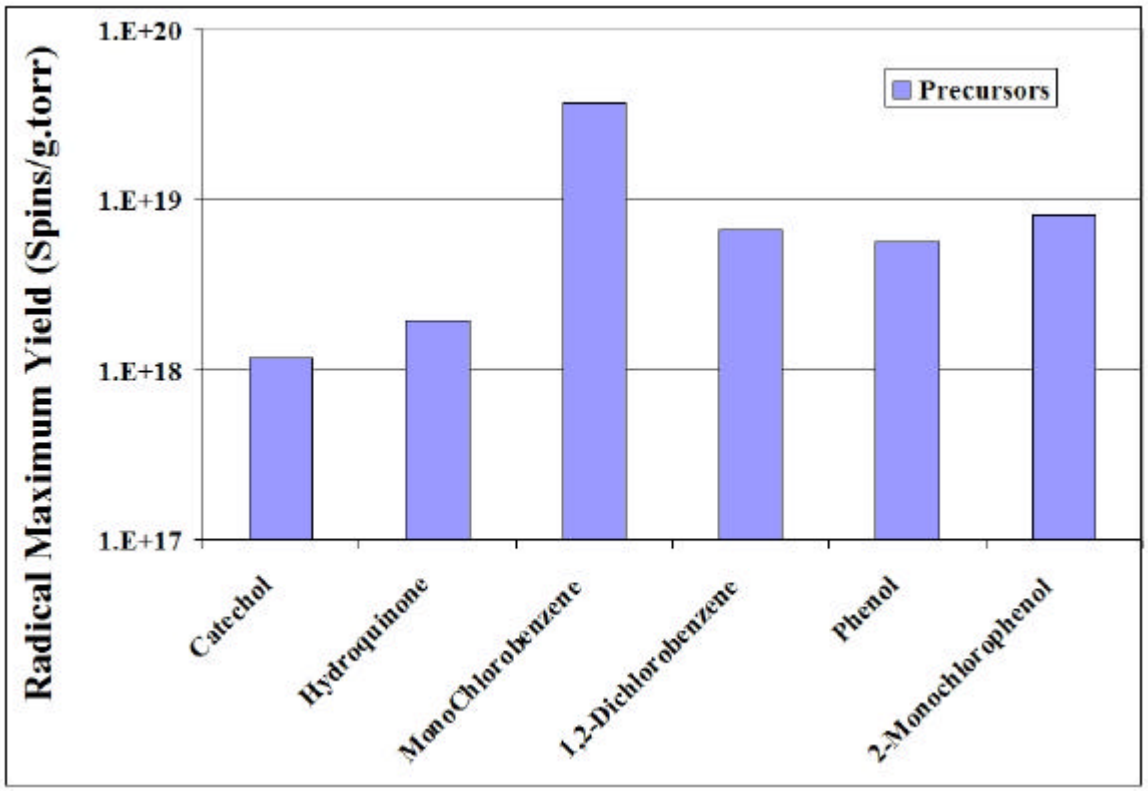

Figure 5.4: Surface-Bound Radical Maximum Yield of Precursors

The hydroxyl substituent containing precursors HQ, CT, 2-CP, and P exhibited lower yield of radical formation than chlorine substituent containing precursors MCBz and 1,2-DCBz because they have strong hydrogen bonding that inhibits chemisorption process. The g-value of aromatic radicals containing halogen atoms is higher than the g-value of aromatic

radical that contain only C, H, and O [13]. In fact, MCBz and 1,2-DCBz initially generated radicals with high g-value at low temperature; however they gradually decreased g-value as increasing temperature because these molecules de-chlorinated with increasing temperature. At low temperature, hydrogen chloride elimination pathway is favor while water elimination path way is favor at high temperature. Thus, g-value of bound radicals from the adsorbed 2-MCP molecule slightly increases with rising temperature. HQ and CT have higher g-value than P because they have an extra hydroxyl group causing high resonance stabilized. These radicals localize on the oxygen atom which increase spin-orbit coupling; consequently, they have higher g-value.

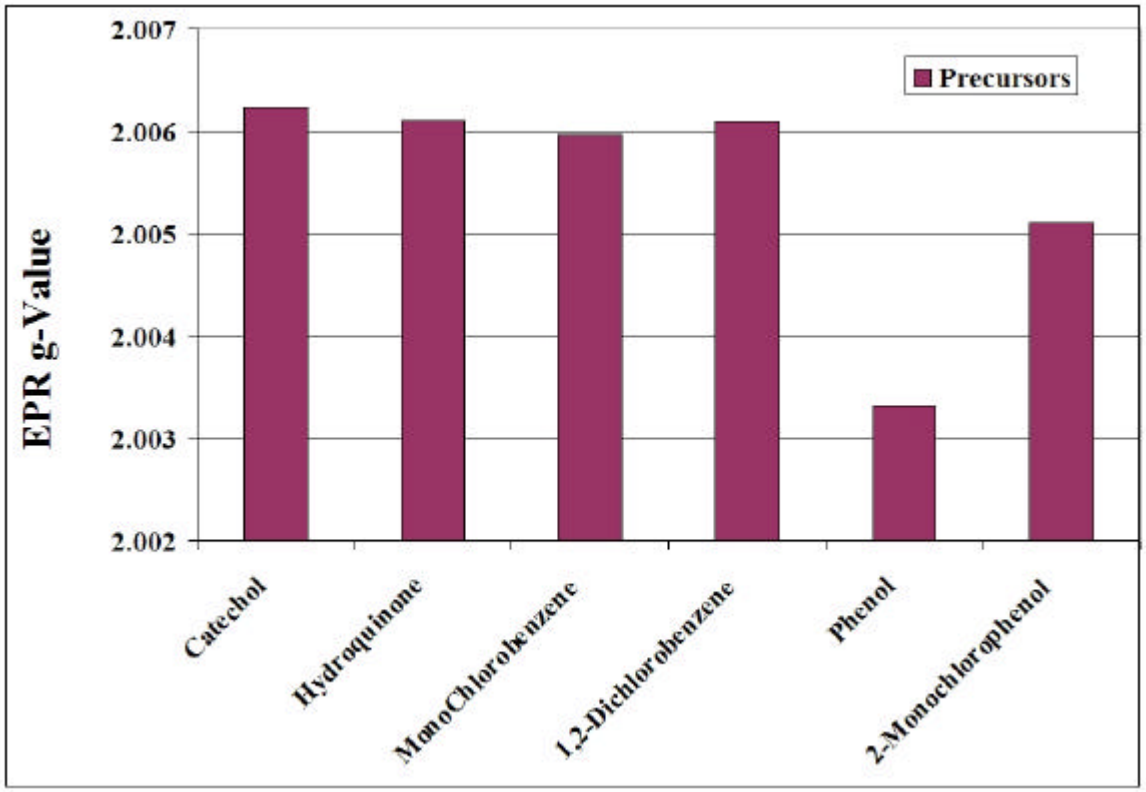

Figure 5.5: EPR g-Value of Surface-Bound Radical at Temperature of Maximum Yield

5.2.3 Persistence of Surface-Bound Radicals

Radicals have very short lifetime in solution or in gas-phase [14-16]. They may stabilize and extend their lifetime when they associate with fine particle containing transition metal [6, 9-12]. In fact, phenoxyl-type radicals have the lifetime t in the range of 43 to74 minutes while semiquinone-type radicals have the lifetime t in the range of 27 to 36 minutes when they chemisorbed on to CuO/SiO_2 surface at 230°C. Lifetime of surface-bound radical from the precursors is presented in **Figure 5.6**.

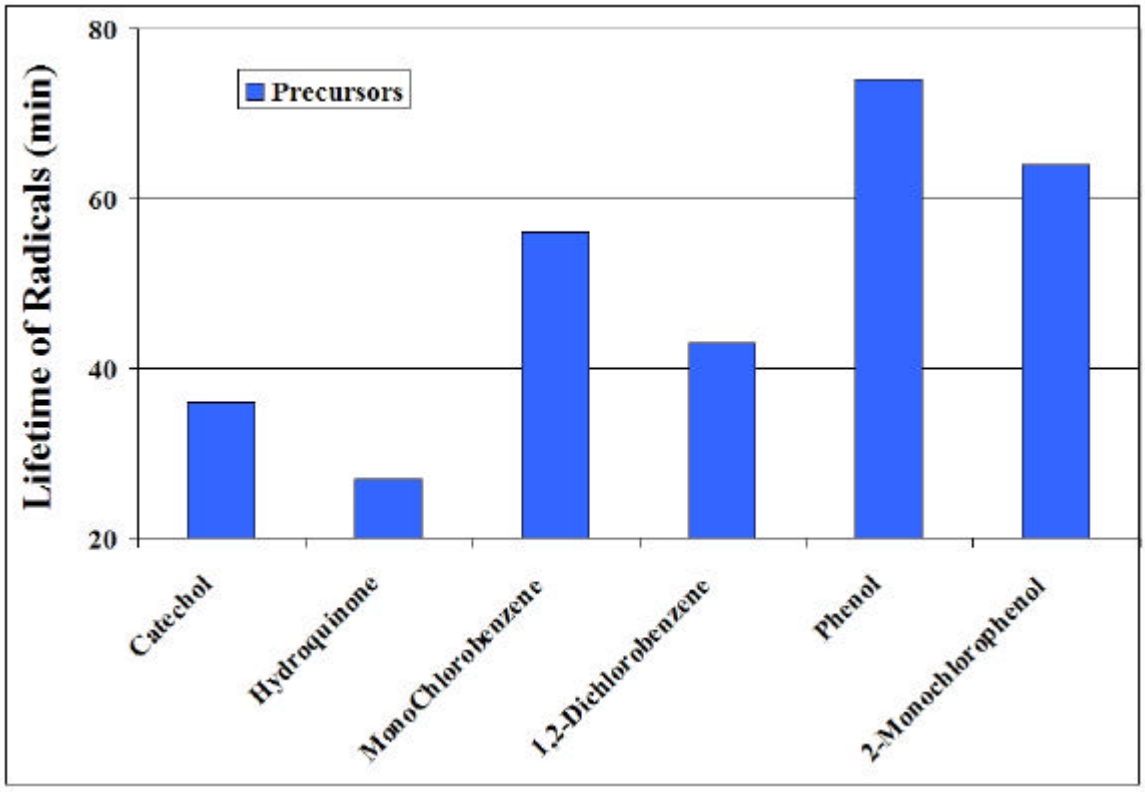

Figure 5.6: Lifetime of Surface-Bound Radicals from Precursors

The reason for this phenomenon due to the unpaired electron is associated with the surface of the particle or metal, and it is apparently protected from reaction with oxygen in

the air causing the radicals being environmentally persistent. Phenoxyl-type radicals appear to be more stable compared to semiquinone-type radicals in the air when they associated with CuO/SiO_2 surface may be that semiquinone-type radicals are more reactive with oxygen in the air than phenoxyl-type radicals. Precursor's bound-radicals form on the surface of CuO/SiO_2 particle and persist for more than a day. However, they may be removable from the surface by some type of solvent extraction for.

5.2.4 Chemical analysis and extractability of chemisorbed radicals

Several polar and non-polar solvents including methyl alcohol (MEA), isopropyl alcohol (IPA), dichloromethane (DCM), toluene (TOL), and *tert*-butylbenzene (TBB) were chosen to study the extractability of surface-bound radicals on CuO/SiO_2 surface from the above six precursors. Figure 5.7 is displayed the percent reduction of EPR signal after extraction with variety of solvents.

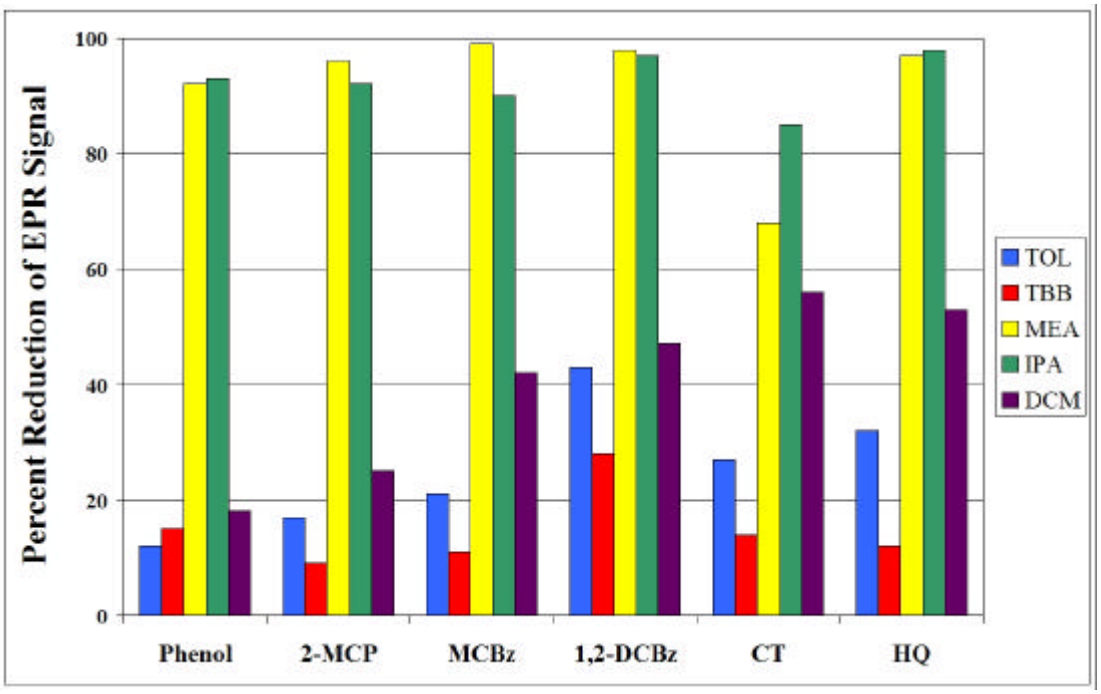

Figure 5.7: Percent Reduction of ERP Signal after Extraction with Solvents

Polar solvent (MEA and IPA) with a high dielectric constant and contain slightly acidic hydrogen extracted more bound-radicals than non-polar (TOL and TBB) and mildly polar solvents (DCM). The presence of dimers and PCDD/F as products of extraction using polar solvent indicated there are radical-radical interactions in the solvent. Combination of the keto-forms of phenoxyl radicals yields DF while interaction of enol-forms of phenoxyl radicals forms DD. This study suggests that once extracted into solution, radicals that were environmentally persistent when associated with particulate matter will also form molecular products in solution. Formation of molecular products in the extract solution may result in misidentification of surface-bound radicals as molecular species by researchers.

The entire of studies have proved that semiquinone-type and phenoxyl-type radicals exist in gas-phase and persist on the surface of combustion generated particles that they are highly redox active and can induce oxidative stress in exposed individual. Collaborations with health effects researchers strongly suggest the radical-particle systems are biologically active in lung, heart, and liver tissue. More research on the origin, nature of stabilization and redox activity of their "persistent free radicals" is clearly justified.

5.3 References

1. Schlotzhauer, W. S.; Walters, D. B.; Snook, M. E.; Higman, H. C., Characterization of Catechols, Resorcinols, and Hydroquinones in an Acidic Fraction of Cigarette-Smoke Condensate. *Journal of Agricultural and Food Chemistry* **1978,** 26, (6), 1277-1288.

2. Simoneit, B. R. T., Biomass burning - A review of organic tracers for smoke from incomplete combustion. *Applied Geochemistry* **2002,** 17, (3), 129-162.

3. Carmella, S. G.; Hecht, S. S.; Tso, T. C.; Hoffmann, D., Chemical Studies on Tobacco-Smoke .77. Roles of Tobacco Cellulose, Sugars, and Chlorogenic Acid as Precursors to Catechol in Cigarette-Smoke. *Journal of Agricultural and Food Chemistry* **1984,** 32, (2), 267-273.

4. Pryor, W. A.; Hales, B. J.; Premovic, P. I.; Church, D. F., The Radicals in Cigarette Tar - Their Nature and Suggested Physiological Implications. *Science* **1983,** 220, (4595), 425-427.

5. Pryor, W. A.; Stone, K.; Zang, L. Y.; Bermudez, E., Fractionation of aqueous cigarette tar extracts: Fractions that contain the tar radical cause DNA damage. *Chemical Research in Toxicology* **1998,** 11, (5), 441-448.

6. Dellinger, B.; Pryor, W. A.; Cueto, R.; Squadrito, G. L.; Hegde, V.; Deutsch, W. A., Role of free radicals in the toxicity of airborne fine particulate matter. *Chemical Research in Toxicology* **2001,** 14, (10), 1371-1377.

7. Berho, F.; Lesclaux, R., The phenoxy radical: UV spectrum and kinetics of gas-phase reactions with itself and with oxygen. *Chemical Physics Letters* **1997,** 279, (5,6), 289-296.

8. Dellinger, B.; Pryor, W. A.; Cueto, R.; Squadrito, G.; Deutsch, W. A., The role of combustion-generated radicals in the toxicity of PM2.5. *Proceedings of the Combustion Institute* **2000,** 28, 2675-2681.

9. Lomnicki, S.; Dellinger, B., A detailed mechanism of the surface-mediated formation of PCDD/F from the oxidation of 2-chlorophenol on a CuO/silica surface. *Journal of Physical Chemistry A* **2003,** 107, (22), 4387-4395.

10. Dellinger, B., Formation and Stabilization of Persistent Free Radicals. *Combustion Institute* **Accepted, 2006**.

11. Rodrigues, M. A.; Bemquerer, M. P.; Tada, D. B.; Bastos, E. L.; Baptista, M. S.; Politi, M. J., Synthesis and characterization of silica gel particles functionalized with bioactive materials. *Adsorption* **2005,** 11, (5/6), 595-602.

12. Hurrell, L.; Johnston, L. J.; Mathivanan, N.; Vong, D., Photochemistry of Lignin Model Compounds on Solid Supports. *Canadian Journal of Chemistry-Revue Canadienne De Chimie* **1993,** 71, (9), 1340-1348.

13. Bersohn, M. a. B., J., *An Introduction to Electron Paramagnetic Resonance*. W.A. Benfamin, Inc.: New York, 1966.

14. Black, G.; Jusinski, L. E., Radiative Lifetimes of the V'3 = 0, 1, and 2 Levels of Ch3s(A2a1). *Journal of Chemical Physics* **1986,** 85, (9), 5379-5380.

15. Falvey, D. E.; Schuster, G. B., Picosecond Time Scale Dynamics of Perester Photodecomposition - Evidence for an Acyloxy Radical Intermediate in the Photolysis of Tert-Butyl 9-Methylfluorene-9-Percarboxylate. *Journal of the American Chemical Society* **1986,** 108, (23), 7419-7420.

16. Okamura, T.; Tanaka, I., Radiative Lifetimes of Benzyl, Deuterated Benzyl, and Methyl-Substituted Benzyl Radicals. *Journal of Physical Chemistry* **1975,** 79, (25), 2728-2731.

APPENDIX 1: EPR SPECTRA AND GC-MS CHROMATOGRAMS OF SAMPLES

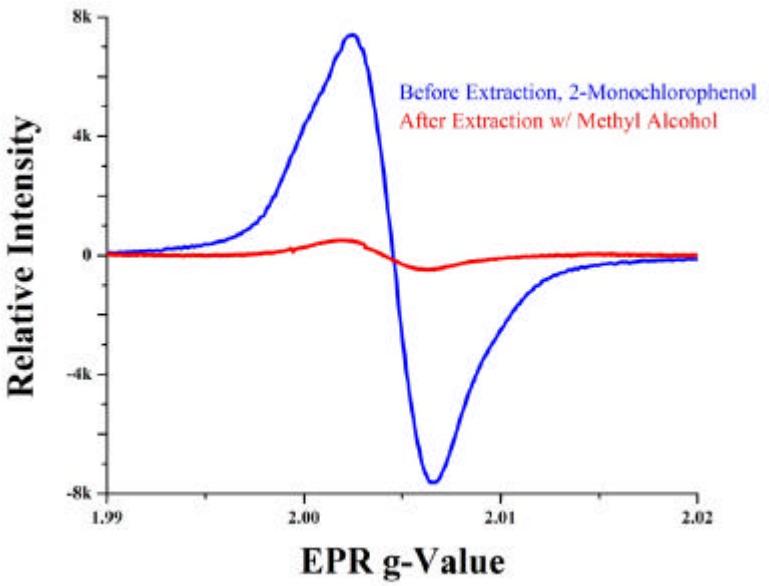

Figure A1.1: EPR Radical Signal of Residue from Chemisorbed 2-MCP on the Surface before and after Extraction with Methyl Alcohol

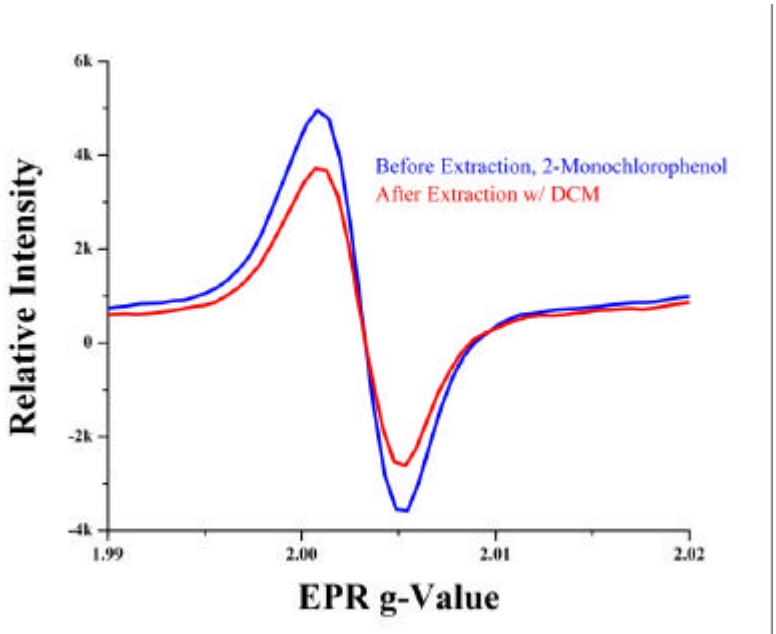

Figure A1.2 EPR Radical Signal of Residue from Chemisorbed 2-MCP on the Surface before and after Extraction with DCM

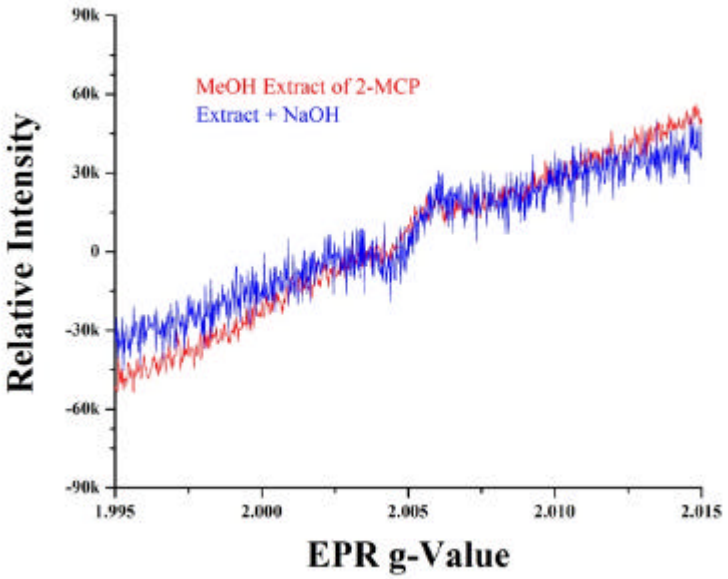

Figure A1.3: EPR Radical Signal of the Extract from Chemisorbed 2-MCP Matrix Using Methyl Alcohol as a Solvent

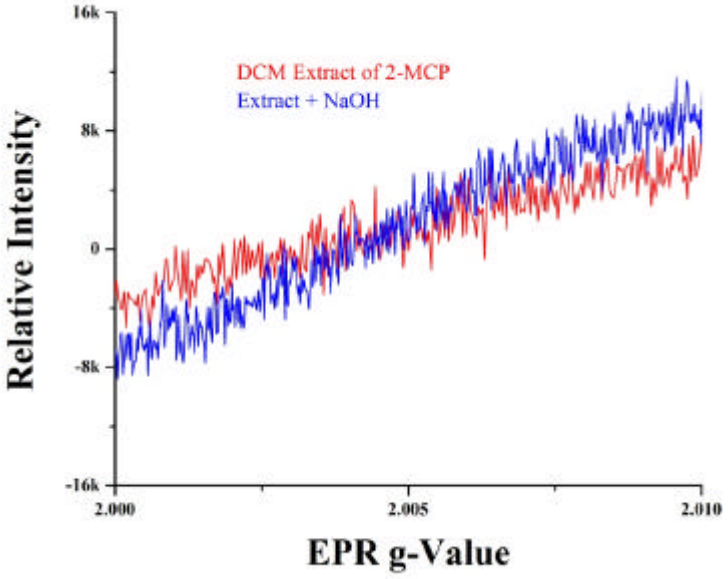

Figure A1.4: EPR Radical Signal of the Extract from Chemisorbed 2-MCP Matrix Using DCM as a Solvent

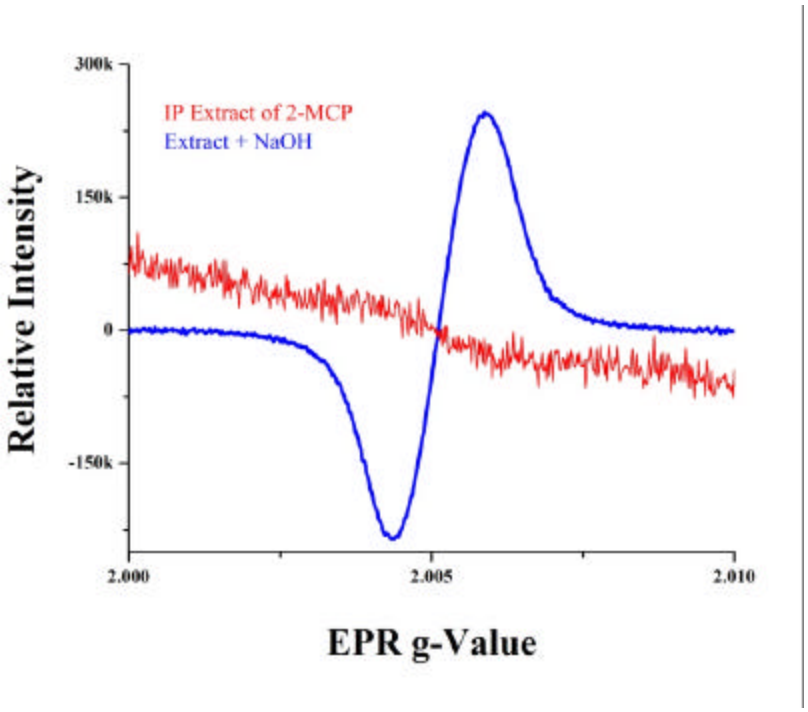

Figure A1.5: EPR Radical Signal of the Extract from Chemisorbed 2-MCP Matrix Using IPA as a Solvent

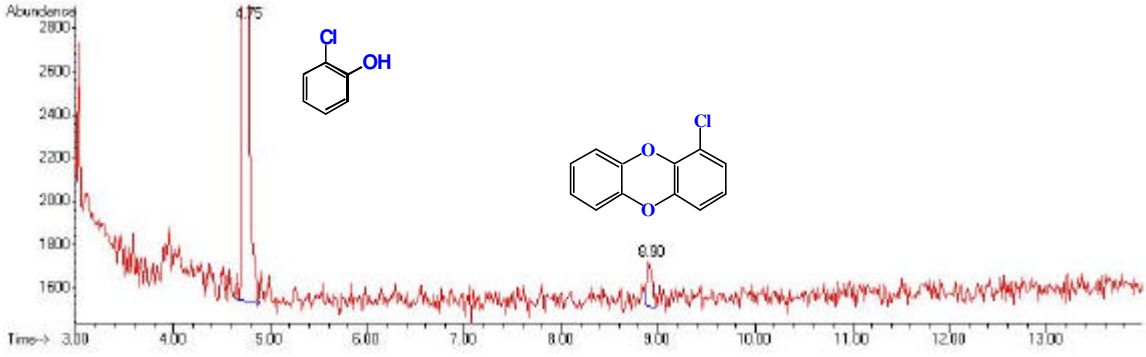

Figure A1.6: GC-MS Spectra of Products of 2-MCP after Extraction by Using MEA-1

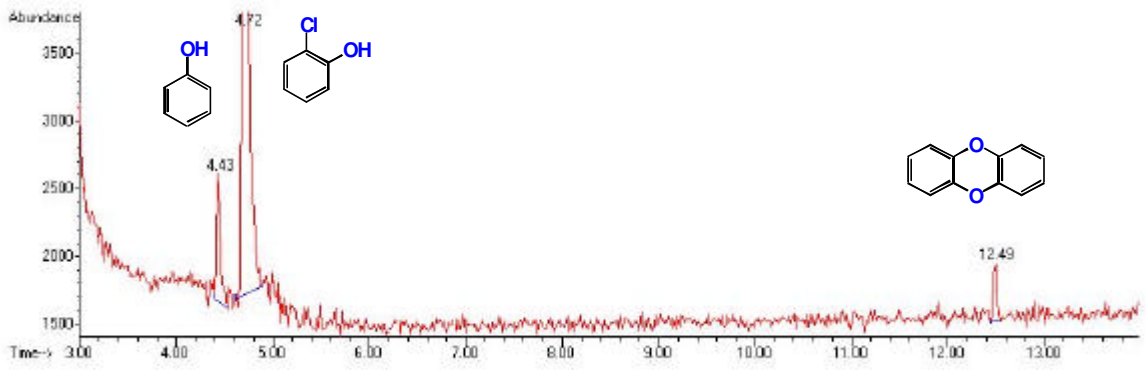

Figure A1.7: GC-MS Spectra of Products of 2-MCP after Extraction by Using MEA-2

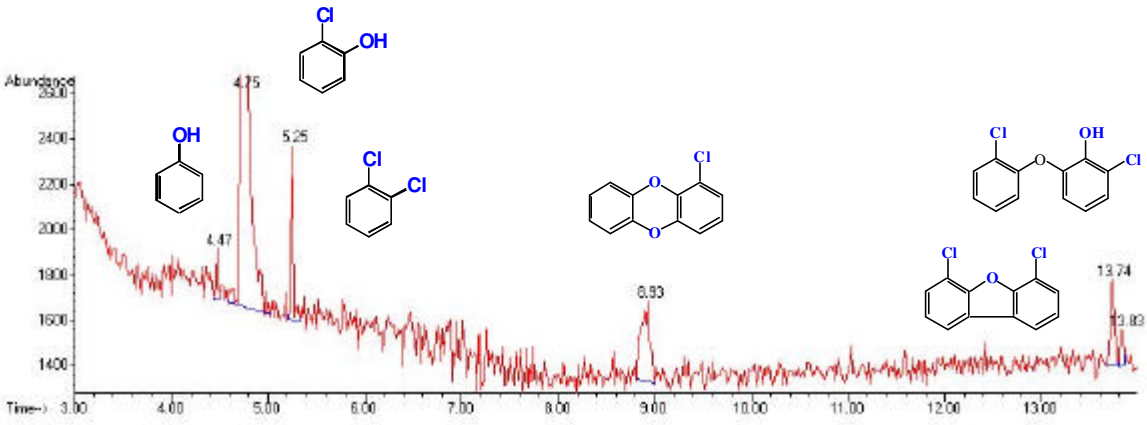

Figure A1.8: GC-MS Spectra of Products of 2-MCP after Extraction by Using IPA

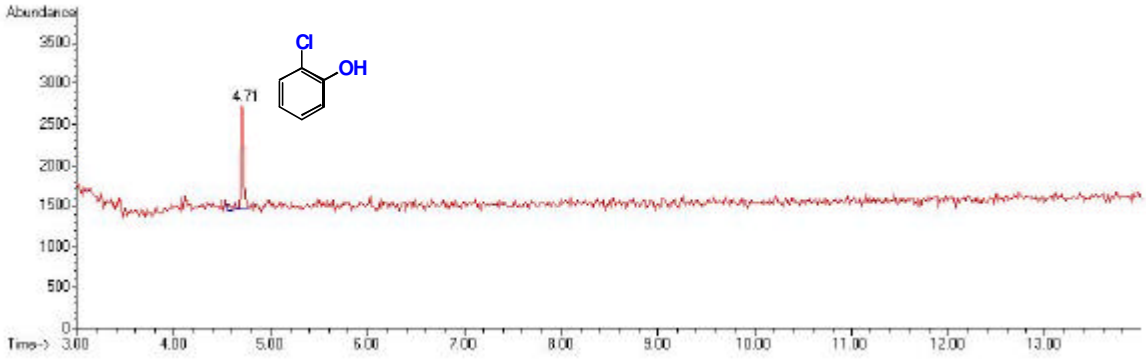

Figure A1.9: GC-MS Spectra of Products of 2-MCP after Extraction by Using DCM

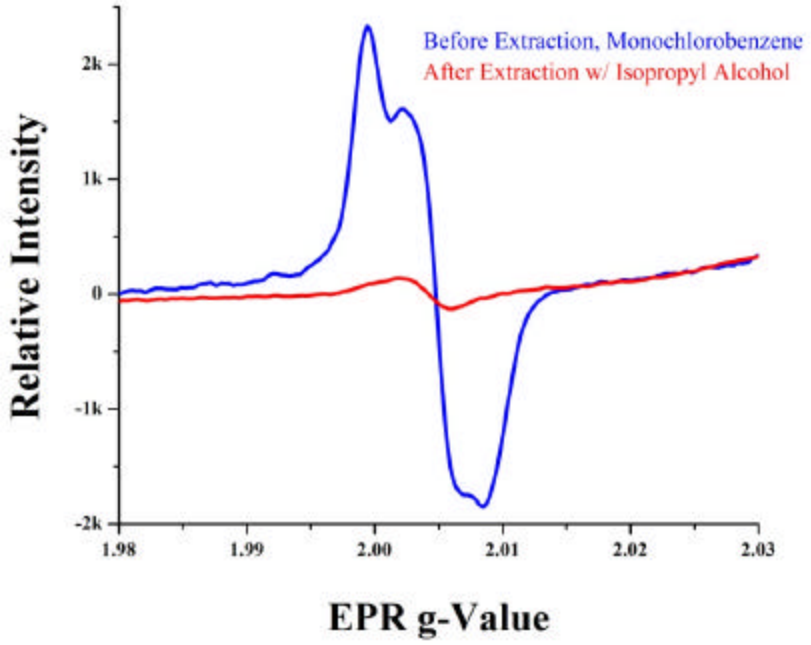

Figure A1.10: EPR Radical Signal of Residue from Chemisorbed MCBz on the Surface before and after Extraction with Isopropyl Alcohol

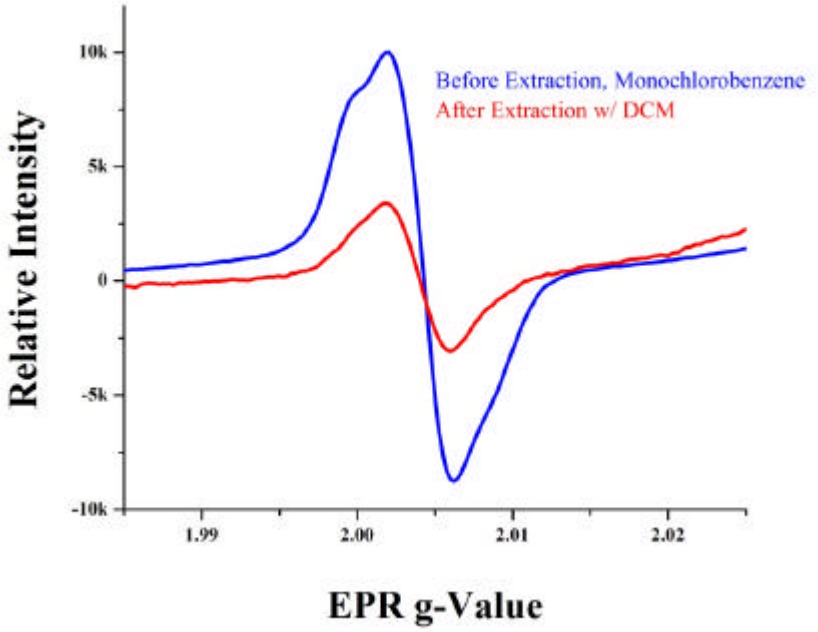

Figure A1.11: EPR Radical Signal of Residue from Chemisorbed MCBz on the Surface before and after Extraction with DCM

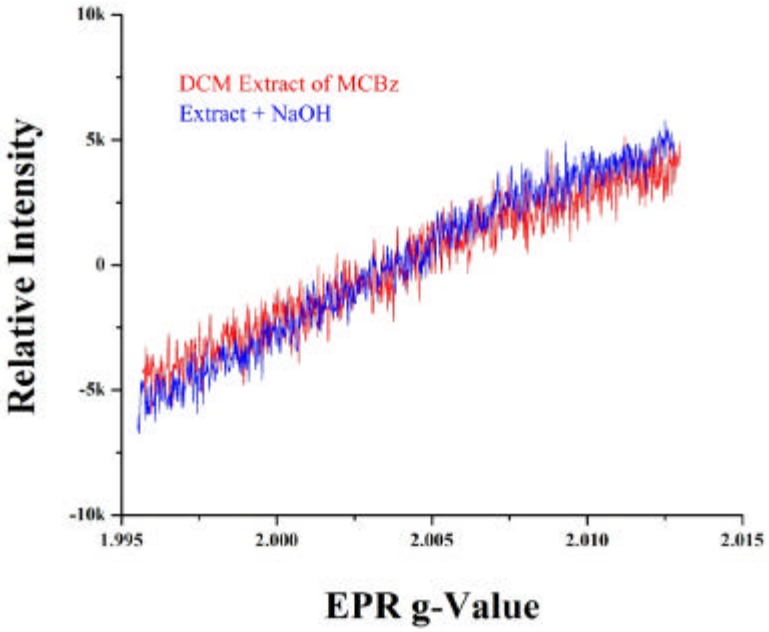

Figure A1.12: EPR Radical Signal of the Extract from Adsorbed MCBz Matrix Using DCM as a Solvent

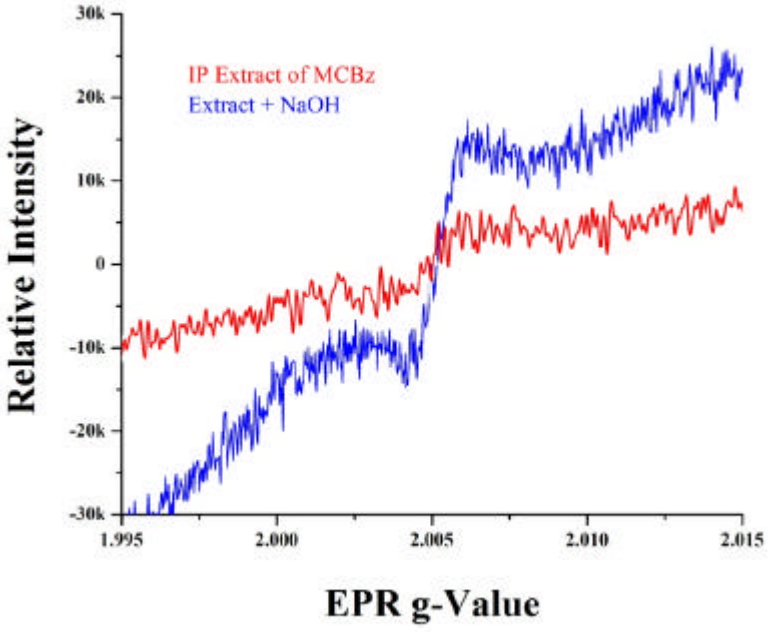

Figure A1.13: EPR Radical Signal of the Extract from Adsorbed MCBz Matrix Using Isopropyl Alcohol as a Solvent

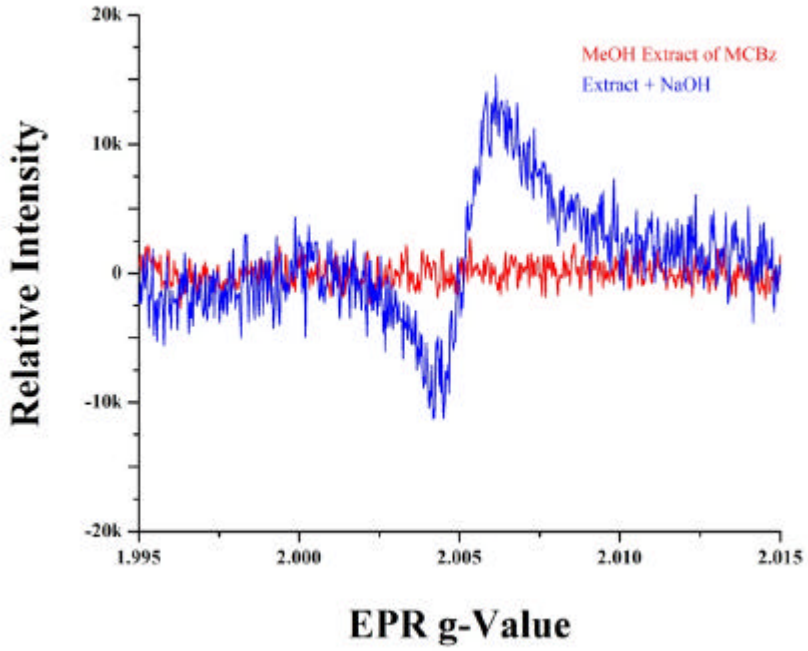

Figure A1.14: EPR Radical Signal of the Extract from Adsorbed MCBz Matrix Using Methyl Alcohol as a Solvent

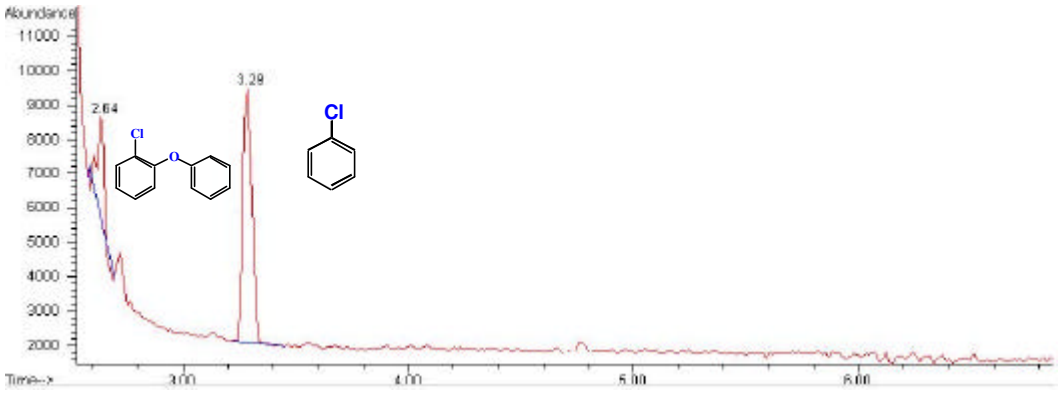

Figure A1.15: GC-MS Spectra of Products of MCBz after Extraction by Using IPA

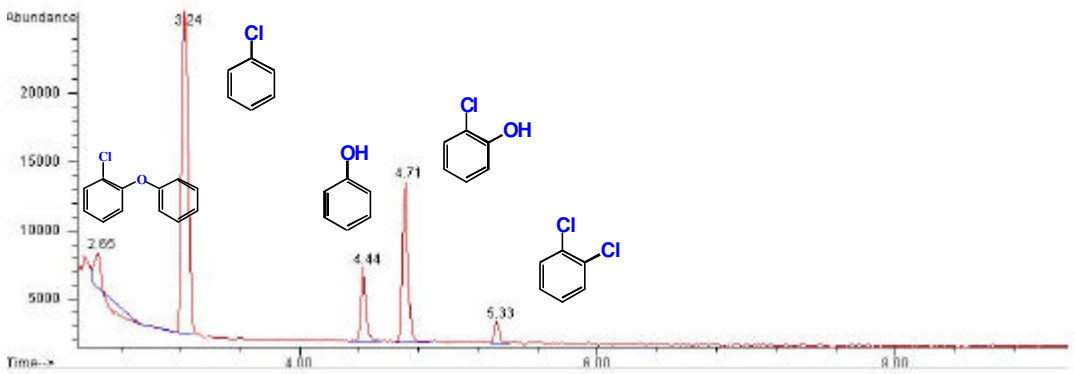

Figure A1.16: GC-MS Spectra of Products of MCBz after Extraction by Using MEA

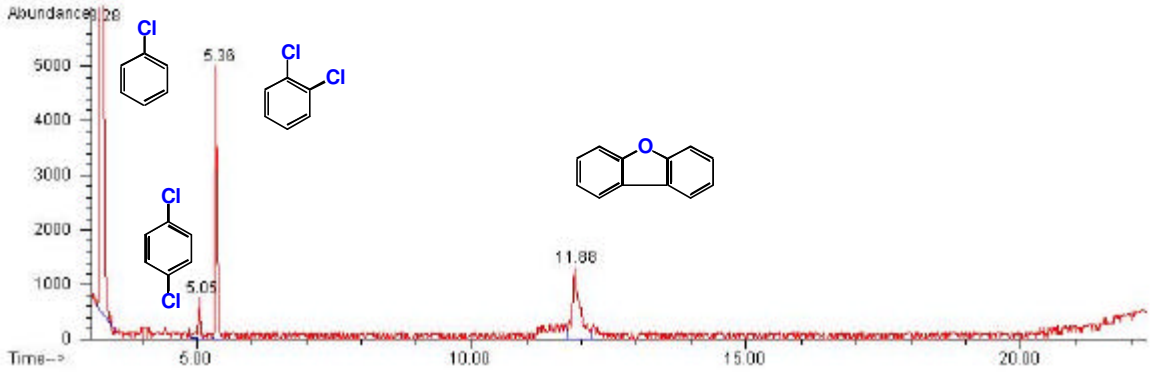

Figure A1.17: GC-MS Spectra of Products of MCBz after Extraction by Using DCM

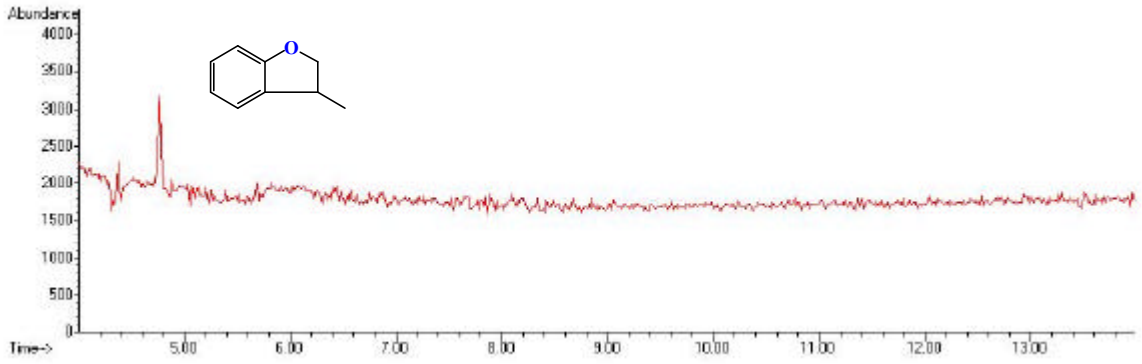

Figure A1.18: GC-MS Spectra of Products of MCBz after Extraction by Using TOL

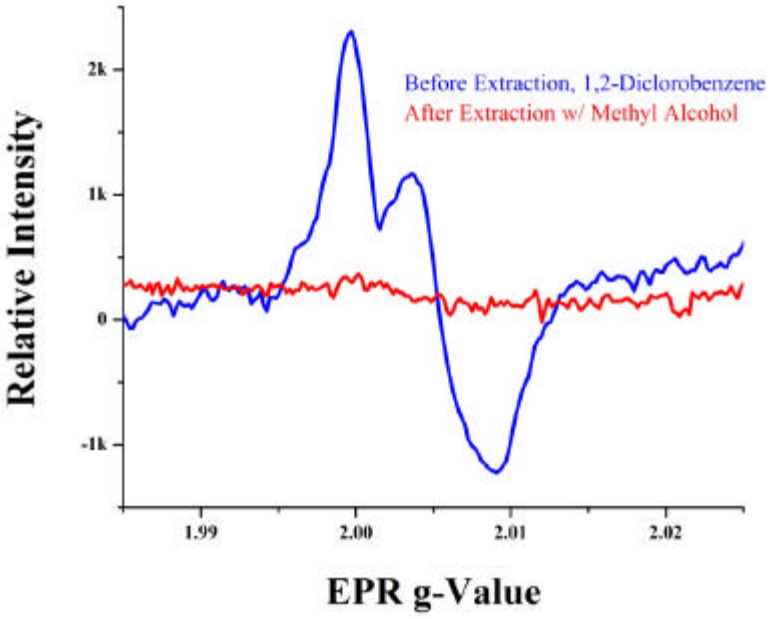

Figure A1.19: EPR Radical Signal of Residue from Chemisorbed 1,2-DCBz on the Surface before and after Extraction with Methyl Alcohol

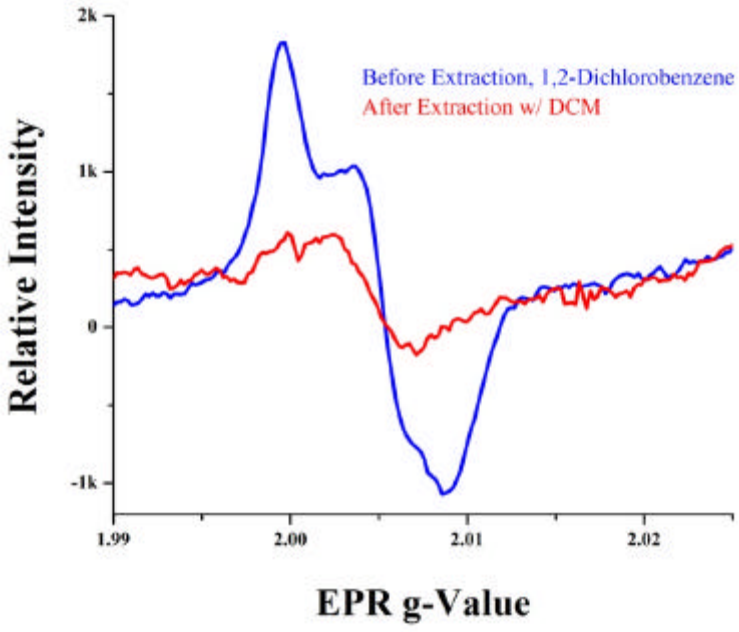

Figure A1.20: EPR Radical Signal of Residue from Chemisorbed 1,2-DCBz on the Surface before and after Extraction with DCM

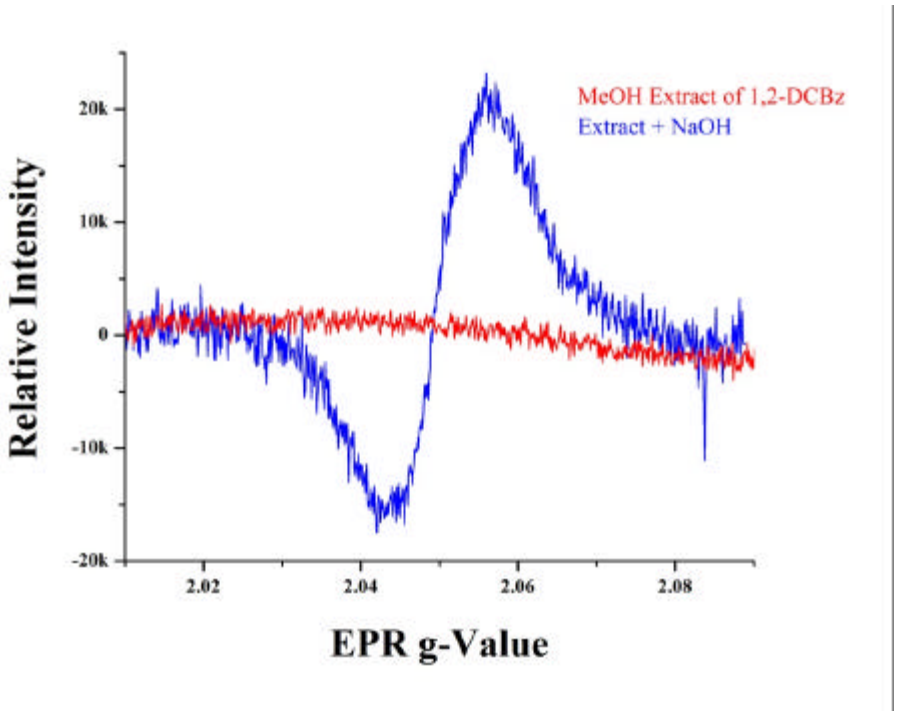

Figure A1.21: EPR Radical Signal of the Extract from Adsorbed 1,2-DCBz Matrix Using Methyl Alcohol as a Solvent

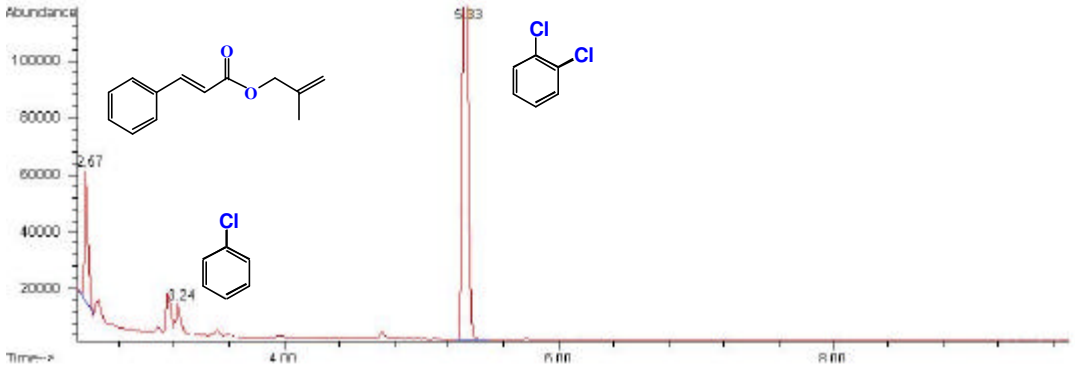

Figure A1.22: GC-MS Spectra of Products of 1,2-DCBz after Extraction by Using IPA

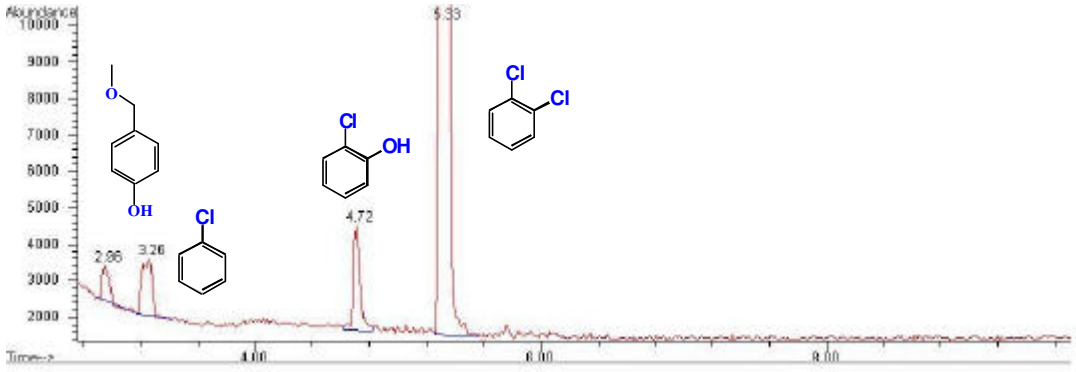

Figure A1.23: GC-MS Spectra of Products of 1,2-DCBz after Extraction by Using MEA

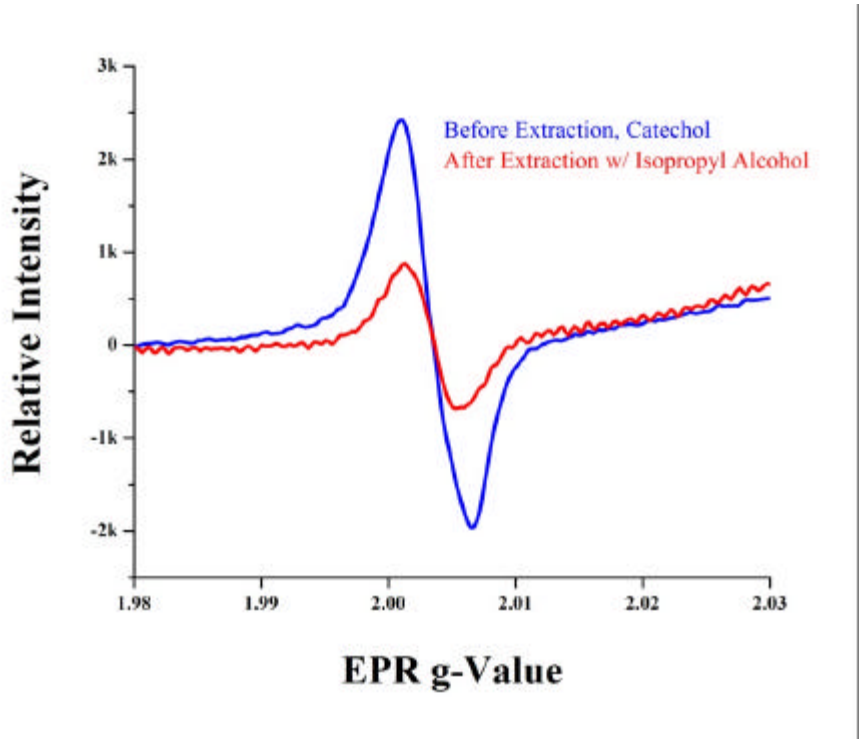

Figure A1.24: EPR Radical Signal of Residue from Chemisorbed CT on the Surface before and after Extraction with Isopropyl Alcohol

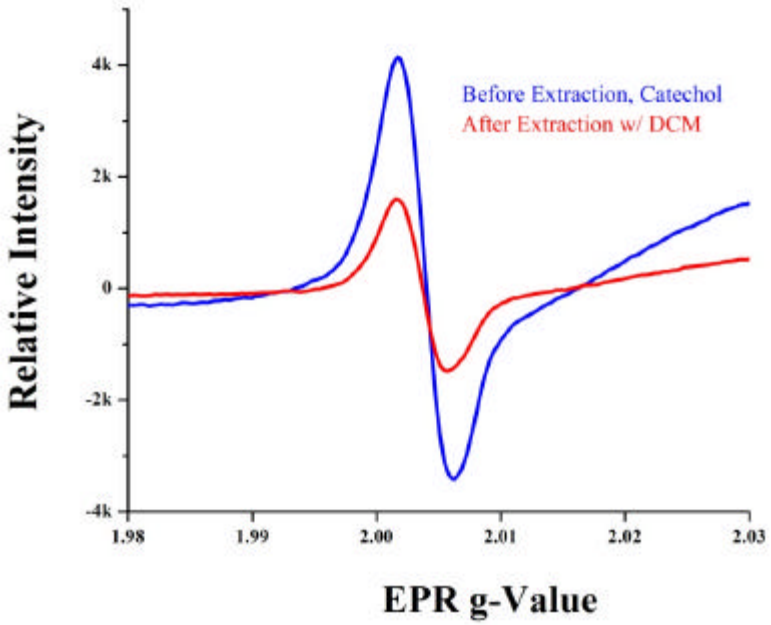

Figure A1.25: EPR Radical Signal of Residue from Chemisorbed CT on the Surface before and after Extraction with DCM

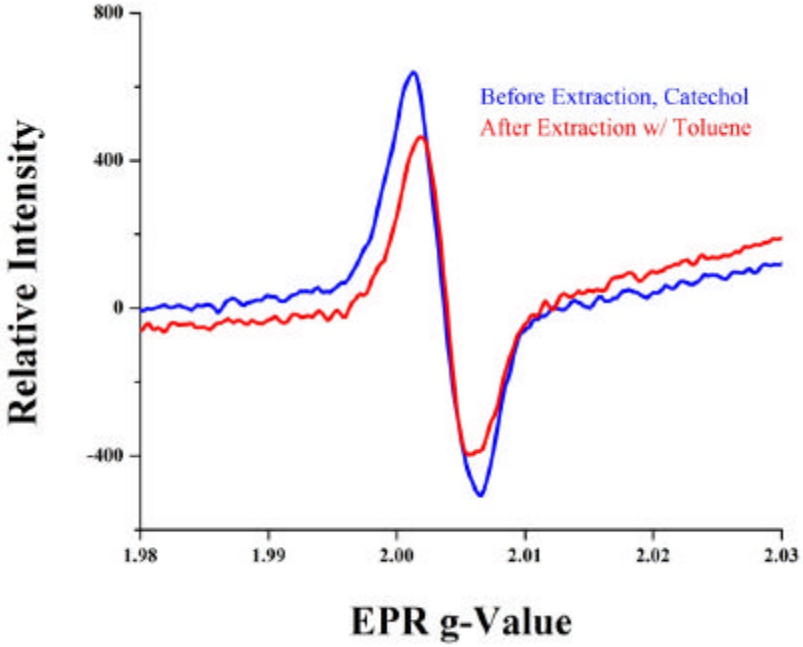

Figure A1.26: EPR Radical Signal of Residue from Chemisorbed CT on the Surface before and after Extraction with Toluene

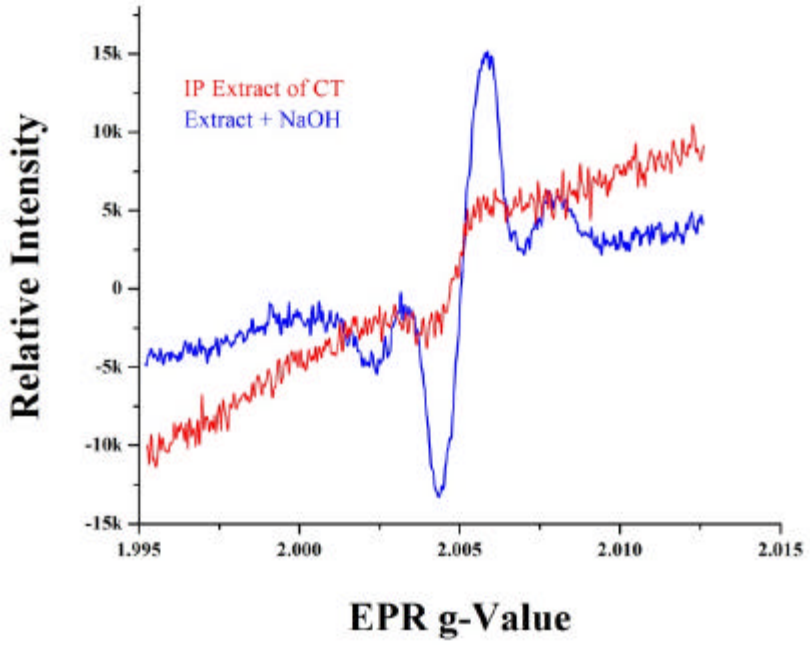

Figure A1.27: EPR Radical Signal of the Extract from Chemisorbed CT Matrix Using Isopropyl Alcohol as a Solvent

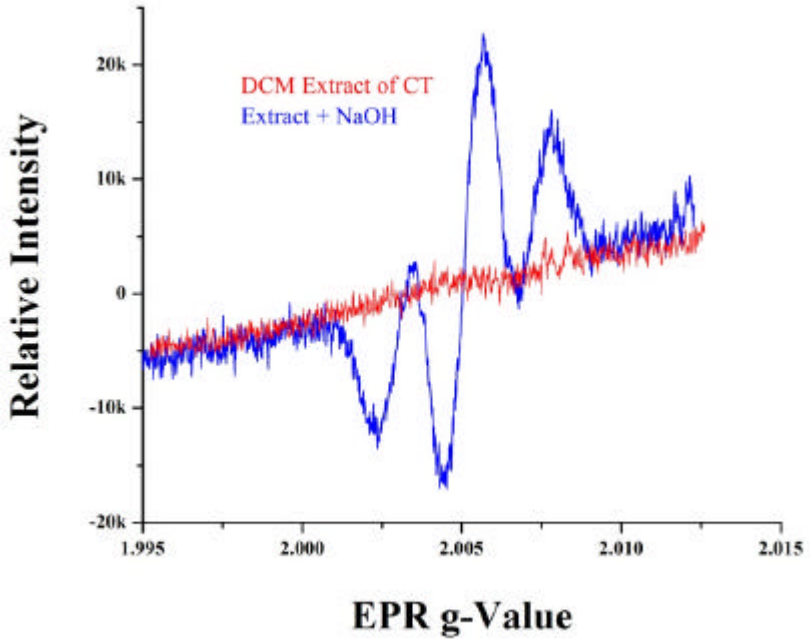

Figure A1.28: EPR Radical Signal of the Extract from Chemisorbed CT Matrix Using DCM as a Solvent

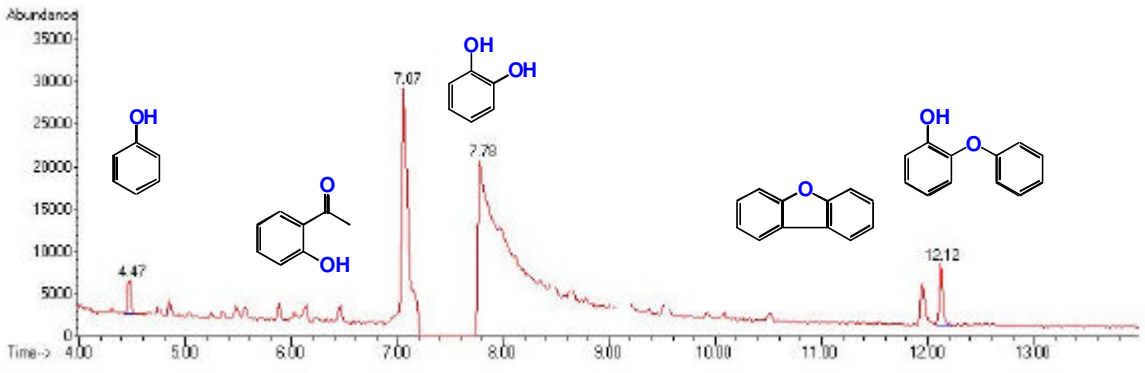

Figure A1.29: GC-MS Spectra of Products of CT after Extraction by Using IPA

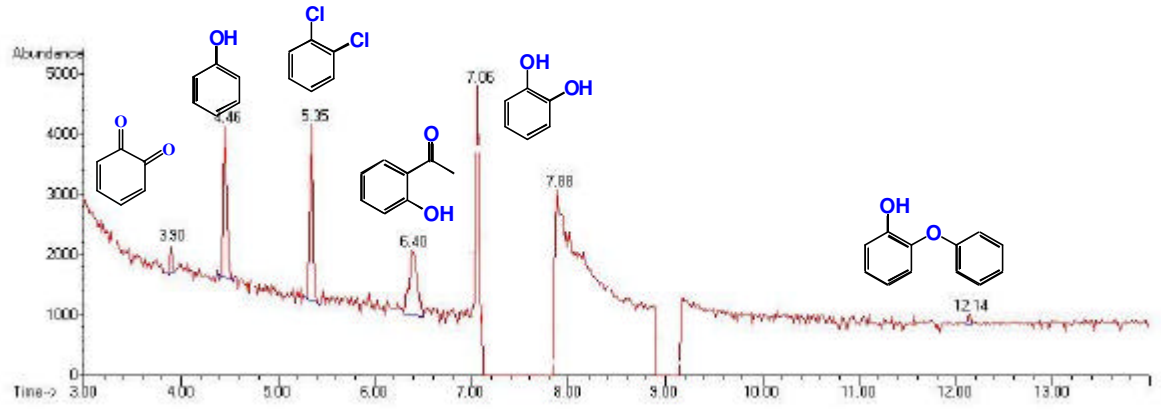

Figure A1.30: GC-MS Spectra of Products of CT after Extraction by Using MEA

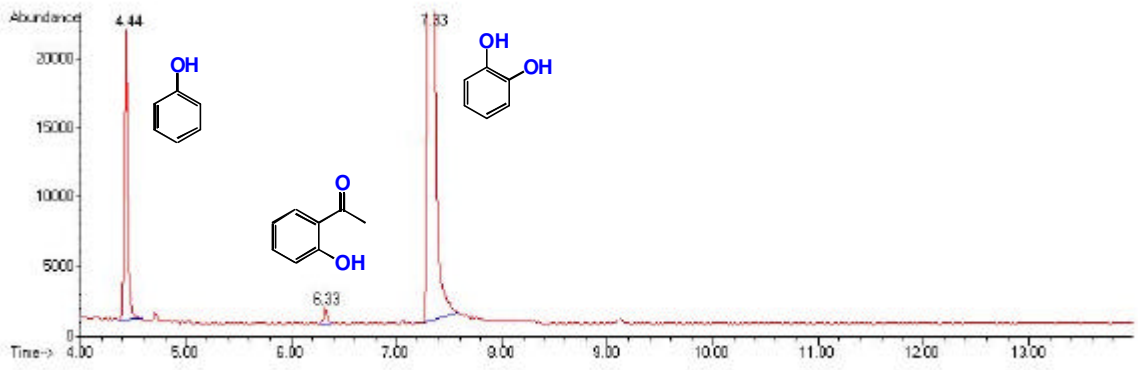

Figure A1.31: GC-MS Spectra of Products of CT after Extraction by Using DCM

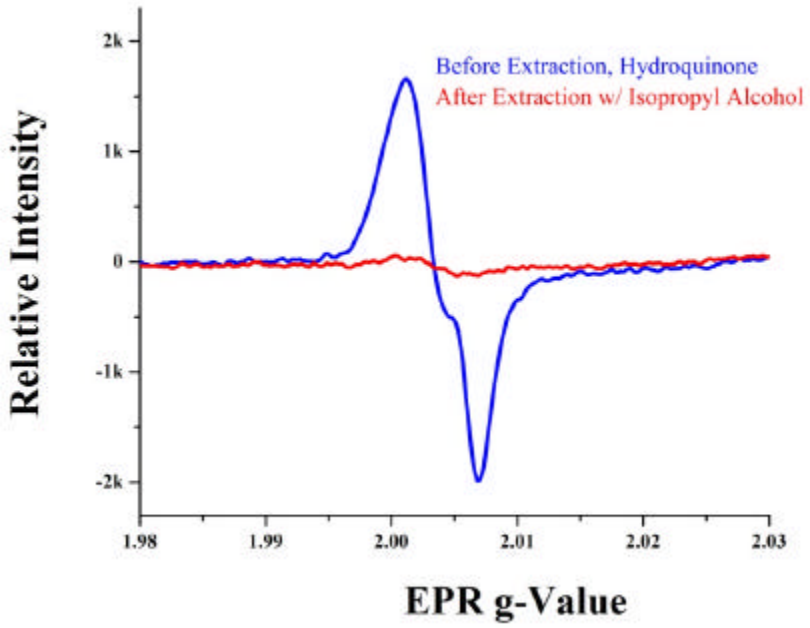

Figure A1.32: EPR Radical Signal of Residue from Chemisorbed HQ on the Surface before and after Extraction with Isopropyl Alcohol

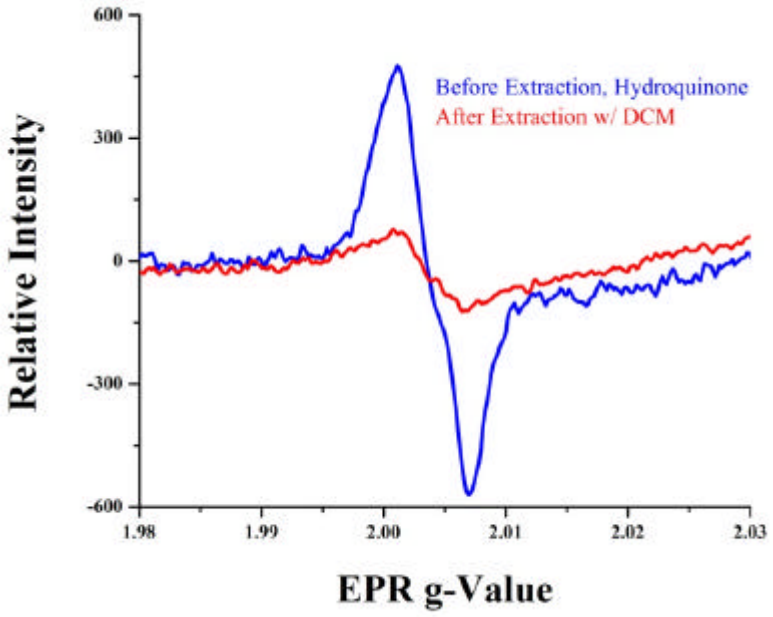

Figure A1.33: EPR Radical Signal of Residue from Chemisorbed HQ on the Surface before and after Extraction with DCM

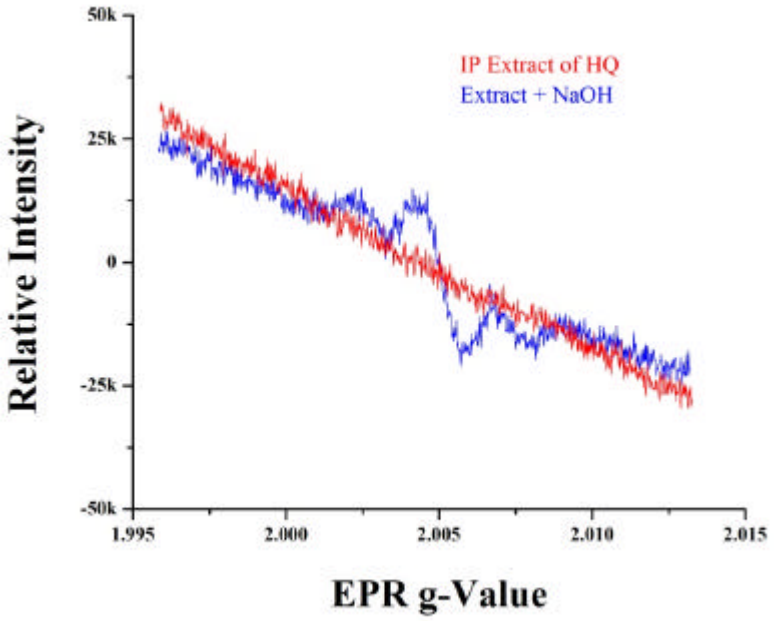

Figure A1.34: EPR Radical Signal of the Extract from Chemisorbed HQ Matrix Using Isopropyl Alcohol as a Solvent

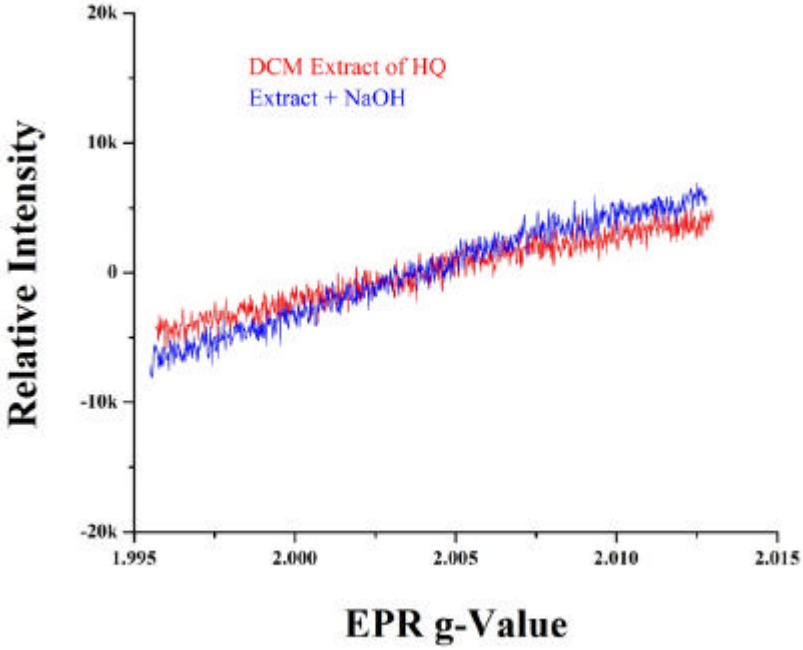

Figure A1.35: EPR Radical Signal of the Extract from Chemisorbed HQ Matrix Using DCM as a Solvent

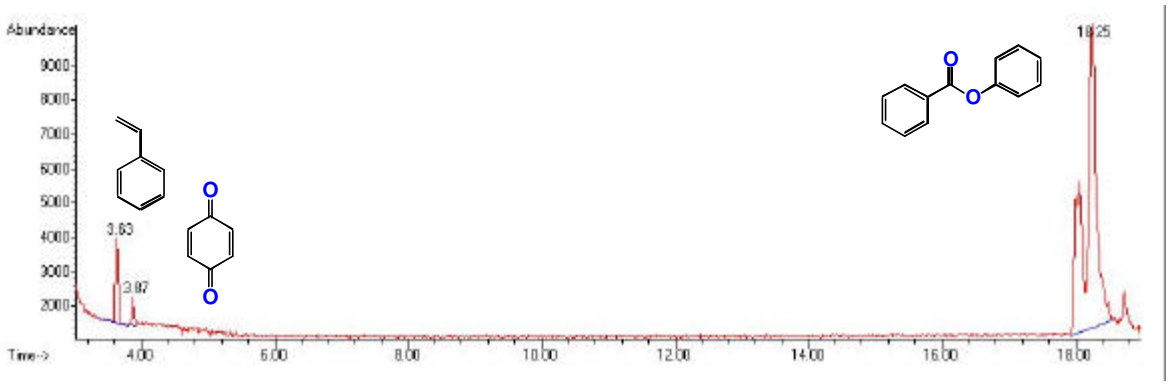

Figure A1.36: GC-MS Spectra of Products of HQ after Extraction by Using IPA

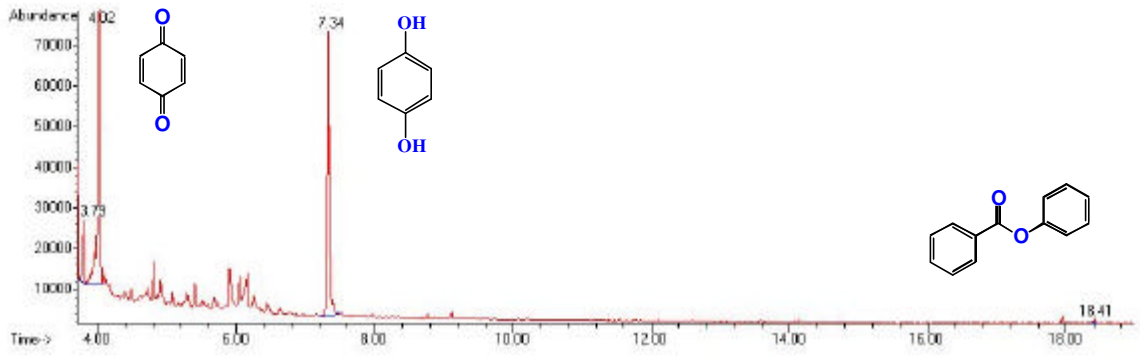

Figure A1.37: GC-MS Spectra of Products of HQ after Extraction by Using MEA

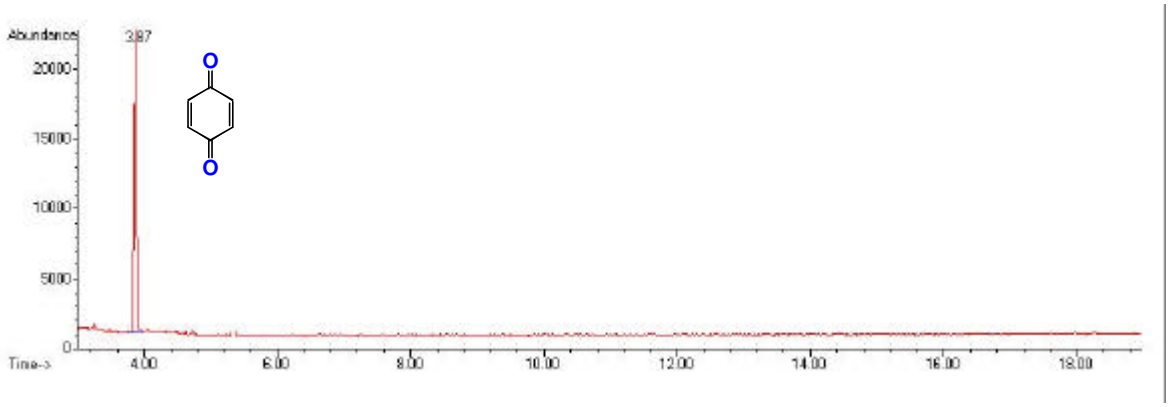

Figure A1.38: GC-MS Spectra of Products of HQ after Extraction by Using DCM

APPENDIX 2: COPYRIGHT PERMISSIONS

Dear Hieu Truong,

We hereby grant you permission to reprint the aforementioned material at no charge in your thesis subject to the following conditions:

1. If any part of the material to be used (for example, figures) has appeared in our publication with credit or acknowledgement to another source, permission must also be sought from that source. If such permission is not obtained then that material may not be included in your publication/copies.

2. Suitable acknowledgment to the source must be made, either as a footnote or in a reference list at the end of your publication, as follows: "Reprinted from Publication title, Vol number, Author(s), Title of article, Pages No., Copyright (Year), with permission from Elsevier".

3. Your thesis may be submitted to your institution in either print or electronic form.

4. Reproduction of this material is confined to the purpose for which permission is hereby given.

5. This permission is granted for non-exclusive world **English** rights only. For other languages please reapply separately for each one required. Permission excludes use in an electronic form. Should you have a specific electronic project in mind please reapply for permission.

6. This includes permission for UMI to supply single copies, on demand, of the complete thesis. Should your thesis be published commercially, please reapply for permission.

Yours sincerely

Manuela Beis
Rights Assistant

VITA

Hieu D. Truong was born on July 26, 1974, in Saigon, Vietnam. He earned a Bachelor of Science degree in biological engineering with minor in environmental engineering from Louisiana State University in May 2001 at Baton Rouge, Louisiana. He went on to pursue a doctoral degree in environmental chemistry at the same university, where he enjoined a wonderful environment and exciting football games. His research was under the direction of Dr. Barry Dellinger, Patrick F. Taylor Chair and Director of Intercollege Environmental Cooperative. He will receive his Doctor of Philosophy degree in August 2007.